

# MASTER THESIS

Thesis submitted in partial fulfillment of the requirements  
for the degree of Master of Science in Engineering at the  
University of Applied Sciences Technikum Wien  
Degree Program MEE

## Utilization of thermostatically controlled loads for demand response and increased energy flexibility in US residential buildings

By: Mario Feldhofer, BSc  
Student Number: 1710578077

Supervisor 1: DI Thomas Zelger  
Supervisor 2: William M. Healy, PhD

Vienna, 16.12.2019



## Declaration of Authenticity

“As author and creator of this work to hand, I confirm with my signature knowledge of the relevant copyright regulations governed by higher education acts (see Urheberrechtsgesetz/ Austrian copyright law as amended as well as the Statute on Studies Act Provisions / Examination Regulations of the UAS Technikum Wien as amended).

I hereby declare that I completed the present work independently and that any ideas, whether written by others or by myself, have been fully sourced and referenced. I am aware of any consequences I may face on the part of the degree program director if there should be evidence of missing autonomy and independence or evidence of any intent to fraudulently achieve a pass mark for this work (see Statute on Studies Act Provisions / Examination Regulations of the UAS Technikum Wien as amended).

I further declare that up to this date I have not published the work to hand nor have I presented it to another examination board in the same or similar form. I affirm that the version submitted matches the version in the upload tool.”

---

Place, Date

---

Signature

# Kurzfassung

Der zunehmende Anteil erneuerbarer Energien an der Energieversorgung stellt hohe Ansprüche an das Stromnetz und kann zu Zuverlässigkeitsproblemen und verminderter Betriebssicherheit führen. Energieflexible Gebäude können die Bedarfsseite an die Versorgungsseite anpassen und so dabei helfen, Überspannungen und andere Komplikationen zu minimieren. Der Einsatz der thermischen Speicherkapazität eines Gebäudes für Demand Response (DR) mit thermostatisch geregelten Lasten (TGL), wie Wärmepumpen und Widerstandsheizungen, kann die Energieflexibilität des Gebäudes verbessern. Das Speichern überschüssiger elektrischer Energie aus erneuerbarer Erzeugung als thermische Energie, in der Gebäudemasse und im Warmwasserspeicher, kann die Residuallast (RL) im Stromnetz reduzieren und die Integration von zusätzlicher erneuerbarer Erzeugungsanlagen ermöglichen.

Der Fokus dieser Arbeit sind Einfamilienhäuser in den USA, welche in Leichtbauweise ausgeführt sind und deswegen nur eine geringe thermische Speichermasse besitzen. Es wird untersucht, welche Systemkonfiguration den Beitrag eines Gebäudes zur RL des Stromnetzes minimiert und dabei die thermische Behaglichkeit aufrechterhält.

Ein validiertes TRNSYS Modell der "Net-Zero Energy Residential Test Facility" (NZERTF) auf dem Campus des National Institute of Standards and Technology (NIST) ist die Grundlage der Simulationen. Die Ergebnisse zeigen, dass die RL um 20 % reduziert werden kann, wenn ausschließlich DR angewandt wird und andere Systemkomponenten unverändert bleiben. Eine Erdwärmepumpe (EWP) reduziert die positive RL effektiver als eine Luftwärmepumpe (LWP), insbesondere in kalten Klimazonen. Im Allgemeinen reduzieren Energieeffizienzmaßnahmen (z. B. bessere Wärmedämmung) die positive RL eines Gebäudes. Eine größere thermische Speichermasse (z. B. Beton, Ziegel, größerer Warmwasserspeicher) verbessert das Potential zur Reduzierung der gesamten RL.

Der Einsatz einer aktiven Schicht aus Phase Change Material (PCM), um die thermische Speichermasse von Leichtbauten zu erhöhen, ist eine effektive Maßnahme zur Reduktion der RL. In Kombination mit einer EWP erreicht diese Variante mit aktivem PCM die größte Reduzierung der RL mit 36 %. Der Wärmestrom zwischen der Innenluft und einer Schicht aus passivem PCM ist zu niedrig, um die RL wirksam zu reduzieren.

Die Erhöhung der Spanne der Temperatursollwerte führt zu einer Reduzierung der RL in allen Varianten. Das Gebäude bietet einen hohen thermischen Komfort in einem Temperaturbereich zwischen 20 °C und 26 °C. Die Bereitschaft des Verbrauchers die Kontrolle über sein Thermostat abzugeben ist essenziell für den Einsatz von TGL. Finanzielle Anreize werden notwendig sein, um Konsumenten zur Nutzung von DR zu ermutigen.

**Schlagwörter:** Energieflexibilität, Thermostatisch geregelte Lasten, Demand Response

# Abstract

The increasing share of fluctuating renewable energy generation places a high demand on the power grid and can lead to issues with reliability and operational security. Energy flexible buildings can help to mitigate electrical surges and other contingencies by matching the demand side to the supply side. Utilizing a building's thermal storage capacity for Demand Response (DR) with Thermostatically Controlled Loads (TCL), such as heat pumps and resistance heaters, can increase a building's energy flexibility. Storing excess electricity from renewable sources as thermal energy, in the thermal mass and the warm water tank, can reduce the power grid's Residual Load (RL) and thus enable the installation of more renewable generation.

This paper focuses on detached single-family homes in the US which are built as lightweight construction and therefore possess little thermal mass. It is examined, what system configuration minimizes a building's contribution to the grid's RL while maintaining thermal comfort.

A validated TRNSYS model of the Net-Zero Energy Residential Test Facility (NZERTF) at the campus of the National Institute of Standards and Technology (NIST) is used for simulations. The results show that the RL can be reduced by up to 20 % when exclusively using a DR control without altering any system components. A ground-source heat pump (GSHP) is more effective at reducing positive RL than an air-source heat pump (ASHP), especially in cold climate zones. In general, energy efficiency measures (e.g. better insulation) decrease a building's positive RL. Greater thermal storage mass (e.g. concrete, brick, bigger warm water tank) increases the potential for reducing the overall RL.

Using an active Phase Change Material (PCM) layer to increase the thermal storage capacity of lightweight construction is an effective measure to reduce RL. In combination with a GSHP this active PCM variant achieves the greatest reduction of RL at 36 %. The heat flux between the indoor air and a passive PCM layer is too low to make it a viable option for reducing RL. Increasing the range of temperature setpoints results in a reduction of RL across all variants. The building provides high thermal comfort in a temperature range between 20 °C and 26 °C. The consumers' willingness to give up control of their thermostat is essential for the use of TCLs. Monetary incentives will be necessary to encourage consumers to use DR.

**Keywords:** Energy Flexibility, Thermostatically Controlled Loads, Demand Response

## **Acknowledgements**

Special thanks to my NIST supervisor William M. Healy for his ongoing support and William Stuart Dols for his help with TRNSYS. I am grateful to my colleagues from the Energy and Environment Division who took time out of their day to help me, even if they were not directly involved in my project.

Finally, I would like to thank my UAS Technikum Wien supervisor Thomas Zelger for his feedback and guidance, especially at the beginning of the project.

# Table of Contents

1	Introduction .....	6
1.1	Research Questions .....	7
2	Methodology.....	7
2.1	Current state of the power Grid in the US .....	9
2.2	Scenarios for the Energy Mix in 2050 .....	11
2.3	Simulation of electricity grid and evaluation of data .....	17
3	Background .....	18
3.1	Demand Response.....	18
3.2	IEA EBC Annex 67 .....	19
3.3	Thermostatically Controlled Loads.....	21
3.4	Phase Change Materials .....	22
3.5	Thermal Comfort .....	25
4	Net-Zero Energy Test Facility NZERTF .....	29
4.1	Climate and building code .....	32
4.2	Building components and Key figures.....	34
4.3	Energy systems.....	40
4.4	Shading .....	42
4.5	Load profiles.....	43
5	Variants .....	45
5.1	Variant 0 - Base Variant without DR .....	46
5.2	Variants 1 and 2 - Base Variant with DR.....	46
5.3	Variants 3 and 4 - Massive Construction .....	47
5.4	Variants 5 - IECC Minimum Standard.....	48
5.5	Variants 6 to 9 - Passive PCM with ASHP .....	48
5.6	Variants 10 to 13 - Active PCM with GSHP .....	49
5.7	Variants 14 to 17 - Concrete Core Activation with AWHP .....	51
5.8	Variants 18 to 21 - Concrete Core Activation with GSHP.....	52
5.9	Variants 22 to 24 - Vienna, Austria .....	53
5.10	Variants 25 to 27 - Phoenix, Arizona .....	53
5.11	Variant 28 to 30 - Miami, Florida.....	54
5.12	Variant 31 to 33 - Fairbanks, Alaska.....	55

5.13	Typical Summer and Winter day/week .....	56
6	Interpretation of results.....	57
6.1	Variants 1 – 2.....	58
6.2	Variant 3 – 5.....	61
6.3	Variant 6 – 9 (PCM with ASHP).....	63
6.4	Variant 10 – 13 (PCM with GSHP).....	65
6.5	Variant 14 – 17 (Concrete Core Activation with AWHP).....	68
6.6	Variant 18 – 21 (Concrete Core Activation with GSHP) .....	71
6.7	Variant 22 – 24 (Vienna).....	74
6.8	Variant 25 – 27 (Phoenix).....	76
6.9	Variant 28 – 30 (Miami) .....	78
6.10	Variant 31 – 33 (Fairbanks).....	80
6.11	Typical Winter Week Gaithersburg .....	83
6.12	Typical Summer Week Gaithersburg .....	85
7	Conclusion .....	87
	Bibliography.....	90
	List of Figures .....	92
	List of Tables .....	94
	List of Abbreviations .....	95

# 1 Introduction

The energy industry is shifting from a regulated monopoly to a competitive market (IEEE 2013). With the introduction of fluctuating renewable energy sources, the entire power system faces new challenges. In the past only the supply side actively regulated energy production to ensure that supply met demand. The supply side was responsible for matching its power generation to the customer's demand at all times. This arrangement was logical because there was no overall necessity to control the demand side in a predictable fossil fuel-based system. If the current system remains in place, however, the power system will not be able to withstand sudden disturbances caused by variable renewable energy sources. An electrical surge could damage the grid infrastructure, and undervoltage could result in an unstable electricity supply or even power outages. The frequency of voltage problems and contingencies will increase, and the operational security and reliability of the power system will decline.

Demand Response (DR) is defined as *“all intentional modifications to consumption patterns of electricity of end-use customers that are intended to alter the timing, level of instantaneous demand, or the total electricity consumption.”* (IEEE 2013).

DR in combination with energy storage can mitigate the aforementioned problems of the current power system. If markets are set up appropriately, the demand/customer side could profit from incentive payments and access to a new market. DR is possible with a variety of different resources. Batteries, electric vehicles, and Thermostatically Controlled Loads (TCLs) can all be used for DR if properly managed. This paper focuses on DR with TCLs. Experiments regarding DR are conducted with a validated TRNSYS model of the Net-Zero Energy Residential Test Facility (NZERTF) which is situated on the campus of the National Institute of Standards and Technology (NIST) located in Gaithersburg, Maryland, U.S.

The NZERTF is a highly insulated detached single-family house (NIST 2015). The building's thermal envelope is a lightweight construction made of wood. Due to low heat transfer coefficients and minimization of thermal bridges, heat flow through the envelope is greatly reduced. Additionally, unwanted heat gains during summer are reduced by windows with low solar heat gain coefficients. However, a common disadvantage of lightweight construction is its low thermal storage capacity. Utilizing thermal storage capacity in the envelope can be highly advantageous for thermal energy storage and user comfort. When combined with an appropriate control strategy the energy consumption of active heating and cooling systems can be increased during times of high renewable production to better match the supply of electricity on the grid. TCLs (e.g., air conditioners and water heaters) can be used for DR. This is accomplished by changing the set points for space heating between 20 °C and 22 °C and space cooling between 24 °C and 26 °C. The user comfort is unlikely to be compromised within these boundaries. Furthermore, the temperature in the hot water storage tank can be increased to 80 °C to further decrease peak loads. Storing excess energy in the building's structure has different advantages. In comparison to residential electrochemical energy storages the thermal

storage capacity of a building, including PCMs (Rathod 2018), does not degrade over time and no additional material besides the construction material needs to be purchased. The outcome of this research is expected to contribute to framework conditions for DR with TCLs and a better understanding of parameters that influence the efficiency of DR with TCLs.

The results of this study should serve to establish a framework that utilizes TCLs for DR to decrease peak loads and support the integration of renewable energy into the electrical grid. It is essential to develop a control system that connects thousands of buildings to provide the power capacity necessary. Simple control mechanisms and fast ramp rates make residential buildings' heating and cooling systems a valuable asset for load management. Furthermore, DR with TLCs is an inexpensive and simple option, which is a crucial factor for decision makers and investors. Additionally, DR can delay the necessity for grid expansion or investments in expensive storage capacity. This delay gives decision-makers more time to work on solutions for a time with a high share of renewables in the grid. The outcome of the proposed research can aid with the transition from fossil fuels to renewable energy and lay the foundation for future research regarding control strategies.

## 1.1 Research Questions

Characterizing energy flexibility based on a mathematical model and a penalty signal is necessary for applying energy flexibility measures across different levels from individual components to entire districts (IEA 2017). Using Residual Load as penalty signal for DR with TCLs to increase the NZERTF's energy flexibility and decrease peak loads on the grid is a major focus of this paper. Additionally, following questions are addressed:

- To what extent can the contribution of a single-family house to the grid's Residual Load be minimized by DR with TCLs while still maintaining acceptable levels of thermal comfort? How are Residual Load and thermal comfort affected if the temperature control range is expanded?
- How is the Residual Load influenced by different parameters such as thermal storage mass, climate, heat pump power, and the utilization of different heat pumps?
- To what extent can Phase Change Materials be used to improve the thermal storage mass of lightweight construction, and what is the impact on thermal comfort?

## 2 Methodology

For answering the aforementioned research questions, it is first necessary to predict a US generation profile with a sufficient share of renewable energy to illustrate the impact of DR. The share of renewable energy is assumed to be higher in the future, but predictions are also less accurate. Therefore, a possible scenario for the year 2050 is chosen to balance share of renewables and prediction accuracy. Since the contiguous US does not have a unified

electricity grid, the regional transmission operator PJM Interconnection is chosen as a representative grid for the US energy mix.

The energy mix in the PJM grid in 2050 is predicted based on reports from the IEA, US Census, and grid development plans. The generation profile is scaled up from the current profile based on population growth and increased electricity demand. The generation profile in 2050 is then divided by the number of predicted detached single-family homes in 2050. The result is a generation profile that provides enough energy to operate a single-family home, or in this case the NZERTF.

The transient systems simulation program TRNSYS is used to model the building, including the hot water system, space heating/cooling, and heat recovery ventilation. Plug loads, appliances, occupancy, and water draws are supplied as input files (Balke 2016). The existing validated model is modified to be a fully electric system without solar thermal collectors. Controlled outside shading is added in preparation for studying the building in different climates. The local PV production is removed and included into the generation profile. This new building is used as Base Variant for all following models. To accurately emulate the behavior of all building components, including the DR controller included in future variants, one minute is chosen as the simulation timestep. Annual energy demand, Residual Loads, and thermal comfort are calculated for this Base Variant. All other variants are compared to this variant to find the best configuration at reducing total annual Residual Load while maintaining high thermal comfort. In this paper high thermal comfort is defined as times when the Predicted Percentage of Dissatisfied (PPD, to be discussed in detail later) < 10 %. The Residual Load is calculated hourly by subtracting the generation profile from the building's load profile. All variants, apart from the Base Variant, are equipped with a DR controller that changes the setpoint temperatures of the heat pump water heater and the space heating/cooling heat pump, depending on Residual Load.

A total of 21 variants are created by changing the following parameters:

- Building envelope (lightweight, massive, minimum IECC insulation standard)
- PCM gypsum boards (active, passive)
- Heat pump technology (GSHP, ASHP, AWHP)
- Compressor technology (single-stage, two-stage, variable speed)
- Heat pump power (70 %, 100 %, 300 %)
- DR controller temperature range

This investigation is not an exhaustive parameter study. Thus, some second- and third-degree correlations cannot be discovered. Nevertheless, this methodology covers the factors that are assumed to be the main contributors to a building's potential for DR. The chosen combinations

are arranged in a way to minimize redundancy and keep the number of models manageable for evaluation.

After determining the variant with the greatest reduction in RL, the Base Variant, the Base Variant with DR, and the variant with the lowest Residual Load are modelled in different climates. The performance of the building is evaluated in hot and humid (Miami, FL), hot and dry (Phoenix, AZ), extremely cold (Fairbanks, AK), and moderate without cooling demand (Vienna, Austria) climates. The goal of these analyses is to determine how different climates impact a building's potential for DR. Twelve variants are evaluated in this section. Including the Base Variant, the total number of variants for the entire study is 34.

Finally, typical cooling and heating weeks are determined to display the effects of DR on Residual Load for a home in Gaithersburg. Typical cooling weeks occur in summer from June 21<sup>st</sup> to September 23<sup>rd</sup> and typical heating weeks occur in winter from December 21<sup>st</sup> to March 19<sup>th</sup>. A typical week is defined as the week with the lowest absolute difference between 168 consecutive hourly temperatures of the weather data file of Dulles, VA and the median hourly temperature in summer/winter of the last 15 years.

## **2.1 Current state of the power Grid in the US**

The US is part of North America's combined transmission and distribution grid (DOE 2015). The grid consists of 4 distinct power grids which are also called interconnections. The Western Interconnection includes the western one-third of the continental United States, the Canadian provinces of Alberta and British Columbia, and a portion of Baja California Norte in Mexico as displayed in Figure 1. The Eastern Interconnection includes the eastern two-thirds of the continental United States and the Canadian provinces from the Great Plains to the Eastern Seaboard. The Texas Interconnection comprises most of Texas, and the Québec Interconnection covers the Canadian province of Québec. The grid in Alaska is not connected to North America's combined grid.

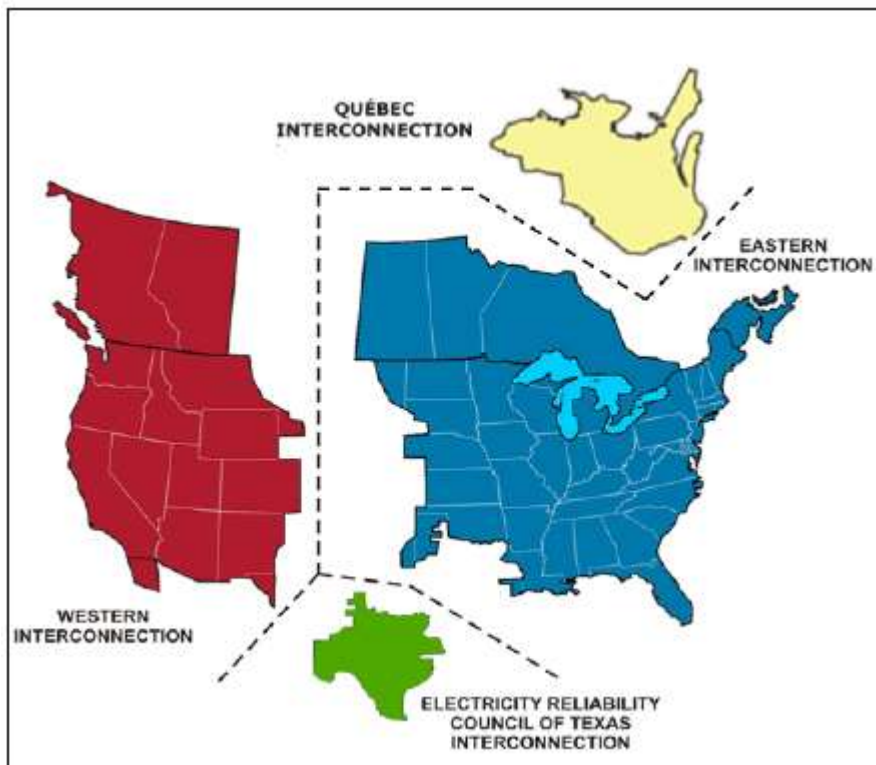


Figure 1: Map of Four North American Power Grid Interconnections (DOE 2015)

The following key players are essential for operating the US power system:

### **FERC**

The Federal Energy Regulatory Commission (FERC) is an independent agency within the US Department of Energy (DOE) that regulates interstate transmission of electricity, gas, and oil as well as natural gas and hydropower projects (DOE 2015). FERC is also responsible for regulating the interstate wholesale market of electricity, protecting the reliability of transmission systems, overseeing environmental matters, and reviewing mergers, acquisitions, and transactions by electricity companies. The FERC does not regulate retail electricity sales or the distribution grid.

### **NERC**

The North American Electric Reliability Corporation (NERC) is a not-for-profit international regulatory authority. NERC's goal is to ensure the reliability of the North American power system, and, for that reason, NERC was designated by FERC as the government's Electrical Reliability Organization (ERO). NERC is responsible for all 4 Interconnections shown in Figure 1.

### **ISO/RTO**

Regional transmission organizations (RTOs) and independent system operators (ISOs) both operate a certain region's electricity grid within 3 of the 4 major Interconnections in North

America (The Electric Reliability Council of Texas ERCOT does not fall under interstate FERC authority). ISOs and RTOs are directly recommended by FERC to oversee a region's electricity grid, wholesale electricity market, and reliability planning. RTOs perform similar tasks as the ISOs but have greater responsibilities regarding the transmission network. As can be seen in Figure 2, there are parts of the US where there are neither ISOs nor RTOs. In these areas, utilities are responsible for coordinating and developing transmission plans under the rules of FERC.

There are more key players in the US power system such as Power Market Administrations, Reliability Coordinators, Utilities, etc. These players do not impact the methodology of this paper and are therefore not considered. The objective of understanding the structure of the US power grid is to make realistic predictions of the electricity production in 2050 in Maryland and its surrounding states. The RTO PJM Interconnection covers this area and provides predictions for the potential for renewable energy and a scenario in which 30 % of electricity on the grid is provided by renewable sources (General Electric 2014).

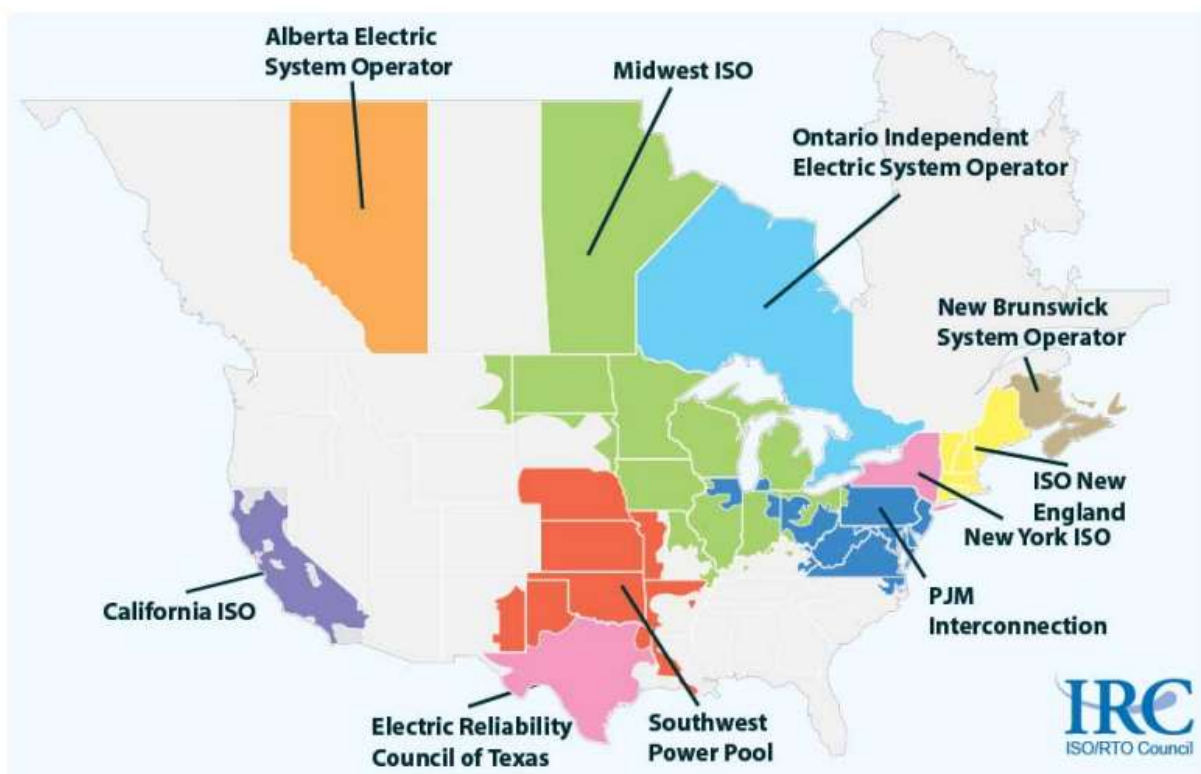


Figure 2: Map of North American Transmission Operators (DOE 2015)

## 2.2 Scenarios for the Energy Mix in 2050

A necessary step to evaluate DR is to create a generation profile with a realistic energy mix. DR is most effective when the share of variable renewable energy is high such that there are numerous peaks in the electricity generation profile. The 18 % share of renewable generation

in the US today is assumed to be insufficient to properly display the potential of DR, especially given that a large fraction of that share is from relatively stable hydropower (EIA 2019a). Therefore, an expected generation profile is created for 2050 with an expected share of fluctuating renewable generation of approximately 50 %. As discussed in 2.1 the US does not have a unified electricity grid. For this reason, creating a generation profile for the whole US would distort local differences in the share of different renewable technologies. Since the NZERTF is situated in Maryland, the Eastern Interconnection is chosen. The Eastern Interconnection includes parts of Canada and the eastern two-thirds of the continental United States. To further specify the boundary conditions, the RTO PJM Interconnection is chosen. PJM is the grid operator for a 960 000 m<sup>2</sup> area that covers all or parts of Delaware, Indiana, Illinois, Kentucky, Maryland, Michigan, New Jersey, North Carolina, Ohio, Pennsylvania, Tennessee, Virginia, West Virginia, and the District of Columbia, with a population of about 65 million (PJM 2019a).

The current electricity mix, as shown in Figure 3, focuses mainly on natural gas, coal and nuclear energy. The total share of renewable generation is under 6 %. Every source of electricity generation under 1 %, apart from solar, is disregarded because there is no significant change expected from these various technologies. The current electricity mix in 2018 results in the electricity generation profile shown in Figure 4. The peaks from renewable electricity generation are insignificant compared to the total generation capacity. The increased electricity generation in summer reflects the cooling demand of commercial and residential buildings. The total electricity production in PJM was 838 TWh in 2018 (PJM 2019b). For the sake of comparability, it is assumed that there are neither exports nor imports. Therefore, electricity generation is equal to electricity demand.

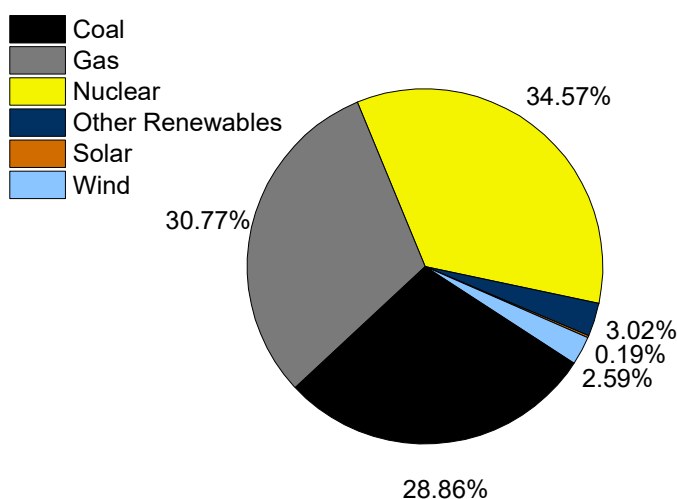


Figure 3: Electricity Mix PJM 2018 (PJM 2019b)

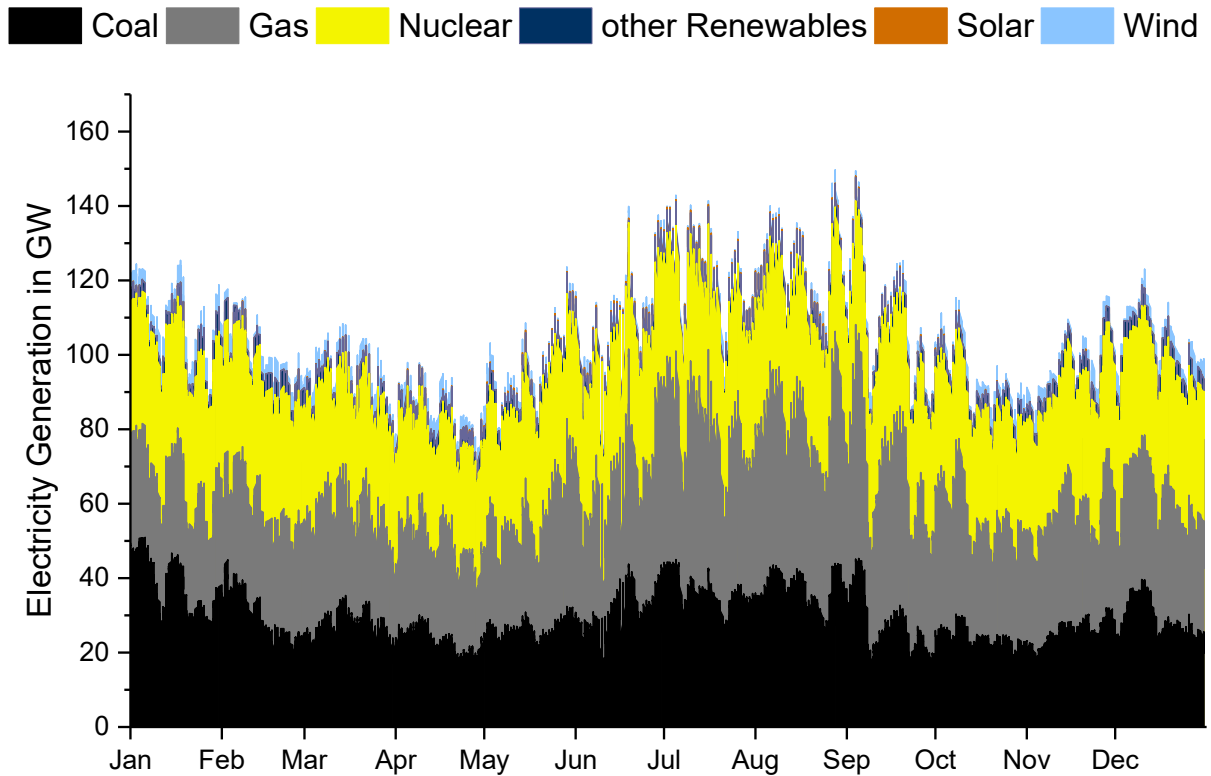


Figure 4: Electricity Generation Profile PJM 2018 (PJM 2019b)

There are multiple possible scenarios for the development of renewable generation in the PJM grid during the next 10 to 15 years (General Electric 2014). One such site selection for centralized solar power plants is displayed in Figure 5 and that for wind in Figure 6. The total potential for renewable generation is 194 GW of wind power and 120 GW of solar power. The scenarios with the highest share of renewable generation expect 30 % renewable generation in 2030. This goal can be achieved by installing a total of 77 GW of wind power (onshore and offshore) and 74 GW of solar power (distributed and centralized) (AWS Truepower 2012). Adding this renewable capacity to the grid is expected to result in the energy mix displayed in Figure 7. An annual increase in electricity consumption of 1 % is assumed, resulting in an electricity demand of 890 TWh in 2030 (EIA 2019a).

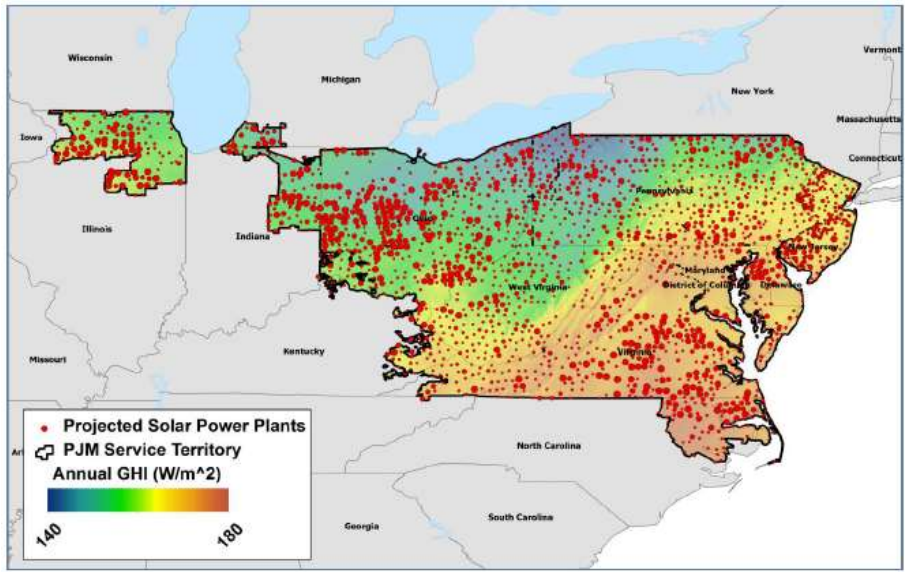


Figure 5: Selected centralized solar power plants PJM (AWS Truepower 2012)

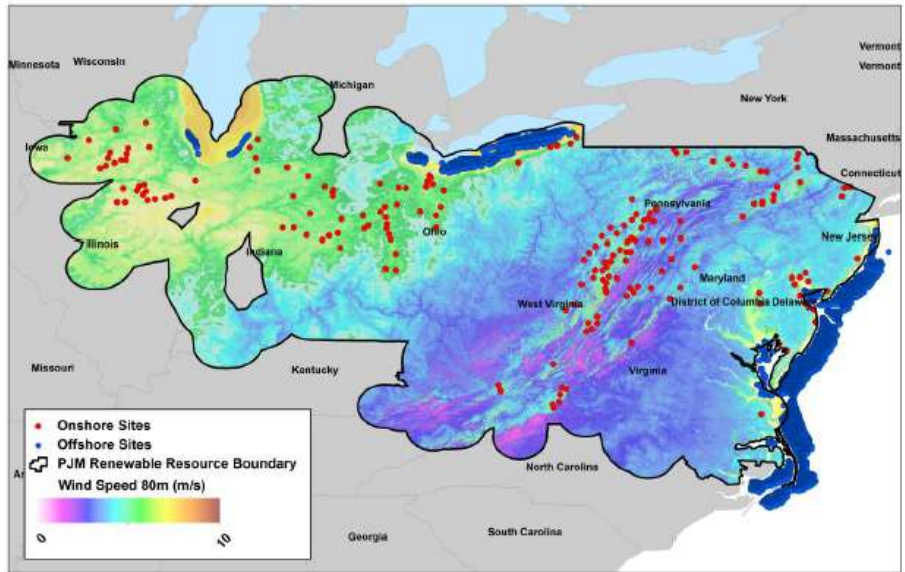


Figure 6: Selected onshore and offshore wind sites PJM (AWS Truepower 2012)

A continuous decline in natural gas prices and the increase of renewable generation will result in lower electricity prices compared to 2018. Additionally, low electricity prices will result in operating losses for coal and nuclear power plants. Therefore, it is assumed that the share of coal and nuclear will decrease by 40 % and 30 % respectively in 2030 (EIA 2019a). The demand for natural gas is expected to increase continuously until 2030 by 7 % in total. Because the overall electricity demand increases as well, the share of natural gas in the electricity mix remains unchanged. The share of solar, wind, and other renewables, such as geothermal and hydro, will increase from 6 % in 2018 to 31 % in 2030. The aforementioned developments result in the electricity generation profile shown in Figure 8. The overall peak generation in

PJM is 190 GW compared to 150 GW in 2018. Additionally, the average peak generation increase caused by wind and solar is 27 GW compared to 3 GW in 2018.

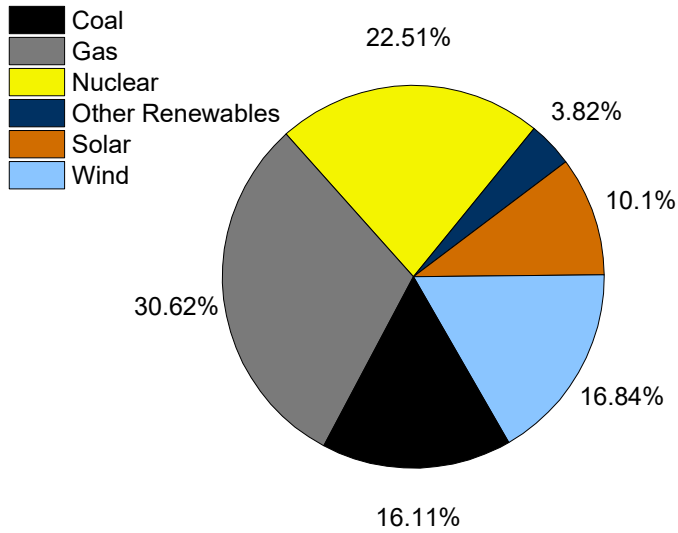


Figure 7: Electricity Mix PJM 2030 (own illustration)

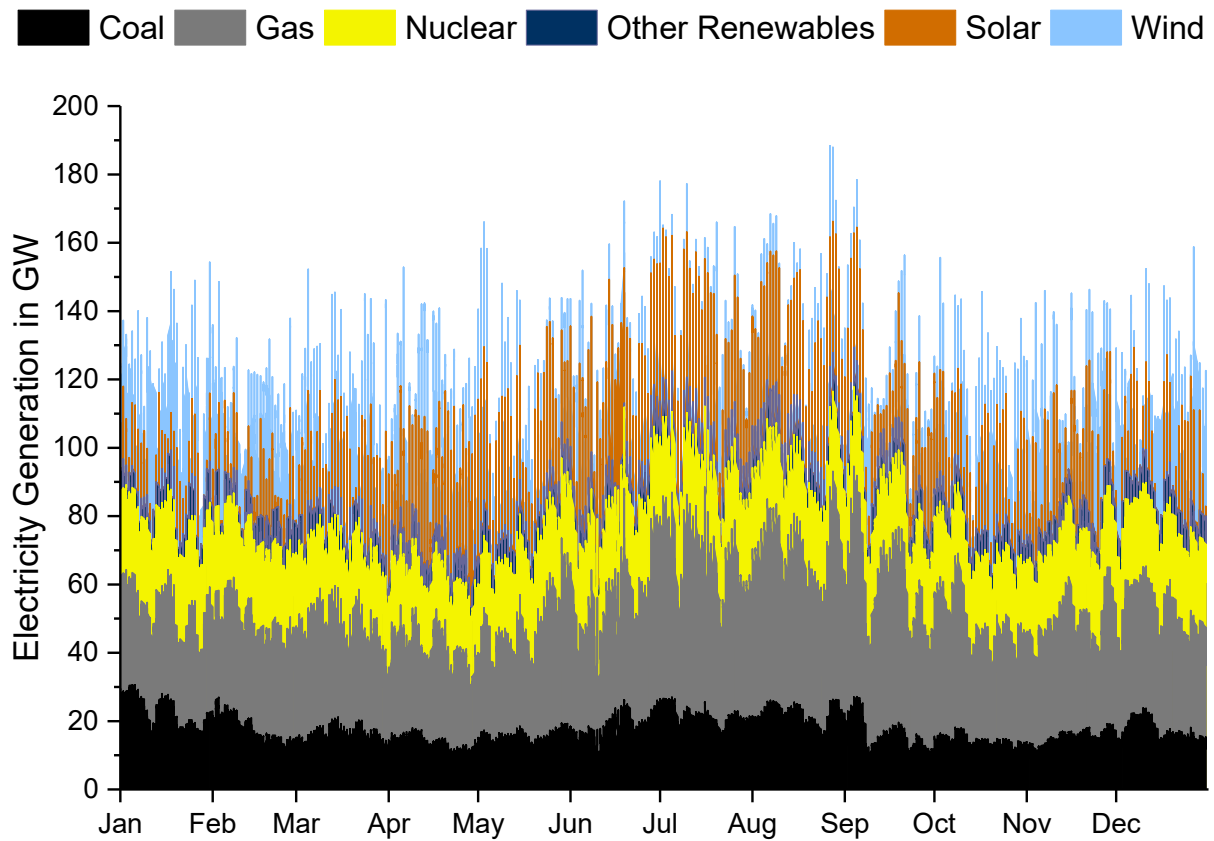


Figure 8: Electricity Generation Profile PJM 2030 (own illustration)

To further increase the renewable electricity generation until 2050 the aforementioned renewable potential of 194 GW wind and 120 GW solar power needs to be utilized. It is

assumed that the electricity demand continues to increase at an annual rate of 1 % to 1152 TWh in 2050 (EIA 2019a). Electricity generation from natural gas is expected to further increase by 10 % compared to 2030. Electricity generation from nuclear and coal are expected to further decrease by 20 %. These changes lead to the energy mix shown in Figure 9 with a total share of renewable generation of 50 %. These changes to the electricity mix result in the generation profile displayed in Figure 10. The overall peak generation in PJM is 250 GW compared to 190 GW in 2030, and the average peak generation increase caused by wind and solar is 60 GW compared to 27 GW in 2030.

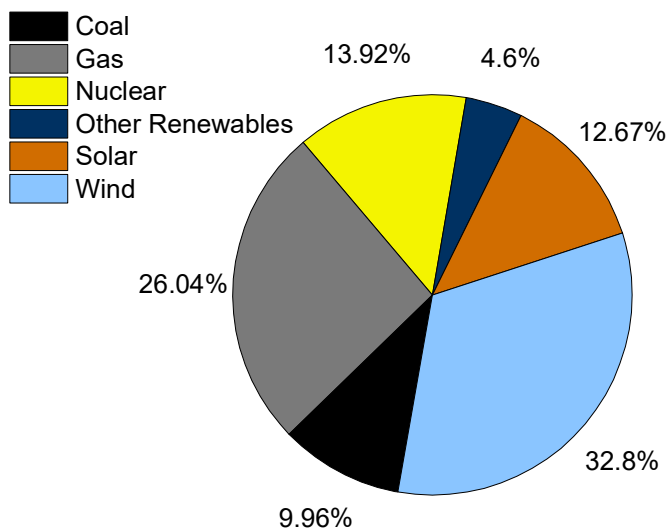


Figure 9: Electricity Mix PJM 2050 (own illustration)

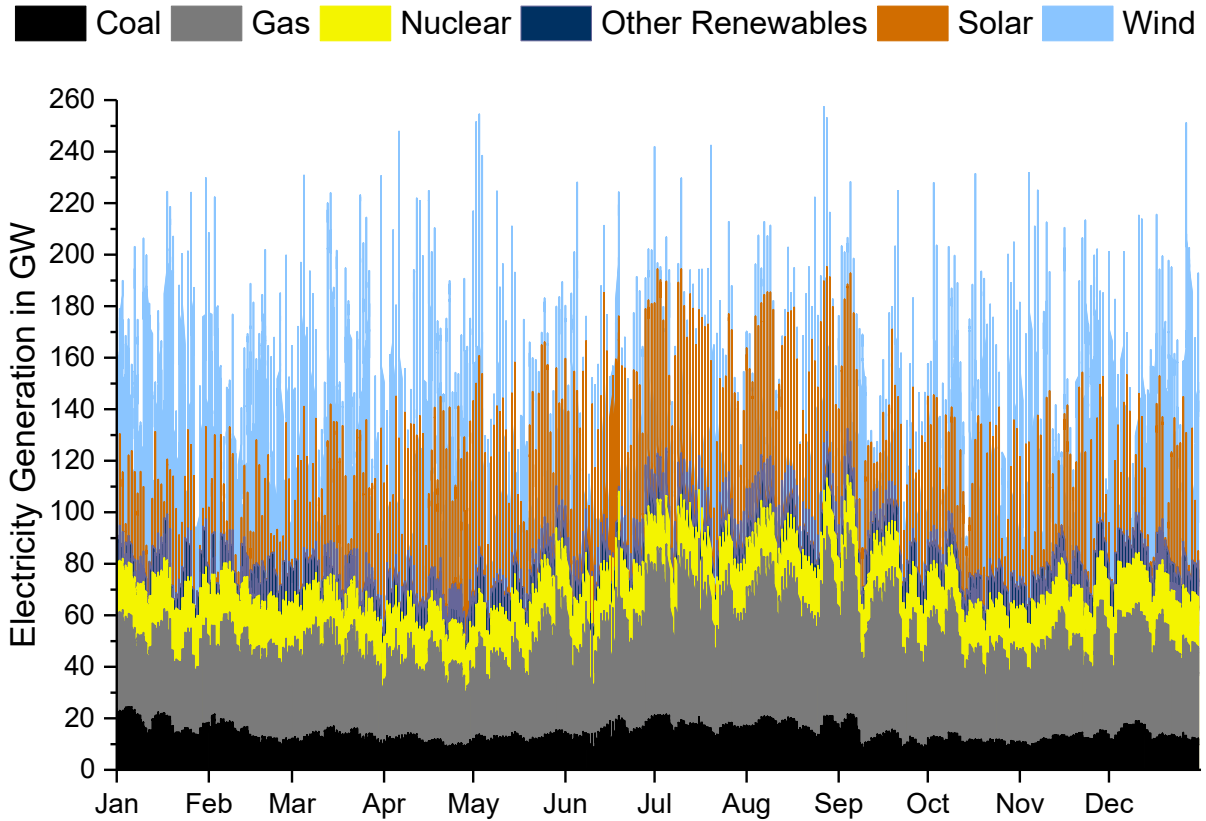


Figure 10: Electricity Generation Profile PJM 2050 (own illustration)

## 2.3 Simulation of electricity grid and evaluation of data

The basis for the simulation of the electricity grid is the generation profile of PJM in 2050 shown in Figure 10. As mentioned in 2.2 the electricity generation is assumed to be equivalent to the demand. To simulate DR the profile needs to be scaled down to one single family house (NZERTF) so the difference between generation and demand, the Residual Load, can be calculated.

To do so, the projection starts with the state of residential electricity demand in 2018. The US residential sector's share of the total electricity demand is 39 % in 2018 (EIA 2019b), sixty-three percent of the housing units are single family homes (US Census 2017).

It is assumed that the residential sector's electricity demand increases by 0.4 % annually due to the increased demand for electricity-using appliances, devices, and equipment (EIA 2019a). Furthermore, the population growth rate is 0.58 % per year resulting in an increase from 65 million to 78 million residents in the PJM grid (US Census 2015). This development results in an increase of the share of single-family homes to 65 %. The total number of single-family homes in PJM in 2050 is estimated to be 20.9 million as shown in Table 1.

Table 1: Development of residential sector in PJM (own illustration)

	<b>PJM 2018</b>	<b>PJM 2050</b>	<b>Sources</b>
Electricity Generation	829 TWh	1152 TWh	(PJM 2019b);(EIA 2019a)
Residential sector	319 TWh	383 TWh	(EIA 2019b);(EIA 2019a)
Single family homes	202 TWh	250 TWh	(US Census 2017)
Residents	65,000,000	78,116,152	(PJM 2019a);(US Census 2015)
Residents per household	2.53	2.43	(US Census 2018)
Housing units	25,691,700	32,117,068	
Single family homes	16,232,675	20,947,255	

The NZERTF is considered a house with an electricity demand at the level of a house in 2050 because all systems and appliances use electrical energy and because its energy usage is beyond that of current code-built homes. Therefore, the electricity demand of the NZERTF is not scaled up by 0.7 % annually like the residential sector.

## 3 Background

### 3.1 Demand Response

Demand Response refers to strategies that can be used in competitive electricity markets to increase the participation of the demand-side, or end-use customers (IEA 2003). When customers are exposed to real-time prices, they can respond in different ways:

- Shift the time of day at which they demand power from the grid to an off-peak period
- Reduce their peak load through energy efficiency measures or self-generation
- Not respond and pay the market price

If the customer reacts in one of the first two approaches, the demand profile in the market is smoothed, which reduces peaks and thus eases system constraints and generates security and economic benefits for the market.

This paper focuses on DR in residential buildings, specifically detached single-family houses. The utilization of several smaller systems for DR has advantages such as higher reliability and spatial distribution, which allows for addressing local bottlenecks in the grid infrastructure (IEEE 2013). While the DR capability per participating unit is low compared to systems with higher power capacity such as commercial buildings, the large number of single-family homes provide an aggregated opportunity for demand reduction on the grid. To create an economically viable way of utilizing DR, however, costs need to be reduced so they do not outweigh the benefits. A major cost factor will be the measurement and communication infrastructure. Partially substituting measurements through estimations and decentralizing the control system can help to bring down costs.

Another major concern regarding DR is privacy and data security. Advanced metering infrastructure (AMI) and programmable communicating thermostats (PCTs) have been key

components of DR approaches that connect homes directly to the power system (Callaway 2009). Measurements taken and communicated via this infrastructure introduce privacy and data security concerns. These privacy concerns are partially mitigated by the fact that is nearly impossible to track the state of every TCL in the power system at any given point in time. Estimation algorithms are used to determine the probability of TCLs being in a certain state, therefore making it nearly impossible to gain information about a specific household.

An important factor for measuring the efficiency of DR is the Residual Load. There are multiple ways of defining Residual Load in the literature. Residual Load can be defined as the difference between actual power demand and the feed-in of non-dispatchable and inflexible generators (Schill 2013). The behavior (ramp rates, partial load efficiencies, etc.) of fossil power plants in 2050 is not predicted in this paper because the complexity of modelling the interrelationship between the demand and supply side exceeds the scope of this paper. Fossil fuel power plants (incl. nuclear) are assumed to provide base load and are treated as inflexible. This approach simplifies the system behavior but leaves PV and wind as main contributors to the fluctuating power generation. Therefore, Residual Load is calculated by subtracting the whole generation profile from the hourly demand data. In this work, the average load over an hour is considered. The mean hourly Residual Loads are then sorted in descending order to derive load-duration curves as used in the results section.

### 3.2 IEA EBC Annex 67

The electricity demand in the future energy system is expected to increase continuously due to the transition from fossil fuels to renewable energy sources (RES), electric cars and heat pumps (IEA 2017). Flexible energy systems are an essential part of the solution to overcome future challenges in balancing the supply of energy to the demand. The IEA EBC Annex 67 explores how energy flexibility in buildings can be achieved and measured. Energy flexibility is defined as follows:

*“Energy Flexibility of a building is the ability to manage its demand and generation according to local climate conditions, user needs and grid requirements. Energy Flexibility of buildings will thus allow for demand side management/load control and thereby demand response based on the requirements of the surrounding grids and on availability of RES ...”* (IEA 2017).

To be able to quantify the amount of energy a building can shift without compromising user comfort, the boundary conditions need to be defined. These conditions can change over time and can be categorized as follows:

**Low frequency factors:** climate change, macro-economic factors, technology improvement, energy costs, use of the building

**High frequency factors:** energy mix/RES availability, energy prices, internal/solar gains, user behavior, hourly energy prices, ambient temperature

All aforementioned factors vary over time. Consequently, energy flexibility is not a constant value but is a function of such forcing factors and control signals (IEA 2017). There are a variety of different factors that can be used as a control signal. The diagram in Figure 11 displays the use of an electricity price signal as control signal. When the electricity price increases, after a delay of  $\tau$ , the electricity demand decreases. The response reaches its maximum  $\Delta$  after the period  $\alpha$ . The response to the price signal lasts for the period  $\beta$ . (A) is the total shifted amount of energy and (B) is the rebound effect of returning the situation back to reference.

In this thesis, the electricity generation from RES is used in combination with a building's load profile to generate a Residual Load signal which is then used as control signal. A negative Residual Load means that there is more energy generated (fluctuating RES) than there is electricity demand.

To bring the Residual Load closer to 0 and consequently reduce the load on the grid the electricity consumption is increased as shown in Figure 12. This approach differs from the method proposed in the IEA EBC Annex 67 where the goal is to decrease consumption and minimize cost. The aim of this thesis is to investigate the DR potential of different building configurations. The magnitude of the response, i.e. the change in electricity demand, is represented by the integrals (A) and (B). The greater these integrals are the higher the DR potential of a specific configuration is because a greater increase in electricity consumption (A) allows for greater savings during the following period (B). Furthermore, the method proposed in this paper utilized a dynamic control signal which is continuously calculated from a load profile and an artificial generation profile. This way the buildings energy flexibility can be tested under more realistic conditions than would be possible with a constant control signal.

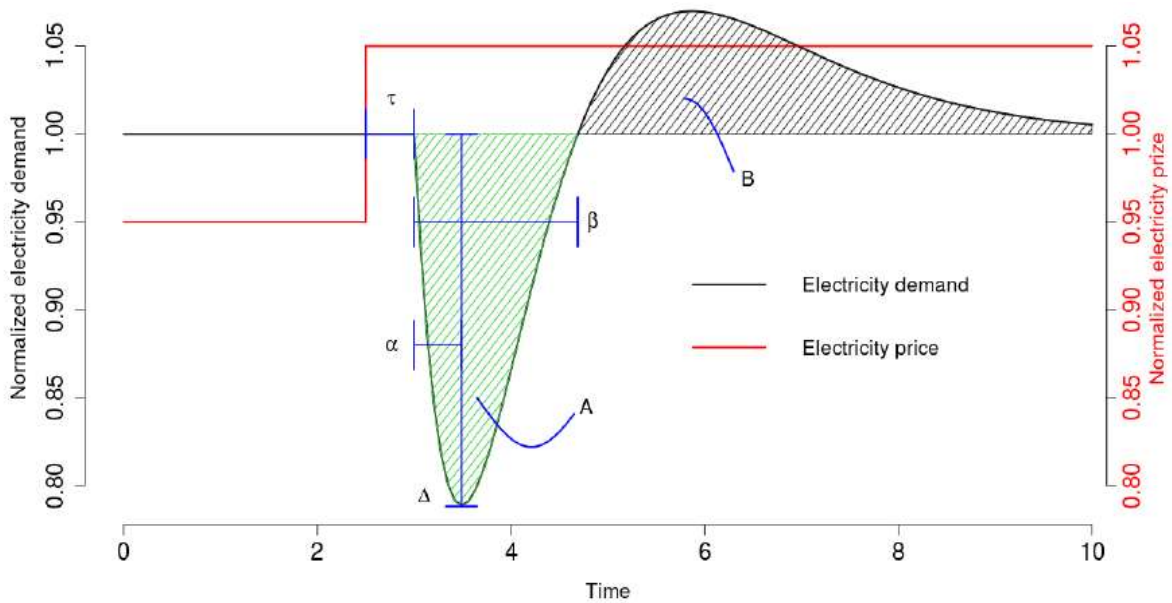


Figure 11: Flexibility function for reduced consumption utilizing a price control signal (IEA 2017)

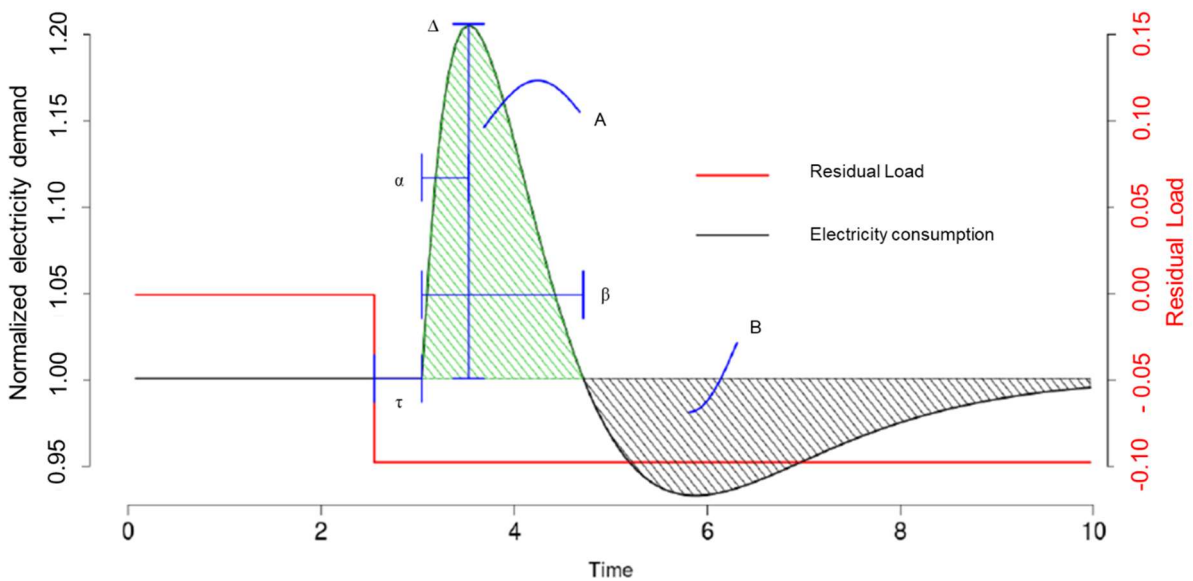


Figure 12: Flexibility function for increased consumption utilizing a Residual Load control signal (IEA 2017, altered)

### 3.3 Thermostatically Controlled Loads

The underlying principle of using TCLs, such as air-conditioners, space heaters, and water heaters, as part of DR is their ability to take advantage of thermal storage capacity within a building (IEEE 2013). Various materials with different heat storage capacities can be used as thermal storage. This paper focuses on the building envelope, water, and PCMs. Careful attention is given to the impact of changing these loads on occupant comfort. For example, when changing the operation of the space conditioning system, temperature deviations that lie

within accepted thresholds for comfort as stated in ASHRAE 55 are assumed to not impact user comfort.

TCLs within a home and across different homes can be synchronized to provide system benefits (IEEE 2013). The aggregated power of multiple heterogeneous loads can be used to respond to an input signal, here being the residual load. To achieve the aforementioned reduction in Residual Loads caused by fluctuating renewable energy generation, the TCLs will track a power system signal by changing temperature set points. In this approach, energy consumption can be temporarily increased or decreased to better match the generation profile.

As an alternative to altering temperature set points, TCLs can also be switched on and off as a response to the grid signal. This comparably simple control strategy is unlikely to negatively impact user comfort as long as the TCLs keep temperature levels within their respective dead bands.

To provide meaningful services to the electricity grid, a large number of TCLs need to be aggregated. A successful synchronization of TCLs provides reliability and flexibility concerning services for the power system. Multiple decentralized loads are more resistant to disruptions than a single load. Furthermore, the spatial distribution of a great number of TCLs can be utilized to address local bottlenecks.

TCLs in residential buildings have simpler dynamics than systems in commercial buildings. Nevertheless, the wide range of TCLs that need to be coordinated while still maintaining individual user comfort makes the development of a suitable control strategy and adequate load models a necessity.

### **3.4 Phase Change Materials**

Phase Change Materials (PCMs) can be used for thermal energy storage (TES) (Pomianowski et al. 2013). TES is a key aspect of peak shifting of electricity consumption of HVAC equipment but can also enhance thermal comfort if designed appropriately. TES can be divided into sensible and latent heat storage. Thermal energy can be stored as sensible heat by varying the temperature of the storage material (Li 2015). Specific heat, density, and thermal conductivity are the main thermal properties of sensible heat storage materials. Ordinary building materials, such as concrete and gypsum, have a sensible TES capacity between 0.75 kJ/kgK and 1 kJ/kgK. The usual temperature levels in buildings are the limiting factor for the TES capacity of materials because of the direct dependency between stored energy and temperature as shown in Figure 13.

The diagram also shows the possibility of latent heat storage where heat is stored or removed during the phase transition of a PCM. The PCM material is absorbing sensible heat up to the

point of its phase transition temperature. At this point additional heat is used to break chemical bonds within the material. This process is energy intensive and a great amount of energy, compared to sensible energy, can be stored as so-called latent energy. The main advantage of PCMs for thermal storage applications is that their phase transition temperature can be at room temperature level. Even small temperature changes cause the PCM to constantly store or release heat and keep the room temperature at a comfortable level.

Organic compounds, inorganic compounds and eutectics are the 3 different classifications of PCMs. This paper focuses on the organic compound paraffin wax because it has high specific heat of fusion and is a predictable and relatively inexpensive material compared to other PCMs. The heat of fusion of paraffin PCMs is approximately  $230 \pm 30 \text{ kJ}\cdot\text{kg}^{-1}$ .

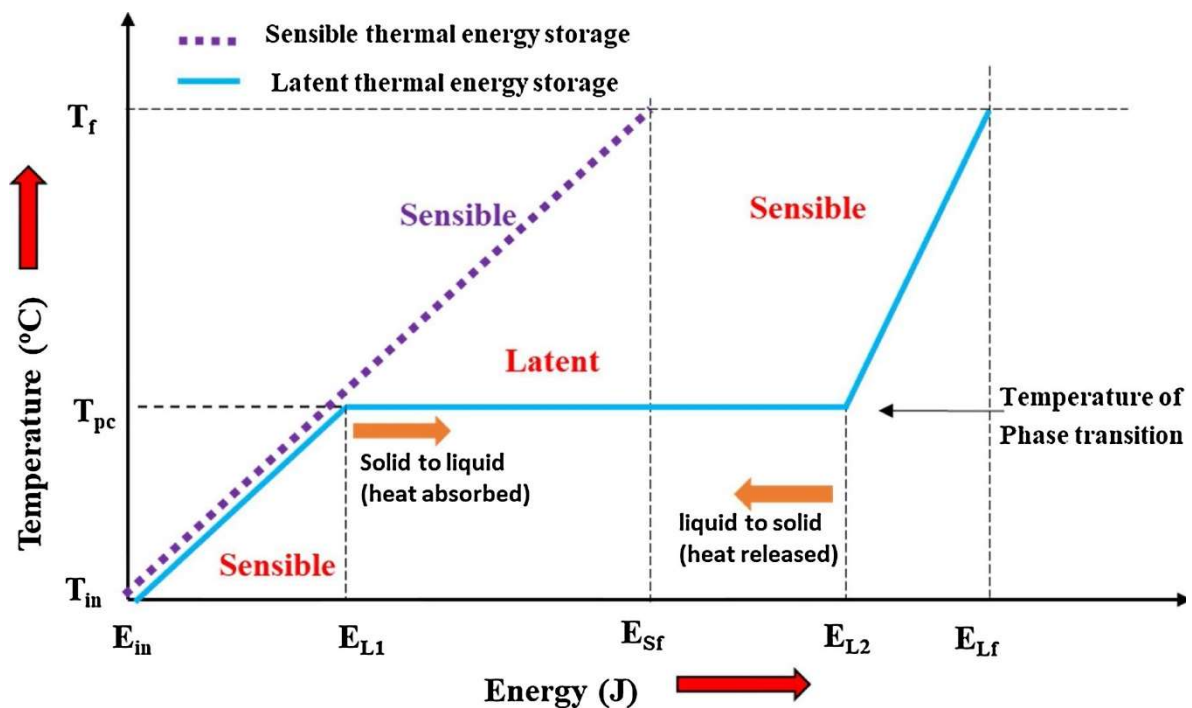


Figure 13: Phase transition profile of phase change material (Reddy et al. 2017)

Additionally, paraffin wax is non-reactive and compatible with conventional construction material which makes it the ideal material for increasing thermal storage mass. A common method to implement paraffin wax into building components is to coat the PCM with an encapsulation material (metallic, inorganic, or plastic) (Reddy et al. 2017). With this method, the PCM is isolated from the construction material and no chemical reaction between the materials can occur. Additionally, the surface area is increased which results in a greater heat transfer rate. Figure 14 shows the cross-section of a spherical encapsulation container. The container can also be shaped rectangular, cylindrical, or tubular. These PCM capsules can then be integrated into building materials.

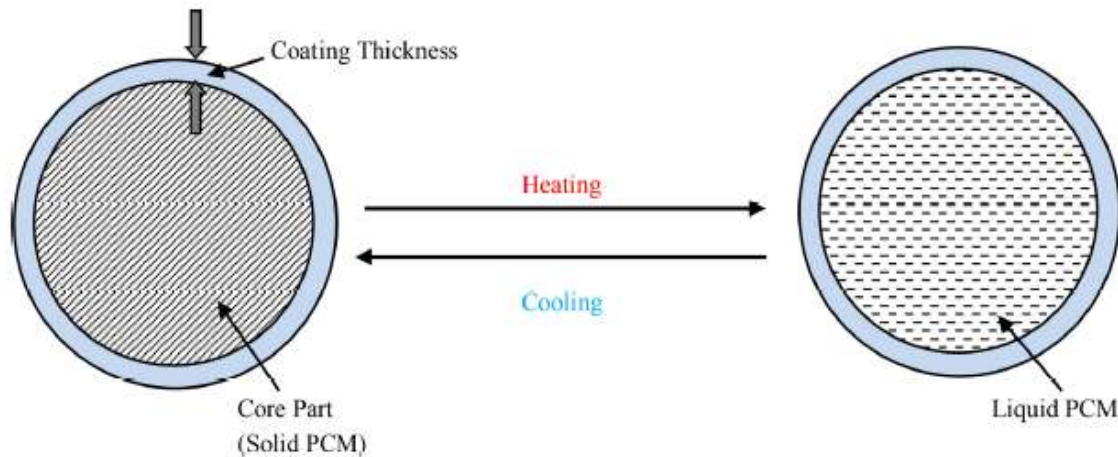


Figure 14: Working principle and structure of encapsulated PCM (Reddy et al. 2017)

A common problem of organic phase change material, and PCMs in general, is its low heat transfer rate (Reddy et al. 2017). Poor heat exchange between the PCM and the surrounding heat transfer material can lead to incomplete freezing and solidification of the PCM which, in turn, increases the charging and discharging time of the PCM. It is possible that the charging and discharging cycles could be too long for building applications (e.g. increasing thermal storage mass) if the cycle of charging and discharging cannot be completed in one day and night cycle. A possible way to increase heat transfer is to utilize micro-encapsulation (size < 1 mm) to increase the PCM's surface area and heat transfer rate. There are also approaches that utilize nanomaterial to increase PCM's heat conductivity.

PCMs can also be used as active construction materials (Pomianowski et al. 2013). One such approach would be to insert capillary tubes in gypsum boards containing PCMs. Warm or cold from a heat pump is circulated through these tubes. In combination with metal fins to improve thermal conductivity, this system can handle loads of up to 40 W/m<sup>2</sup>K. Another possible application is to incorporate PCMs into radiant floor heating panels. In this configuration, the PCM passively reduces peak temperatures when the heat pump is turned off. Switching on the heat pump provides the aforementioned benefit of higher heat transfer rates

### 3.5 Thermal Comfort

“Thermal comfort is that condition of mind that expresses satisfaction with the thermal environment” (ASHRAE 2013). It is difficult to satisfy every single person because of people’s physiological and psychological differences. There are several environmental factors that contribute to comfort and each of them can vary with time. These six factors that contribute to thermal comfort are:

- a. Metabolic rate
- b. Clothing insulation
- c. Air temperature
- d. Radiant temperature
- e. Air speed
- f. Humidity

Physical activity and the resulting heat emissions are described with a Metabolic Rate. Metabolic rates for various tasks are shown in Table 2. Typical activities in a single-family home have Metabolic Rates between 0.7 and 2. Intensive house cleaning can result in a metabolic rate of up to 3.4.

To get an absolute value for heat emission the skin area of an average adult (DuBois area = 1.8 m<sup>2</sup>) is used (ASHRAE 2013). A Metabolic Rate of 1 is equal to a total heat emission of around 110 W.

Table 2: Metabolic Rates for Typical Tasks (ASHRAE 2013)

Activity	Metabolic Rate	
	Met Units	W/m <sup>2</sup>
Sleeping	0.7	40
Seated	1	60
Standing	1.2	70
Walking about	1.7	100
Cooking	1.6-2.0	95-115
House Cleaning	2.0-3.4	115-200

Apart from the Metabolic Rate the amount of thermal insulation worn by a person has a significant impact on thermal comfort (ASHRAE 2013). Clothing insulation is expressed as “clo” value. Different clothing combinations are displayed in Table 3. The extent to which people adapt their clothing factor to outdoor conditions usually lies between 0.45 and 1 as shown in Figure 15.

Table 3: Clothing Insulation Values for Typical Ensembles (ASHRAE 2013)

Clothing	$I_{cl}$ (clo)
None	0
Shorts, short-sleeve shirt	0.36
Knee-length skirt, short-sleeve shirt	0.54
Trousers, short-sleeve shirt	0.57
Trousers, long-sleeve shirt	0.61
Sweat pants, long-sleeve sweatshirt	0.74
Trouser, suit jacket	0.96
Trouser, long-sleeve sweater, T-shirt	1.01
Thick winter indoor clothing	1.25

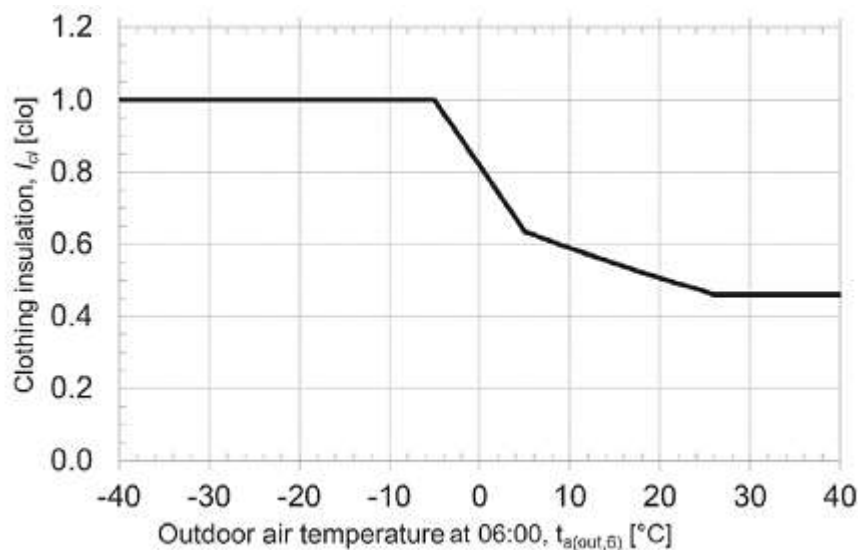


Figure 15: Clothing insulation as a function of outdoor temperature (ASHRAE 2013)

The operative temperature ( $t_o$ ) combines air temperature ( $t_a$ ) and mean radiant temperature (MRT) into one numerical value. For representative occupants with metabolic rates between 1.0 and 1.3, air speeds under 0.2 m/s, and a difference between MRT and  $t_a$  less than 4 °C, the operative temperature can be calculated as the mean of MRT and  $t_a$  (ASHRAE 2013). The comfortable range of the operative temperature can be expanded by adjusting the clothing factor.

Figure 16 shows that at a lower  $t_o$  people have a higher tolerance for relative humidity than at a higher  $t_o$ . There are no established lower humidity limits for thermal comfort. ASHRAE 55 does not cover non-thermal comfort factors, such as dryness of skin and eyes.

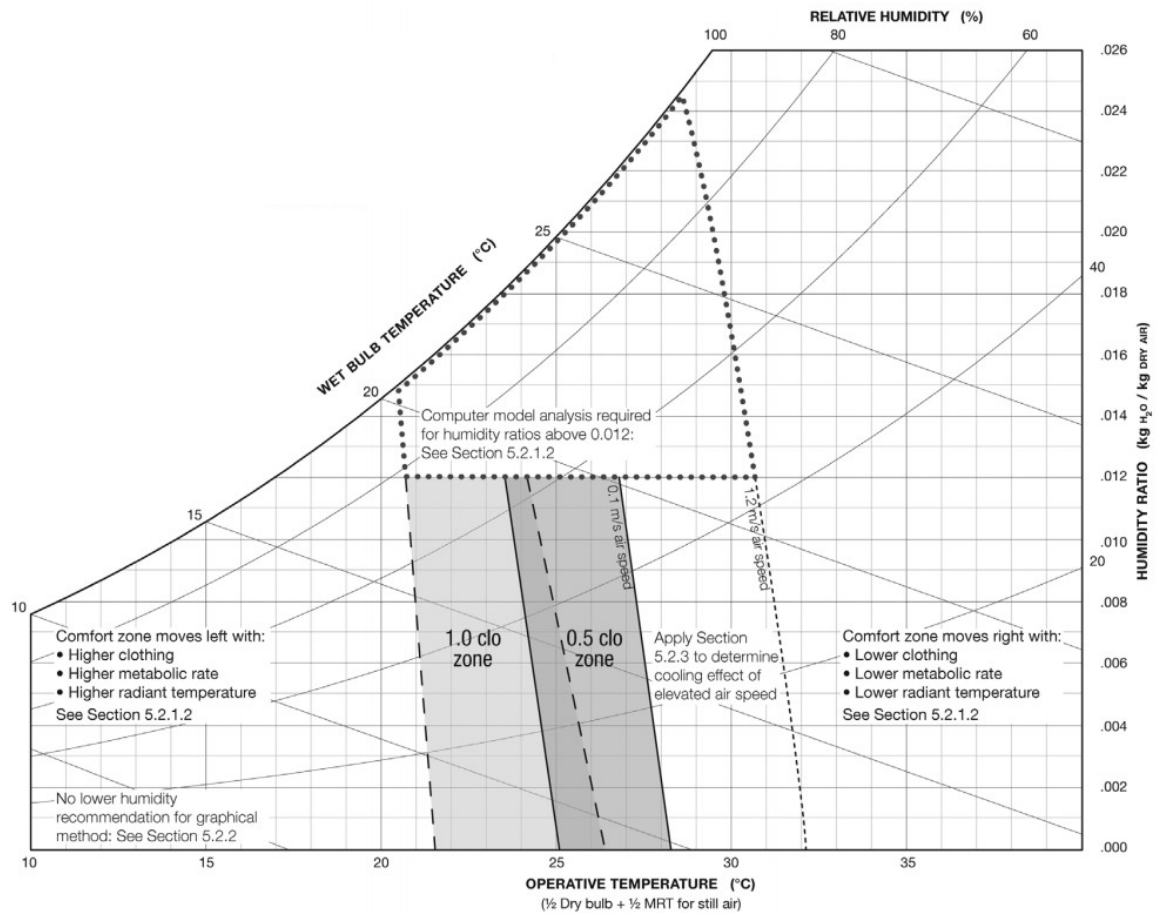


Figure 16: Acceptable range of operative temperature and humidity (ASHRAE 2013)

Thermal comfort can be quantified by using the numerical values PMV (predicted mean vote) and PPD (predicted percentage of dissatisfied). PMV is an index that predicts the mean value of the thermal sensation of a large group of people. PMV depends on all 6 parameters mentioned at the beginning of this chapter and is evaluated using following sensation scale:

- 3 Hot
- 2 Warm
- 1 Slightly warm
- 0 Neutral
- 1 Slightly cool
- 2 Cool
- 3 Cold

The PPD is directly related to the PMV and predicts, under the assumption that the PPD is symmetric around a neutral PMV, what percentage of people is thermally dissatisfied. The relation between PPD and PMV is displayed in Figure 17. It is notable that the PPD cannot be lower than 5 % because even at neutral thermal conditions at least 5 % of people are dissatisfied. The acceptable thermal environment for general comfort is defined as follows:

PPD	PMV Range
< 10	-0.5 < PMV < 0.5

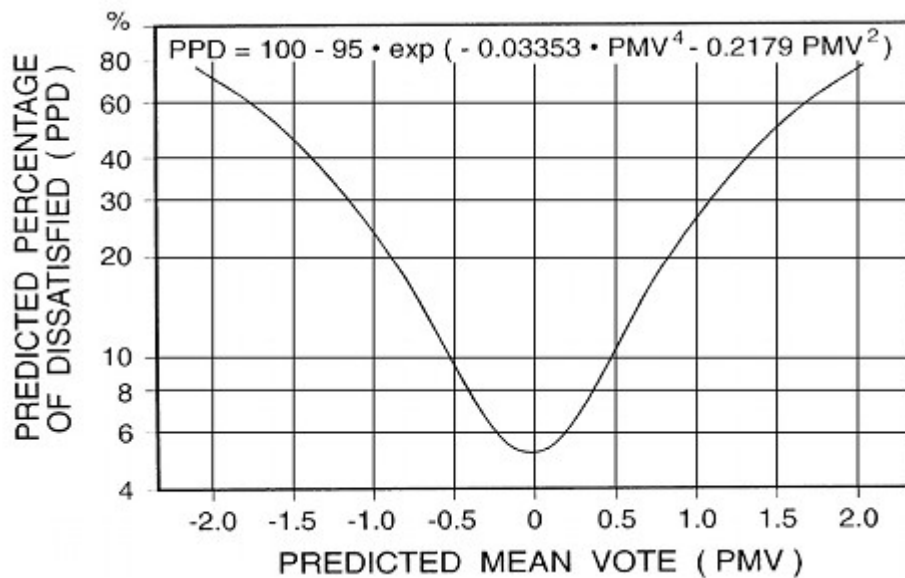


Figure 17: PPD as a function of PMV (ASHRAE 2013)

Keeping room conditions within the aforementioned thresholds does not guarantee thermal comfort. Spatial variations in the MRT can affect occupant's thermal comfort and cause local discomfort. These variations are especially important for this thesis because the heat distribution system is changed to radiant heating in a number of variants. As shown in Figure 18, a warm ceiling has a negative impact on the PPD compared to a cool ceiling. A warm ceiling that is more than 4 K warmer than the air temperature increases the PPD compared to its 5 % baseline. Variants in this thesis with radiant heating also use radiant cooling. With cool ceilings, a radiant temperature asymmetry of up to 13 K can be tolerated before increasing the PPD above its 5 % baseline. The interior design temperatures used for heating and cooling load calculations shall be a maximum of 22 °C for heating and minimum of 24 °C for cooling (ICC 2016).

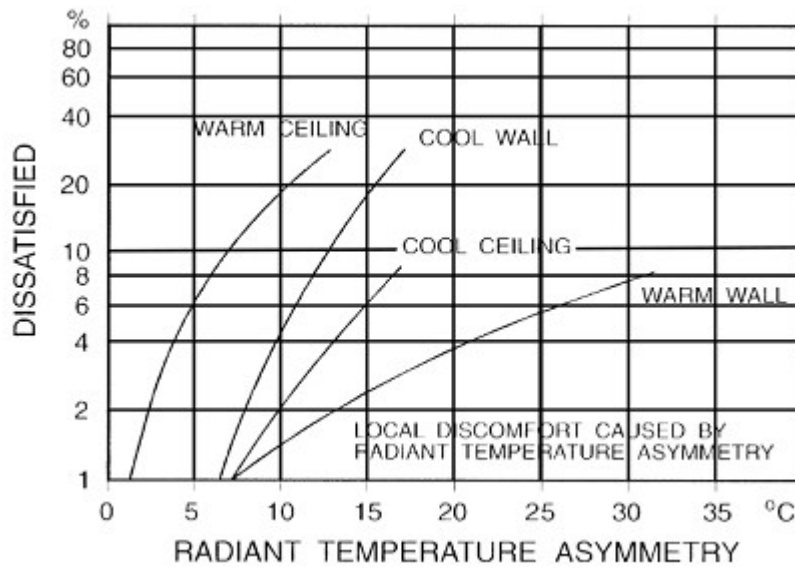


Figure 18: Local thermal discomfort caused by radiant asymmetry (ASHRAE 2013)

## 4 Net-Zero Energy Test Facility NZERTF

Approximately 50 % of newly built single-family houses in the US in 2017 have a floor area between 170 m<sup>2</sup> and 280 m<sup>2</sup> (US Census 2017). The NZERTF has a floor area of 251 m<sup>2</sup> excluding the conditioned basement (Balke 2016). Therefore, the NZERTF is a suitable benchmark for the average building size of single-family houses in the US.

Zone	Floor Area (m <sup>2</sup> )	Volume (m <sup>3</sup> )	Interior Thermal Capacitance [kJ/K]
Zone 1 (Basement)	142	432	4299
Zone 2 (First Floor)	142	447	4317
Zone 3 (Second Floor)	114	360	3467
Zone 4 (Attic)	114	122	147

Figure 19: NZERTF Zones (Balke 2016)

The building envelope, including the unconditioned garage, is shown in Figure 20 and Figure 21. The basement is an open space containing the building's mechanical and electrical equipment.

The Kitchen, living room, dining room, office and a bathroom are on the main floor as shown in Figure 22. There are two bathrooms and three bedrooms on the second floor as shown in Figure 23. The unconditioned attic is inside the thermal envelope.



Figure 20: NZERTF south view



Figure 21: NZERTF north view

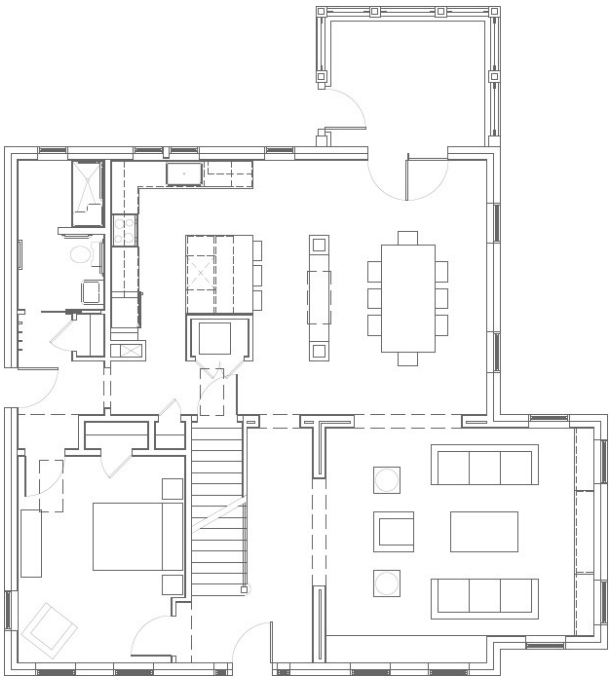


Figure 22: NZERTF 1st Floor (NIST)

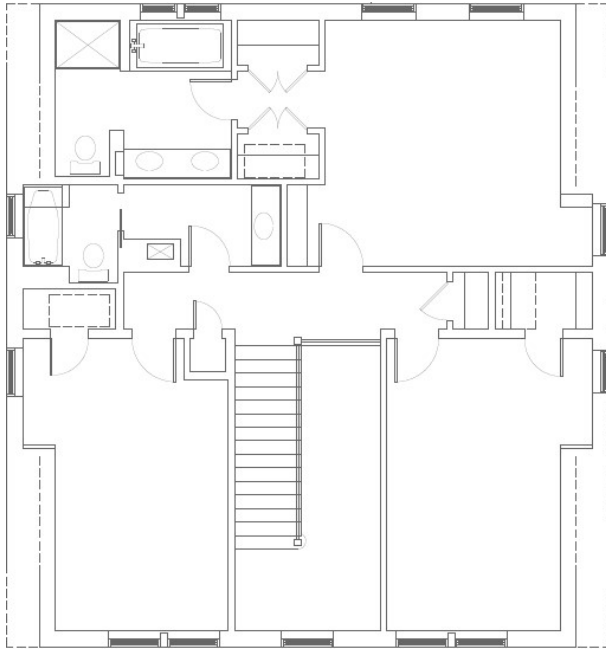


Figure 23: NZERTF 2nd Floor (NIST)

## 4.1 Climate and building code

The NZERTF is situated in Montgomery County, Maryland. Maryland is marked in blue in Figure 24. Montgomery County's international climate zone definition is 4A (ICC 2016). The climate is mixed-humid with the following thermal criteria: cooling degree days with a basis of 10 °C (CDD10°C) ≤ 2500 degree-days and heating degree days with a basis of 18 °C (HDD18°C) ≤ 3000 degree-days. This relative balance of CDD and HDD means that buildings in this climate zone need to be flexible enough to accommodate seasonal changes in temperature as well as peak heating and cooling loads.

The climate diagram in Figure 25 displays average monthly temperatures and precipitation from 2010 to 2017. One of the closest weather stations to the NZERTF is at Dulles International Airport. The weather station's location is 38°57"N, 77°27"Q (NOAA 2017). The average solar radiation in Maryland from 1961 to 1990 is 1480 kWh/m<sup>2</sup> (NREL 1990).

In the main energy code in place in the US, the International Energy Conservation Code, the requirements concerning a building's thermal envelope are dependent on the climate zone. The insulation and fenestration requirements by component are displayed in Table 4. The values displayed have been converted as follows:  $1 \frac{BTU}{h \cdot ft^2 \cdot ^\circ F} = 5.678 \frac{W}{m^2 \cdot K}$

Furthermore, the maximum Solar Heat Gain Coefficient (SHGC) for windows in climate zone 4 is 0.4.

Table 4: Minimum requirement for U-Values by the IECC in W/m<sup>2</sup>K (ICC 2016)

Fenestration	Roof	Frame Wall	Mass Wall	Basement Floor	Basement Wall
2.00	0.15	0.34	0.56	0.57	0.34

### Energy Rating Index (ERI)

In addition to minimum requirements for building components there are also criteria for compliance using an Energy Rating Index (ERI). A building that meets the requirements of the 2006 International Energy Conservation Code has an ERI of 100. A building that uses no net purchased energy has an ERI of 0. A building that is a net exporter to the grid can have a negative ERI.

The ERI necessary for compliance in climate zone 4 is 54. That value means that a residential building must use at least 46 % less total energy than the reference building from 2006.

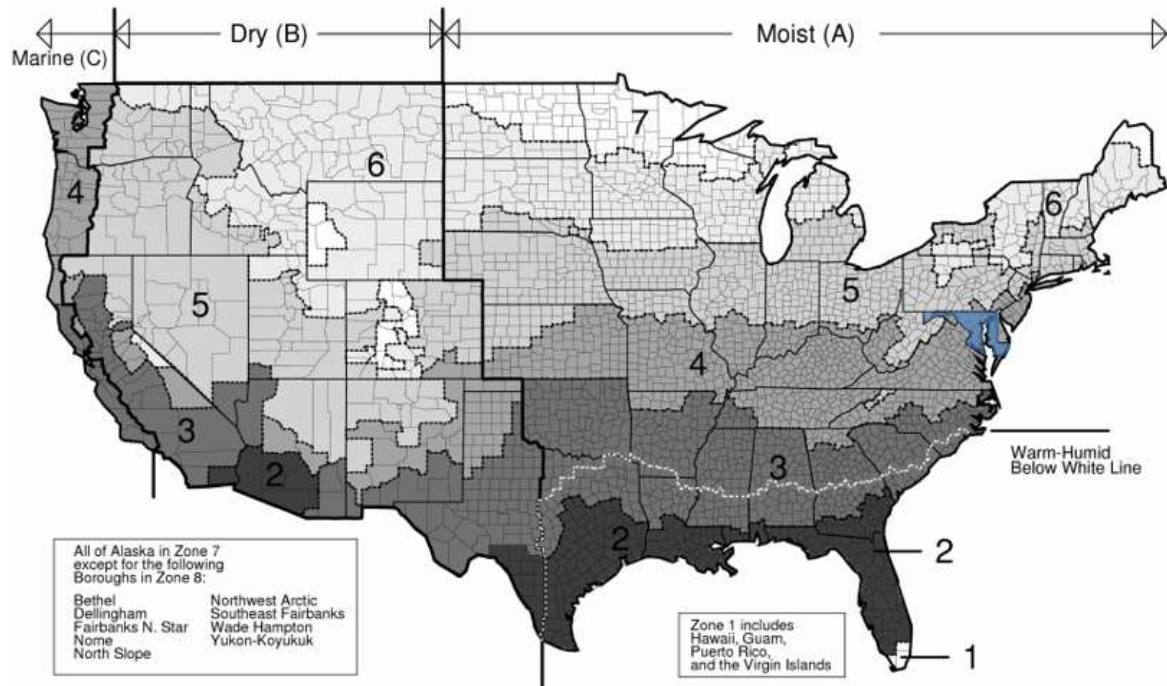


Figure 24: Climate Zones US (ICC 2016)

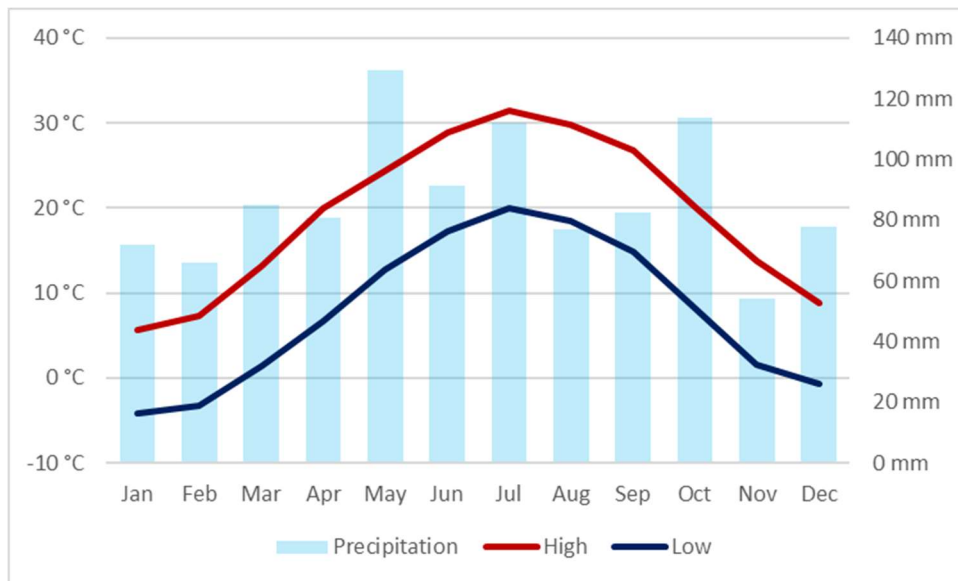


Figure 25: Climate diagram Washington Dulles (2010-2017) (NOAA 2017)

## 4.2 Building components and Key figures

This chapter includes all building components used in the Base Variant of the NZERTF (Table 5 through Table 10) as well as the modified building components that represent a typical massive construction (Table 11 through Table 14).

The lightweight roof and outer wall are built as a wooden frame construction. Cellulose fibers are blown into the gaps between the wooden studs as insulation material. Additionally, Polyisocyanurate (PIR) panels are applied exterior to the sheathing to further reduce the u-values and minimize thermal bridging. The gypsum wall board is the only layer of both building components that contributes to thermal capacitance because it is the only layer inside of the first insulation layer. Wooden studs and roof rafters do not account for more than 15 % of the insulation layer's volume. Therefore, the whole layer is assumed to be an insulation layer. The windows have double glazing with a u-value of 1.16 W/m<sup>2</sup>K and a solar transmission coefficient (g-value) of 0.27. This low g-value is attributed to low emissivity glass which is necessary to minimize solar gains and consequently cooling loads during summer. The window's total u-value is 1.40 W/m<sup>2</sup>K.

Table 5: NZERTF Lightweight Roof (IBO 2019)

O	1	Asphalt Shingles	0.20 cm
	2	Plywood Sheathing with H-Clips	1.60 cm
	3	Foil-Faced Polyisocyanurate	4.00 cm
	4	Foil-Faced Polyisocyanurate	5.00 cm
	5	Foil-Faced Polyisocyanurate	4.00 cm
	6	Air Barrier Membrane	0.02 cm
	7	Plywood Sheathing	1.25 cm
	8	Roof Rafters with Cellulose Insulation	30.00 cm
I	9	Gypsum Wall Board	1.25 cm
			U-Value 0.093 W/m <sup>2</sup> K
			Mass 64 kg/m <sup>2</sup>
			Capacitance 12 kJ/m <sup>2</sup> K

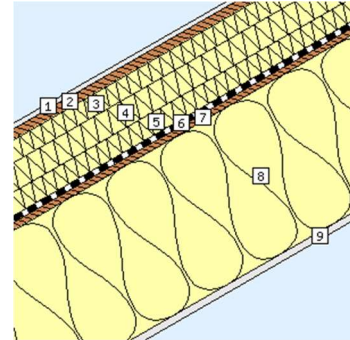
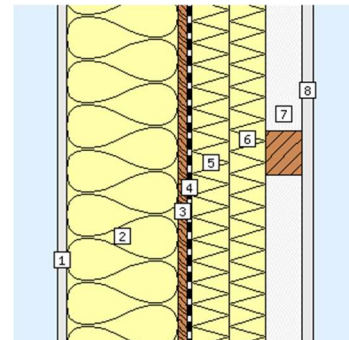


Table 6: NZERTF Lightweight Wall (IBO 2019)

I	1	Gypsum Wall Board	1.25 cm
	2	Wood Stud Wall filled with Cellulose	15.25 cm
	3	Plywood Sheathing	1.25 cm
	4	Air Barrier Membrane	0.02 cm
	5	Foil-Faced Polyisocyanurate	5.00 cm
	6	Foil-Faced Polyisocyanurate	5.00 cm
	7	Wood Furring Strips	5.00 cm
O	8	Fiber Cement Siding	1.50 cm
			U-Value 0.145 W/m <sup>2</sup> K
			Mass 51 kg/m <sup>2</sup>
			Capacitance 12 kJ/m <sup>2</sup> K



The lightweight ceiling as well as the lightweight interior wall have no insulation layer between the wooden studs. The enclosed air layer does not provide any sound proofing and there is little thermal storage mass due to the thin layers of wood and gypsum. The basement wall and floor are made of concrete to provide structural integrity. These building parts are not altered during the course of the calculations because there is no lightweight alternative.

Table 7: NZERTF Lightweight Ceiling (IBO 2019)

T	1	Parquet	1.00	cm	
	2	Floor Sheathing	2.20	cm	
	3	Deep Open Web Wood Joist	35.50	cm	
B	4	Gypsum Wall Board	1.25	cm	
			Mass	47 kg/m <sup>2</sup>	
			Capacitance Ceiling	12 kg/m <sup>2</sup>	
			Capacitance Floor	32 kJ/m <sup>2</sup> K	

Table 8: NZERTF Lightweight Interior Wall (IBO 2019)

I	1	Gypsum Wall Board	1.25	cm	
	2	Wood Studs	10.00	cm	
I	3	Gypsum Wall Board	1.25	cm	
			Mass	27 kg/m <sup>2</sup>	
			Capacitance	12 kg/m <sup>2</sup>	

Table 9: NZERTF Basement Wall (IBO 2019)

I	1	Gypsum Wall Board	1.25	cm	
	2	Foil-Faced Polyisocyanurate	5.00	cm	
	3	XPS Slotted Insulation	5.00	cm	
	4	Reinforced Concrete	25.40	cm	
	5	Dampproofing	0.20	cm	
O	6	Drainage Mat	0.50	cm	
			U-Value	0.306 W/m <sup>2</sup> K	
			Mass	604 kg/m <sup>2</sup>	
			Capacitance	12 kJ/m <sup>2</sup> K	

Table 10: NZERTF Basement Floor (IBO 2019)

I	1	Concrete Slab with Welded Wire Mesh	10.00 cm	
	2	PE Vapor Barrier	0.40 cm	
	3	XPS	5.00 cm	
	4	Stone Pad	10.00 cm	
O	5	Filter Fabric	0.20 cm	
		U-Value	0.566 W/m <sup>2</sup> K	
		Mass	433 kg/m <sup>2</sup>	
		Capacitance	267 kJ/m <sup>2</sup> K	

To properly represent massive construction, the material composition of the roof, exterior wall, interior wall, and ceiling are changed while maintaining the same u-value as their lightweight counterparts. A constant u-value is necessary for obtaining comparable results that are only influenced by the difference in mass and, consequently, thermal capacitance. The thermal capacitance of the concrete roof is on average more than 40 times greater compared to the lightweight construction whereas the thermal capacitance of the brick wall is 22 times greater. The mass per square meter of the concrete roof and brick wall are 10 and 7 times greater, respectively.

Table 11: NZERTF Concrete Roof (IBO 2019)

O	1	Clay roof tiles	2.50 cm	
	2	Battens	3.00 cm	
	3	Counter Battens	5.00 cm	
	4	PE Roofing underlayment	0.02 cm	
	5	Plywood Sheathing	2.40 cm	
	6	Glass Wool between Rafters	6.00 cm	
	7	Glass Wool between Rafters	29.50 cm	
	8	Glass Wool between Rafters	6.00 cm	
	9	Reinforced concrete	18.00 cm	
I	10	Gypsum plaster	0.30 cm	
		U-Value	0.093 W/m <sup>2</sup> K	
		Mass	499 kg/m <sup>2</sup>	
		Capacitance	483 kJ/m <sup>2</sup> K	

Table 12: NZERTF Brick Wall (IBO 2019)

T	1	Lime-cement plaster	1.50 cm	
	2	Vertically perforated brick + Mortar	25.00 cm	
	3	EPS	25.00 cm	
B	4	Silicate Plaster	0.20 cm	
			U-Value	0.145 kg/m <sup>2</sup>
			Mass	347 kg/m <sup>2</sup>
			Capacitance	266 kJ/m <sup>2</sup> K

The concrete ceiling's thermal capacitance is 45 times greater compared to the lightweight ceiling while the mass per square meter is 12 times greater. In variants with radiant floor heating, the pipes are installed near the surface of the cement screed. The footfall sound insulation not only provides sound proofing but also ensures proper heat transfer into the room by preventing heat transfer into the reinforced concrete ceiling.

Table 13: NZERTF Concrete Ceiling (IBO 2019)

I	1	Parquet	1.00 cm	
	2	Cement Screed	6.00 cm	
	3	PE Sealing Membrane	1.25 cm	
	4	EPS	4.00 cm	
	5	Reinforced Concrete	20.00 cm	
O	6	Gypsum plaster	0.30 cm	
			Mass	580 W/m <sup>2</sup> K
			Capacitance Ceiling	537 kg/m <sup>2</sup>
			Capacitance Floor	135 kJ/m <sup>2</sup> K

The interior walls of the building's massive construction variant are built from vertically perforated bricks with lime-cement plaster on both sides. This wall has a 7 times greater mass and a 13 times greater thermal capacitance than its lightweight counterpart.

Table 14: NZERTF Brick interior wall (IBO 2019)

I	1	Lime-cement plaster	1.50 cm	
	2	Vertically Perforated Brick + Mortar	12.00 cm	
I	3	Lime-cement plaster	1.50 cm	
			Mass	198 kg/m <sup>2</sup>
			Capacitance	150 kg/m <sup>2</sup>

For the variants with PCMs the gypsum board on the inside of the lightweight exterior wall and roof are replaced with 2,5 cm thick gypsum board with micro-encapsulated PCM. These PCM gypsum boards are installed on both sides of the lightweight interior wall.

## 4.3 Energy systems

In this section the major systems and subsystems in the NZERTF are described.

### HVAC

The NZERTF has different systems for providing ventilation and space conditioning (Balke 2016). For space conditioning, there are an air source heat pump (ASHP) and a ground source heat pump (GSHP). For ventilation, there are a heat recovery ventilator (HRV) and an energy recovery ventilator (ERV) available. The demonstration of net-zero operation of the NZERTF during its first two years were done using an ASHP in conjunction with an HRV. Therefore, a combination of ASHP/GSHP and HRV is assumed to be implemented in future net-zero buildings and used throughout this paper.

#### Heat Recovery Ventilation (HRV)

The HRV provides 171 m<sup>3</sup>/h of fresh air at the lowest fan speed, which is more than the required 137 m<sup>3</sup>/h specified in ASHRAE Standard 62.2. (Balke 2016). When outdoor temperatures fall below -5 °C the HRV goes into defrost mode every 25 minutes for 7 minutes. The heat exchanger in the HRV cannot be bypassed which makes economizer cooling during summer nights impossible.

It is assumed that economizer cooling provides a potential to reduce cooling energy consumption and will be commonly implemented in most buildings in 2050. Therefore, the HRV in this paper's TRNSYS models includes a "free" cooling option with an economizer to represent future developments in the building sector more accurately.

The HRV cannot be used for demand response because higher fan speeds would cause draft, and lower fan speeds would decrease air quality. Both scenarios have an immediate negative impact on occupant comfort. The HRV contributes 3.3 % to the building's total energy consumption which results in a relatively low potential for DR compared to the 48 % share of the ASHP. Furthermore, an increase in fan speed does not reduce the need for ventilation later in the day because air quality cannot be stored.

#### Air Source Heat Pump (ASHP)

The ASHP used in the NZERTF has 3 heating stages (the third stage is 10 kW resistance heat), 2 cooling stages, and a dehumidification mode (Balke 2016). The ASHP's heating seasonal performance factor (HSPF) is 2.65 W/W and its seasonal energy efficiency ratio is (SEER) is 4.63 W/W. If the cooling mode is not on and the relative humidity is above 50 %, the heat pump switches to dehumidification. The air is cooled down below the dew point by the evaporator and then reheated by the condenser.

The rated heating capacity of the ASHP is 8 kW and the rated cooling capacity is 7 kW. The temperature setpoint in heating mode is 21 °C, and the setpoint in cooling mode is 25 °C.

The ASHP has a high potential for DR. It accounts for nearly half of the NZERTF's annual electricity consumption and changes in setpoint temperature do not have an immediate impact on user comfort. Changes in setpoint temperature can be sustained for longer the greater the building's thermal storage capacity is. This relation between storage mass and setpoint temperature results in a decreased electricity consumption during the time period following DR.

## **Domestic Hot Water (DHW)**

### Solar Hot Water (SHW)

The NZERTF has a solar hot water (SHW) system in place to preheat water going to the heat pump water heater, but the SHW system is not part of any variant in this thesis. It is assumed that photovoltaics will be the predominant source of on-site energy production for residential homes in 2050 (Balke 2016).

### Heat Pump Water Heater (HPWH)

The HPWH is an integrated system that has the heat pump unit mounted on top of the storage tank (Balke 2016). The HPWH tank has a volume of 189 L (50 gallons). The air to water heat pump has a maximum heating capacity of 2025 W. In addition, the HPWH has a resistance heating element with 3800 W heating capacity installed inside the tank. The existing model has a setpoint of 49 °C for the hot water temperature. To improve the HPWH's potential for DR the setpoint can be raised up to 80 °C in the base variant of this thesis. A tempering valve then limits the temperature of the water leaving the water heater to 49 °C to reduce the risk of scalding. Additionally, the capacity of the HPWH tank is increased to 400 L in the base variant of this thesis to compensate for the fact that the SHW system is not included in these simulations. Additionally, this added storage capacity could be beneficial when examining DR possibilities.

The HPWH system has a high potential for DR after making the aforementioned changes. DHW accounts for 14.8 % of the annual electricity consumption. An increased hot water temperature in the storage tank has no impact on user comfort. The user is supplied with the desired water temperature at all times because of the tempering valve. Additionally, the electricity demand for hot water can be reduced in the time period following DR. The potential reduction in electricity consumption depends on the size of the tank and the water temperature.

## **Photovoltaics (PV)**

The use of PV for DR is not within the scope of this paper. The share of PV in the generation mix is accounted for in the generation profile. Therefore, the modules, with a maximum power of 10.24 kW, are not part of the simulation (Balke 2016).

## 4.4 Shading

The current model of the NZERTF does not include automated external window shading. Minimization of solar gains is achieved solely by the low solar transmission of the windows as indicated by their g-value of 0.27 (Balke 2016).

The NZERTF's roof, as shown in Figure 26, includes a canopy construction on the south side of the first floor. The canopy minimizes unwanted solar gains during summer and allows solar gains during winter, due to the shallow inclination-angle of the sun.

In addition to the shading provided by the roof geometry, the building as modeled in this thesis is assumed to have controlled outside shading for each window. The shading is activated if the tilted surface radiation on the window exceeds  $150 \text{ kJ}/(\text{h}\cdot\text{m}^2)$  during the cooling season. The shading factor,  $F_c$ , (1 = no shading, 0 = opaque wall) for outside shading is approximately 0.25 which represents a reduction in total energy transmittance of 75 % (Richarz and Schulz 2013). The changes to the model are made based on the assumption that in 2050 building control systems and building automation will be ubiquitous in residential building. Shading caused by trees and neighboring structures is not considered in the model.

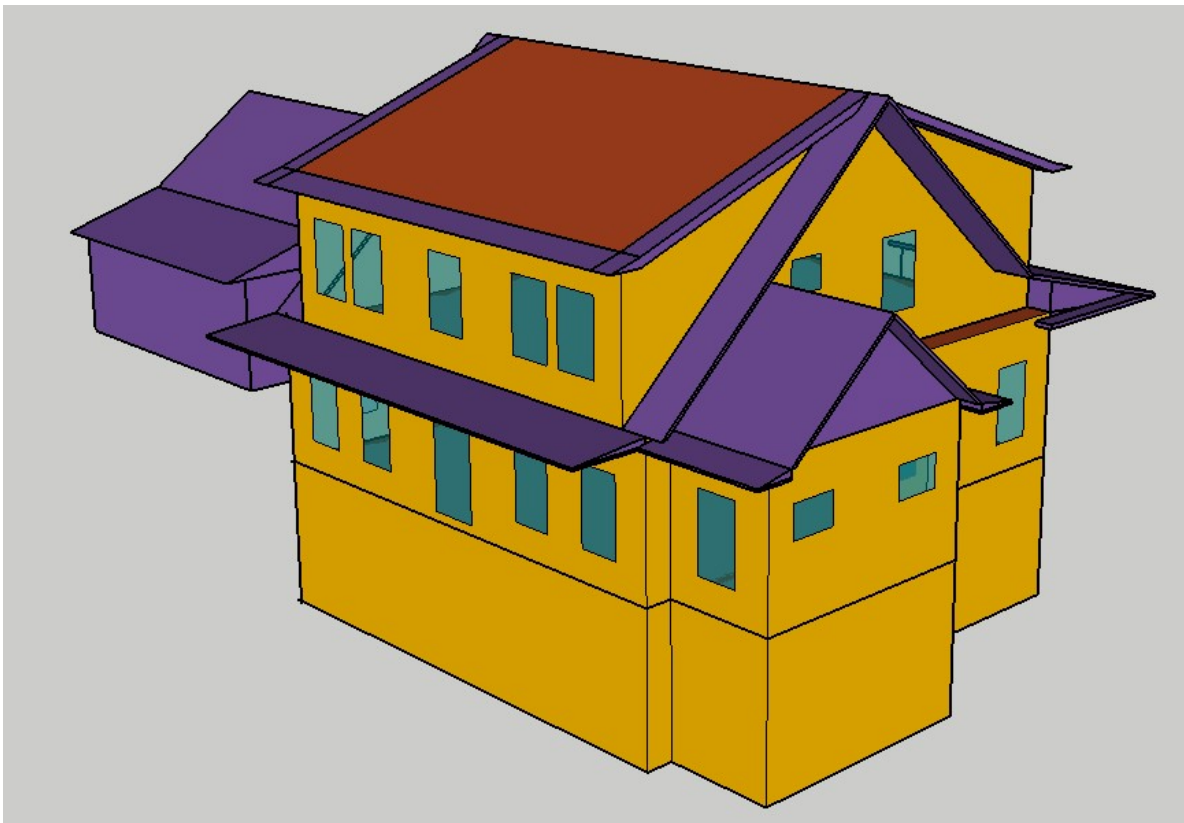


Figure 26: Roof geometry of the NZERTF (own illustration)

## 4.5 Load profiles

Occupant behavior can have a major impact on the energy performance of a house (Omar and Bushby 2013). The occupancy and behavior of a virtual family of four (2 parents, 14-year-old child and 8-year-old child) is simulated based on recommendations developed for the US Department of Energy “Building America” program. The virtual family is simulated by utilizing both hardware (resistance heaters, household appliances, humidifiers, etc.), as shown in Figure 27 and Figure 28, and software (control strategies to simulate occupant behavior).

Utilizing the results of studies and guidelines for energy usage in conjunction with the assumed occupancy schedule, the following loads are specified (Balke 2016):

### Occupancy

Each occupant generates a constant load of 70 W of sensible heat and 45 W of latent heat. The sensible heat is emulated using resistance heaters. The 45 W of latent heat is converted to liters/hour and emulated by humidifiers.

### Water Draw

Five types of water draw events are emulated in the NZERTF. Sink draws, baths, showers, washing machine cycles, and dishwasher cycles result in a total weekly water draw of approximately 2200 liters.

### Lighting

The lighting schedule follows the occupancy schedule. If a room is occupied and there is insufficient daylight, then the lights are turned on. The lights are always turned on in case of a bathroom event. The basement and attic are unoccupied.

### Plug Loads

The plug loads in the NZERTF are assumed to be owned by more than 50 % of US households. Miscellaneous electric plug loads (e.g. TV, Laptop, Vacuum, Microwave, Iron etc.) follow a weekly schedule and are represented by actual devices or latent/sensible heat generators.

### Appliances

All appliances in the NZERTF are located on the first floor. The electricity consumption of the washing machine, clothes dryer, dishwasher, oven, cooktop, refrigerator and microwave are measured.

### Moisture

The moisture generated from cooking and the family’s occupancy is emulated by using ultrasonic humidifiers.



Figure 27: Resistance heaters, sensors for dry air temp, relative humidity and radiant temperature (NIST)

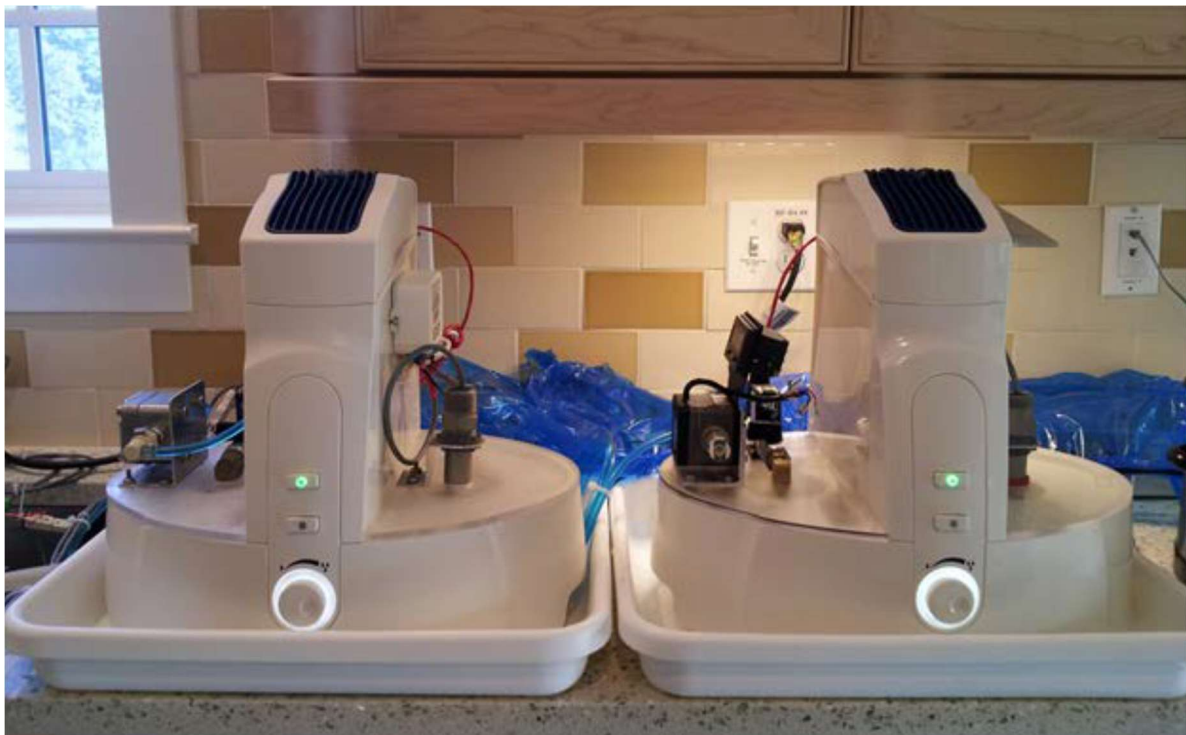


Figure 28: Latent Heat Generators (Ultrasonic humidifiers) (Omar and Bushby 2013)

## 5 Variants

The chart in Figure 29 depicts the hierarchy of all variants simulated with the climate data of Gaithersburg. The variants are categorized by the building envelope style and further subdivided depending on the heat pump technology. Figure 30 shows the comparison of 3 variants in different climates.

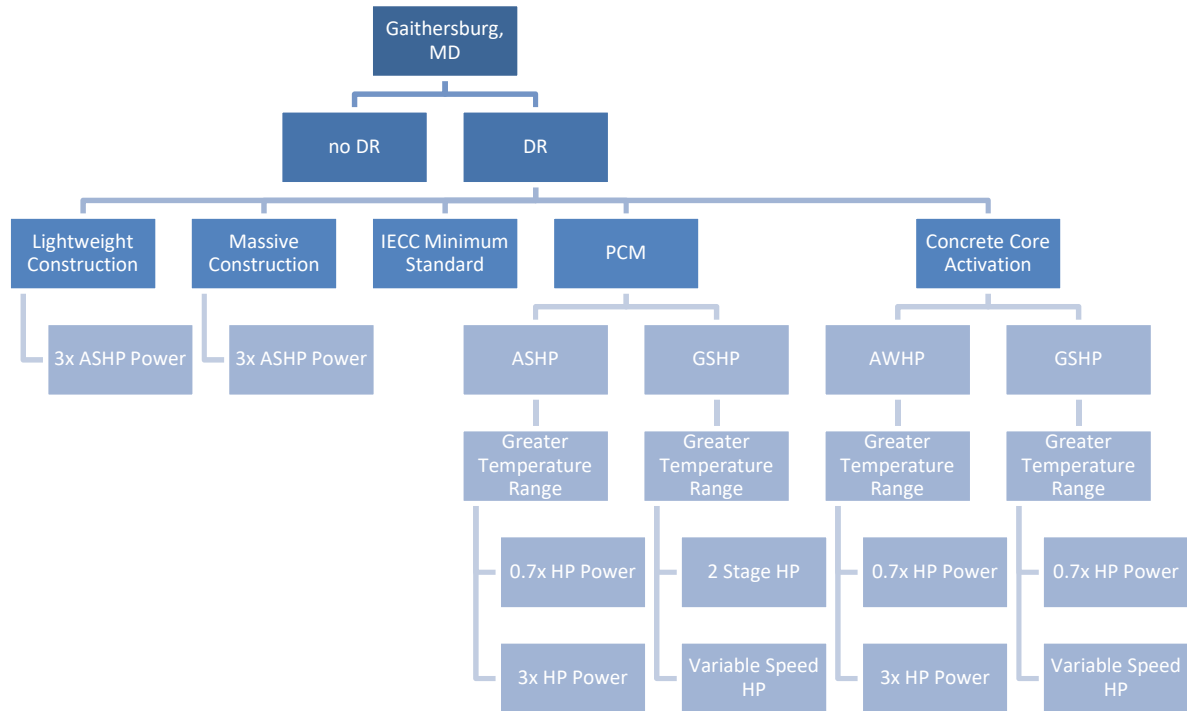


Figure 29: Variants Simulated in Gaithersburg Climate

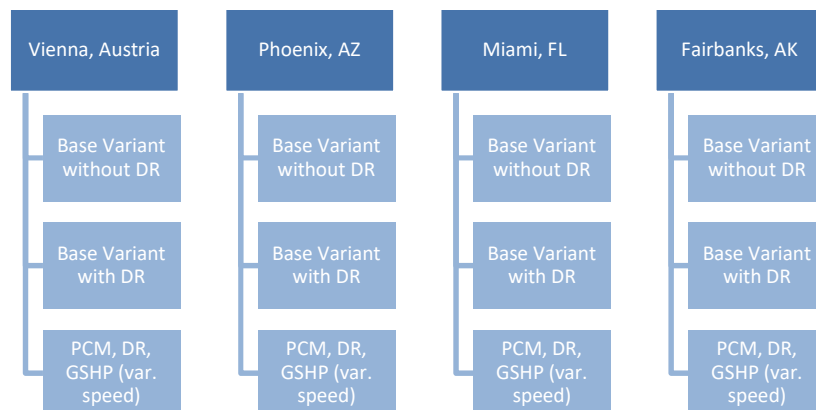


Figure 30: Variants Simulated in Climates of Vienna, Phoenix, Miami, and Fairbanks

## **5.1 Variant 0 - Base Variant without DR**

### **Variant 0**

This variant is the foundation of all subsequent variants. The building envelope is composed of the building components specified in Table 5 to Table 10. The windows are equipped with irradiation controlled outside shading. An ASHP is used for space conditioning including dehumidification. Each stage of the ASHP (heat/cool/dehumidify) has a minimum runtime of 5 minutes. DHW is supplied with a heat pump water heater. The ventilation system is equipped with an HRV. The NZERTF's solar thermal system is not included in the model. A fully electric energy system offers more potential for DR compared to a mixed system with thermal and electric energy. Electricity from photovoltaics is considered in the grid generation. Consequently, no local PV system is modeled. The setpoint temperatures are fixed at 21 °C for space heating, 25 °C for space cooling, and 55 °C for water heating.

## **5.2 Variants 1 and 2 - Base Variant with DR**

### **Variant 1**

This variant is identical to Variant 0 with the addition of a DR control strategy. The control strategy shown in determines the setpoint temperature of the ASHP during heating and cooling mode, as well as the DHW setpoint temperature.

The first stage of the ASHP runs at approximately 70 % maximum capacity. As a result, the power draw cannot be increased by more than 30 %. To prevent the control from overshooting (e.g., heat pump turns on at a small positive Residual Load and causes a greater negative Residual Load) the decision boundary uses a deadband. If the absolute Residual Load is smaller than half of the ASHP's first stage electrical load, the setpoint temperatures are not altered. Otherwise the setpoint temperatures are changed depending on the Residual Load as shown in Figure 31.

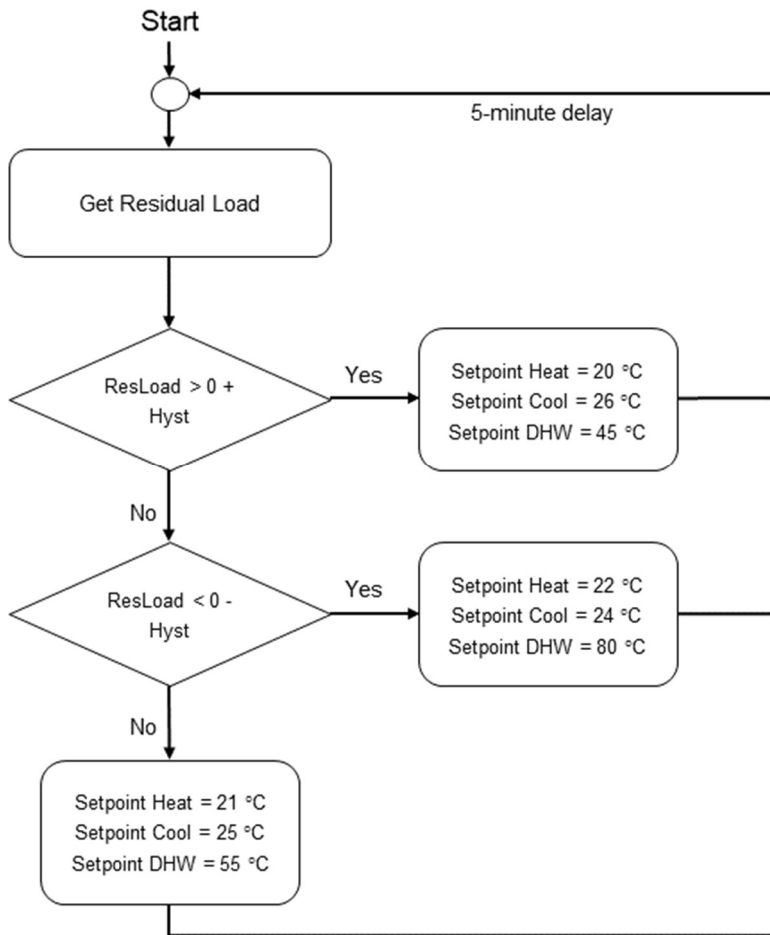


Figure 31: Single-Stage Heat Pump Control

### Variant 2

The power of the ASHP from Variant 1 is increased by 200 %. It is examined how a greater heating/cooling capacity impacts the building's capacity for DR in combination with lightweight construction. Of particular interest is whether the building's thermal capacitance is sufficient to be used for DR while sustaining high levels of thermal comfort.

## 5.3 Variants 3 and 4 - Massive Construction

### Variant 3

The building envelope is changed to massive construction according to the building components in Table 11: NZERTF Concrete Roof (IBO 2019)Table 11 to Table 14. The u-values of the massive building components are identical to the lightweight components, but they differ in thermal capacitance.

It is examined whether the increased thermal storage mass impacts the building's capabilities for DR. Additionally, the effect of thermal inertia, caused by high thermal capacitance, on thermal comfort is investigated.

#### **Variant 4**

The envelope from Variant 3 is maintained, but the power of the ASHP is increased by 200 %. It is examined, how a greater heating/cooling capacity impacts the building's capacity for DR in combination with massive construction. Greater heating/cooling capacity leads to faster temperature changes and can cause discomfort. It is examined if thermal capacitance can counteract this behavior such that a high level of thermal comfort can be maintained.

### **5.4 Variants 5 - IECC Minimum Standard**

#### **Variant 5**

The components of the building envelope are changed so that their u-values comply with the IECC minimum standard as specified in Table 4. It is investigated if an increased energy demand, caused by greater heat losses compared to the Base Variant, impacts the annual Residual Load.

### **5.5 Variants 6 to 9 - Passive PCM with ASHP**

#### **Variant 6**

The inside of the building's exterior lightweight walls is covered by 2.5 cm thick PCM boards with a total surface area of 293 m<sup>2</sup>. The PCM boards are used passively, i.e., no fluid flows through interior tubes. The main type of heat transfer is convection between the interior air and the PCM boards' surface. TRNSYS Type 399 from "Transsolar Energietechnik GmbH" is used to model the PCM.

#### **Variant 7**

Variant 6 is modified by increasing the range of heating setpoints from (20 °C to 22 °C) to (19 °C to 23 °C) and cooling setpoints from (24 °C to 26 °C) to (23 °C to 26 °C). This variant will explore whether larger heating and cooling deadbands impact the potential for DR. Furthermore, it is evaluated if the heat transfer between air and PCM is enough to sustain high levels of thermal comfort given the adjusted temperature band.

#### **Variant 8**

This Variant is identical to Variant 7 except that the heat pump's capacity is decreased by 30 %. It is examined if HP capacities can be decreased in a system with high thermal capacitance while still maintaining thermal comfort.

#### **Variant 9**

This Variant is identical to Variant 7 except that the heat pump's capacity is increased by 200 %. It is assessed if the DR capacity of a building is increased with increasing HP power in combination with high thermal capacitance. Furthermore, it is evaluated if the passive PCM system can be loaded at a faster rate with an increased HP capacity.

## 5.6 Variants 10 to 13 - Active PCM with GSHP

### Variant 10

A single-stage water-to-water GSHP is installed. The geothermal field consists of a borehole heat exchanger with a total length of 150 m. The ground's thermal conductivity is 2.4 W/(m·K). The GSHP is connected to a hydronic system that is run through the PCM boards to create an "active" phase change system. To sustain comfortable relative humidity levels smaller than 60 % during summer, a dehumidifier is used. The building envelope is identical to those used in Variants 5 to 8. It is examined how the greater heat transfer to the PCM, compared to the passive system, impacts the building's DR capabilities.

### Variant 11

The envelope and systems used in Variant 10 are modified to examine how increasing the range of heating setpoints from (20 °C to 22 °C) to (19 °C to 23 °C) and cooling setpoints from (24 °C to 26 °C) to (23 °C to 26 °C) impacts the building's capacity for DR.

### Variant 12

The single-stage GSHP in Variant 11 is exchanged for a 2-stage GSHP. Stage 1 runs at 50 % of the maximum capacity and stage 2 runs at maximum capacity. Each stage has a minimum runtime of 5 minutes. Otherwise the model is identical to Variant 11.

The control strategy for choosing the compressor stage is shown in Figure 32. The control strategy for the temperature setpoints, as displayed in Figure 31, remains unchanged. A 2-stage HP can respond more precisely to a change in Residual Load compared to a single stage HP. To reduce overcompensation for small Residual Loads, stage 1 only turns on if the Residual Load exceeds 25 % of the HP's capacity. To always maintain comfortable air temperatures the control checks if the indoor air temperature is in a range between 20 °C and 26 °C. If the indoor air temperature is outside of this range the control overrules the Residual Load-controlled signal and activates stage 1 for heating/cooling depending on the season.

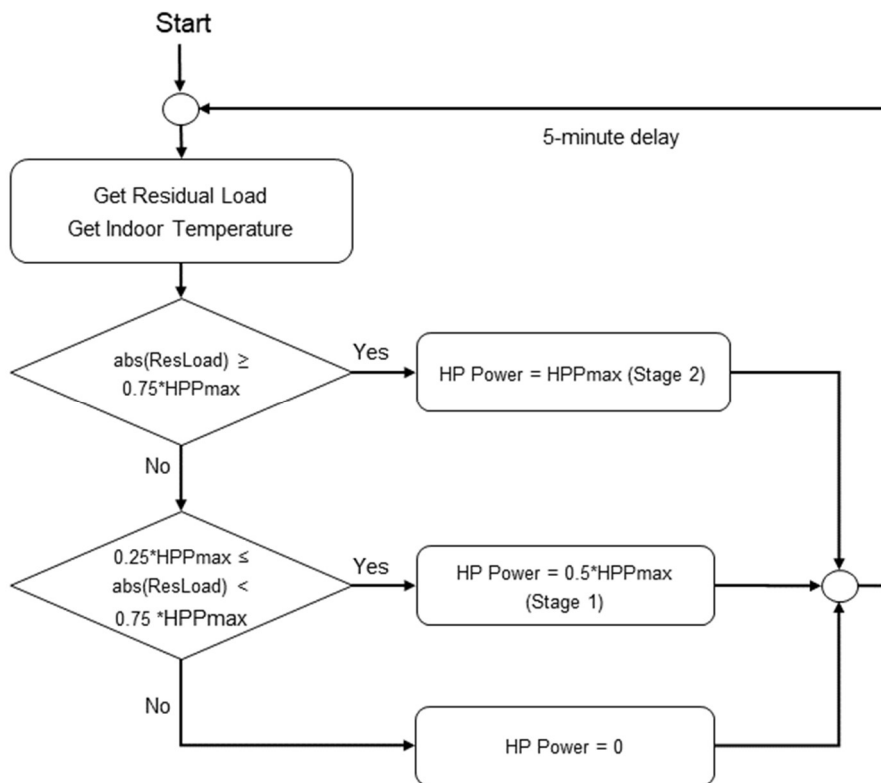


Figure 32: 2-Stage Heat Pump Control - Stage Selection

**Variant 13**

The single stage GSHP from Variant 11 is replaced with a variable speed GSHP. The HP can run at any capacity between 50 % and 100 %. There is no minimum runtime and the compressor speed is continuously adjusted based on a Residual Load signal as shown in Figure 33. The 1-minute delay is caused by the simulation timestep of 1 minute. A variable speed HP can respond more precisely to a change in Residual Load than a single-stage or 2-stage HP.

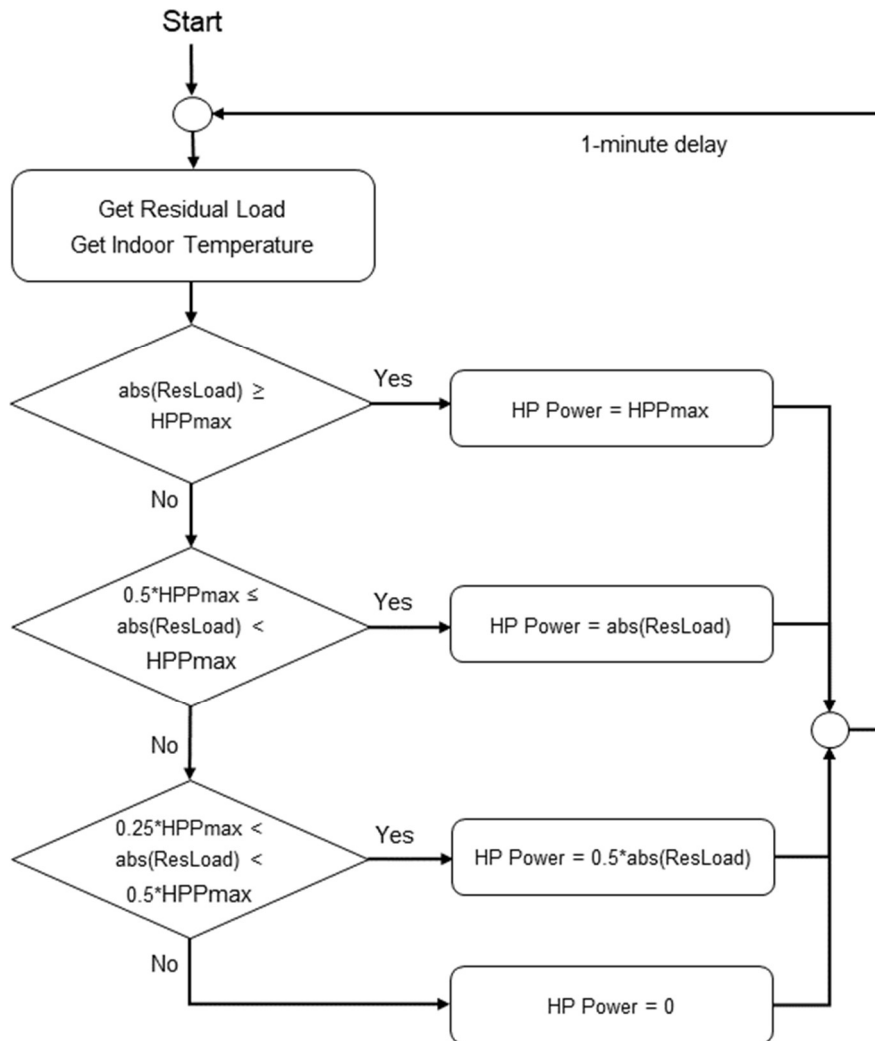


Figure 33: Variable Speed Heat Pump Control - Power Selection

## 5.7 Variants 14 to 17 - Concrete Core Activation with AWHP

### Variant 14

The building envelope is changed to massive construction as in variant 3. The concrete ceiling in this variant has embedded tube coils that are connected to a single stage AWHP with the same capacity as the ASHP. Interior walls are made of brick. A separate dehumidifier is used to keep relative humidity levels below 60 %. It is examined, how active concrete ceilings with significant thermal storage mass perform regarding DR and thermal comfort.

### Variant 15

The range of heating setpoints in Variant 14 is increased from (20 °C to 22 °C) to (19 °C to 23 °C) and the range of cooling setpoints from (24 °C to 26 °C) to (23 °C to 26 °C). The peak shifting capabilities of high thermal storage mass are examined by monitoring the thermal comfort within the increased temperature range.

### **Variant 16**

The heat pump's capacity is decreased by 30 %. Otherwise the model is identical to Variant 15. It is examined if HP capacities can be decreased in a system with high thermal capacitance while still maintaining thermal comfort.

### **Variant 17**

The heat pump's capacity is increased by 200 %. Otherwise the model is identical to Variant 15. It is evaluated if the concrete ceiling's storage mass can be used more efficiently with a high-power HP to reduce Residual Load while maintaining thermal comfort.

## **5.8 Variants 18 to 21 - Concrete Core Activation with GSHP**

### **Variant 18**

A GSHP with a borehole heat exchanger identical to the one in variant 10 is connected to the activated concrete ceiling. Otherwise the variant is identical to variant 14.

### **Variant 19**

Variant 18 is modified by increasing the range of heating setpoints from (20 °C to 22 °C) to (19 °C to 23 °C) and the range of cooling setpoints from (24 °C to 26 °C) to (23 °C to 26 °C). It is examined if the GSHP has an advantage over the AWHP regarding DR with this configuration.

### **Variant 20**

The heat pump's capacity is decreased by 30 %. Otherwise this variant is identical to variant 19. GSHP's are in general more efficient than AWHP because of the lower temperature difference between the condenser and the evaporator compared to air-source heat pumps. It is evaluated if an undersized single-stage GSHP reduces the Residual Load by a greater amount than an undersized AWHP.

### **Variant 21**

A variable speed GSHP is used in this variant, otherwise it is identical to Variant 19. It is examined if a variable speed GSHP reduces Residual Load by a similar magnitude in heavyweight construction as it does in lightweight construction with PCM.

## 5.9 Variants 22 to 24 - Vienna, Austria

### Variant 22

The Base Variant without DR is simulated with the climate data of Vienna. **Error! Reference source not found.** provides key climate conditions on a monthly basis for Vienna. It is examined, how a low cooling demand, due to less humid and cooler summers, affects Residual Load.

### Variant 23

A DR strategy is implemented into the model of Variant 22. No other system parameters are changed. In this variant the reduction of RL in a climate with low cooling demand is examined.

### Variant 24

The ASHP is exchanged for a variable speed GSHP. PCM gypsum boards are attached to the inside of the lightweight building envelope. The maximum possible reduction in RL in the prevalent climate conditions is examined.

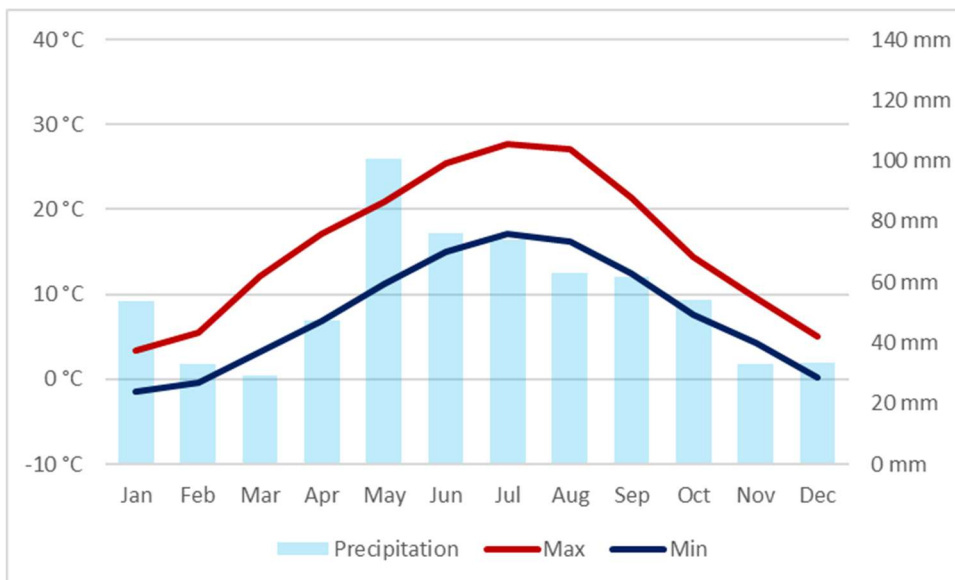


Figure 34: Climate Diagram Vienna, Austria (MA23 2019)

## 5.10 Variants 25 to 27 - Phoenix, Arizona

### Variant 25

The Base Variant without DR is simulated with the climate data of Phoenix (Figure 35). It is examined, how a high sensible cooling demand and low heating demand affect RL.

### Variant 26

A DR strategy is implemented into the model of Variant 25. No other system parameters are changed. In this variant the reduction of RL in a dry and hot climate with high sensible cooling demand is examined.

### Variant 27

The ASHP is exchanged for a variable speed GSHP. PCM gypsum boards are attached to the inside of the lightweight building envelope. The maximum possible reduction in RL in the prevalent climate conditions is examined.

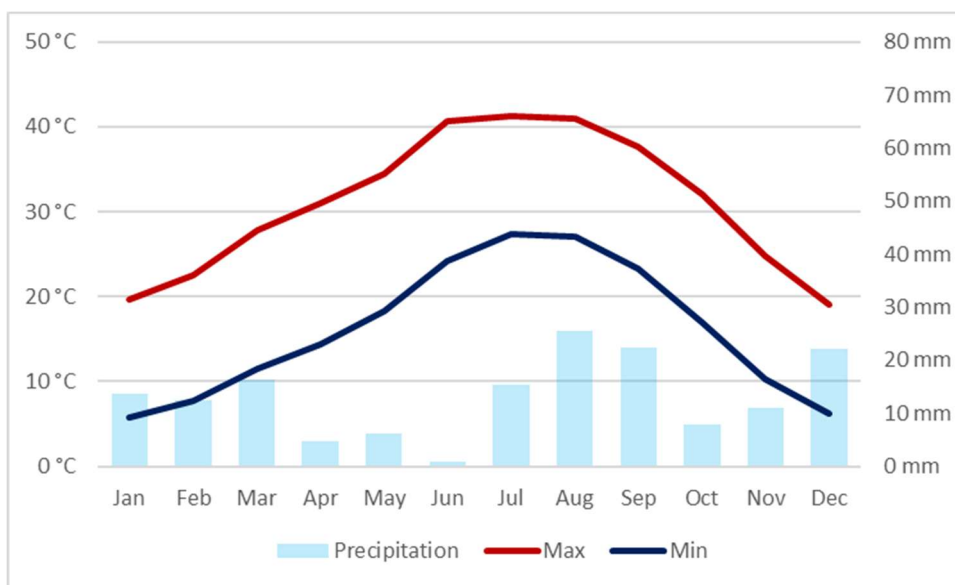


Figure 35: Climate Diagram Phoenix, AZ (NOAA 2017)

## 5.11 Variant 28 to 30 - Miami, Florida

### Variant 28

The Base Variant without DR is simulated with the climate data of Miami (Figure 36). It is examined, how a high latent cooling demand and low heating demand affect RL.

### Variant 29

A DR strategy is implemented into the model of Variant 28. No other system parameters are changed. In this variant the reduction of RL in a hot and humid climate with high latent cooling demand is examined.

### Variant 30

The ASHP is exchanged for a variable speed GSHP. PCM gypsum boards are attached to the inside of the lightweight building envelope. The maximum possible reduction in RL in the prevalent climate conditions is examined.

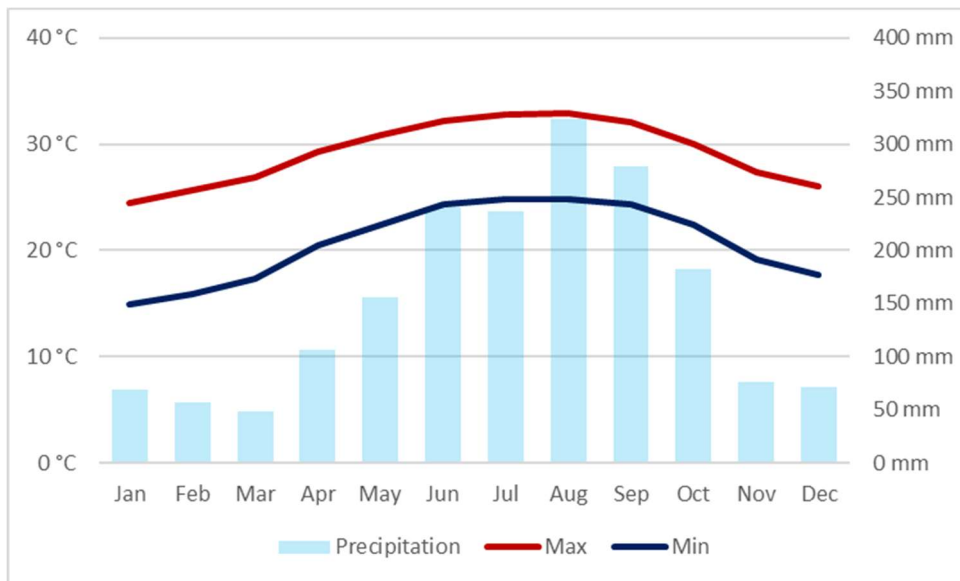


Figure 36: Climate Diagram Miami, FL (NOAA 2017)

## 5.12 Variant 31 to 33 - Fairbanks, Alaska

### Variant 31

The Base Variant without DR is simulated with the climate data of Fairbanks (Figure 37). It is examined, how a very high heating demand and no cooling demand affect RL, especially when using an ASHP.

### Variant 32

A DR strategy is implemented into the model of Variant 31. No other system parameters are changed. In this variant the reduction of RL in an extremely cold climate with a very high heating demand is examined.

### Variant 33

The ASHP is exchanged for a variable speed GSHP. PCM gypsum boards are attached to the inside of the lightweight building envelope. The maximum possible reduction in RL in the prevalent climate conditions is examined.

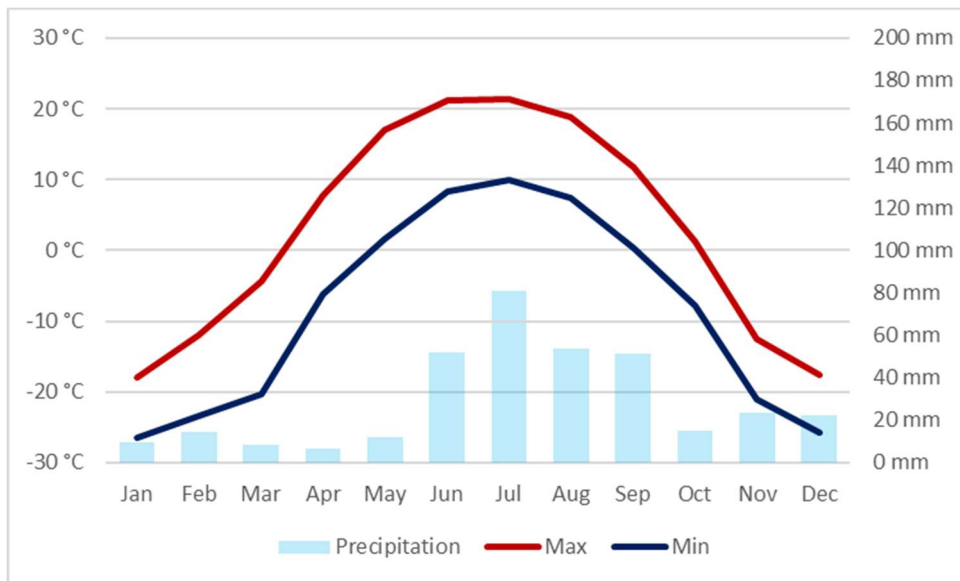


Figure 37: Climate Diagram Fairbanks, AL (NOAA 2017)

### 5.13 Typical Summer and Winter weeks

To better understand the ways in which each of these variants impact the Residual Load, the time variation of the energy demand, energy supply, and Residual Load are examined over a week with a typical temperature profile. The weather data of Dulles Int. Airport, VI is used to calculate the average hourly dry bulb temperature for summer and winter from 2000 to 2015. Summer is assumed to be from June 21 to September 23 and winter from December 21 to March 19. Then, the absolute difference between the average dry bulb temperatures and the dry bulb temperatures from the simulation’s weather data (Dulles 2015) is calculated. The 7 consecutive days with the smallest absolute temperature difference are chosen as typical summer and winter weeks.

July 27 to August 2 is a typical summer week. The absolute difference between this week and the average from the last 15 years is 244 K.

February 3 to February 9 is a typical winter week. The absolute difference between this week and the average from the last 15 years is 379 K.

The temperature profiles of typical summer and winter days are displayed in Figure 38 and Figure 39 respectively.

The typical summer/winter weeks of Variant 0, 1 and 27 are compared concerning their load profiles and the generation profile. It is assessed, how accurately the DR controller fits the load profile to the generation profile with minimum measures (Variant 1) and maximum measures (Variant 27).

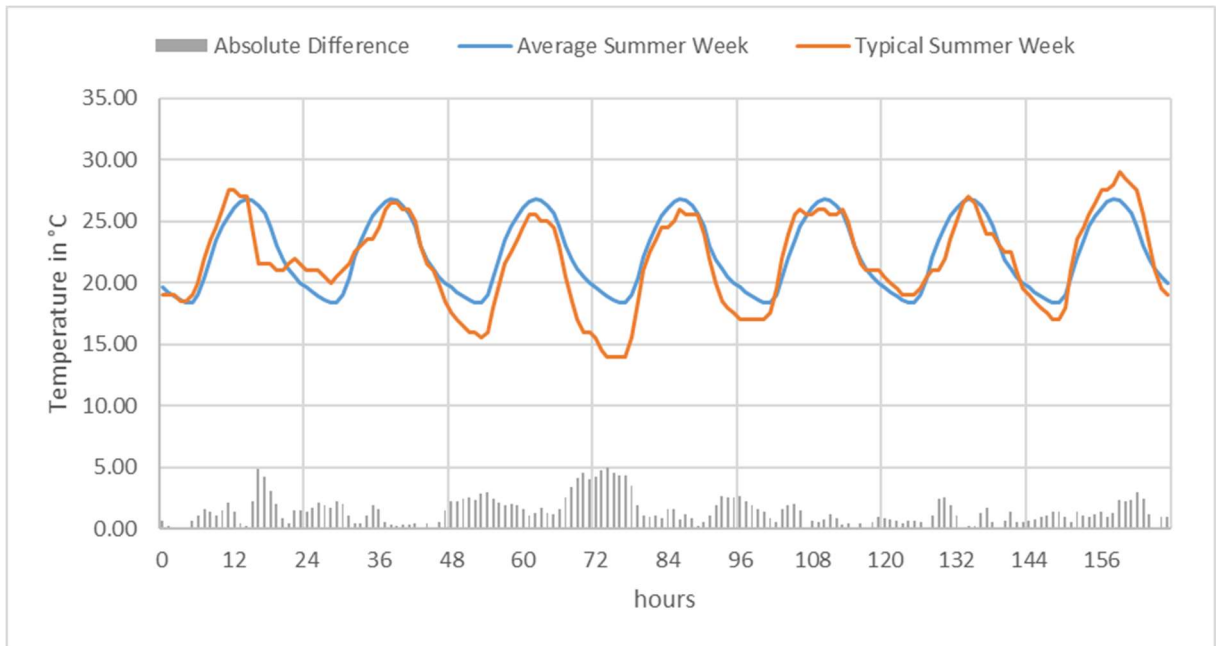


Figure 38: Typical summer week July 23 to August 2

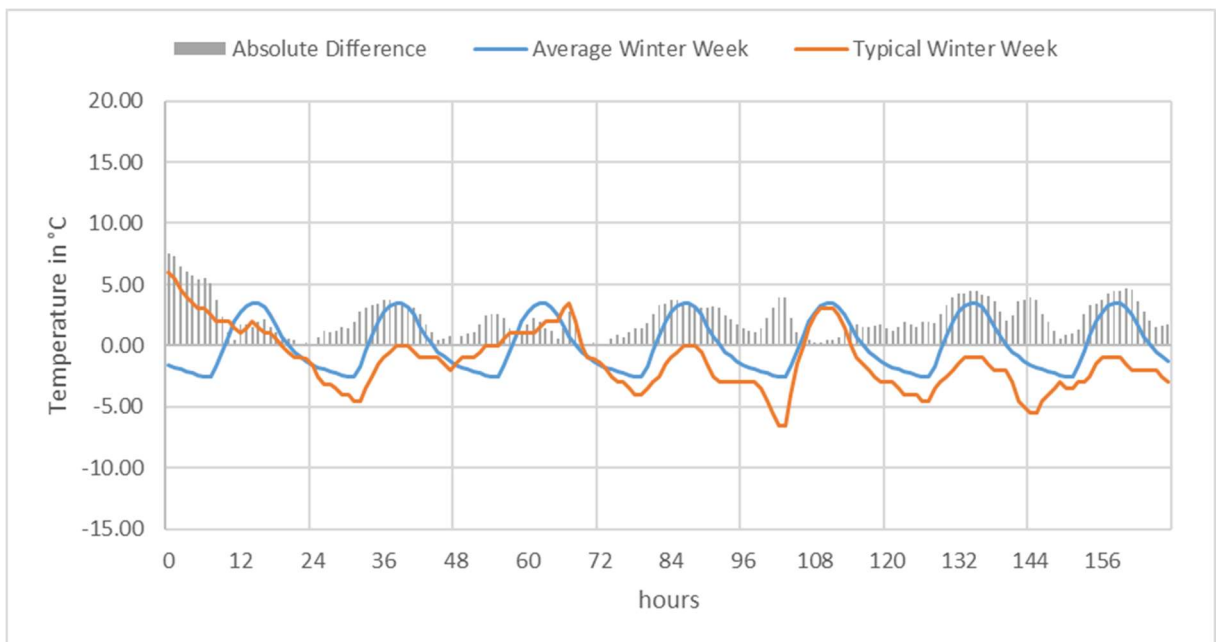


Figure 39: Typical winter week February 3 – February 9

## 6 Interpretation of results

The simulation results are compared to the Base Variant (Variant 0) as described in 5.1. In an ideal case with no Residual Load the generation profile is matched by the building's load profile at all times. The discrepancy between load and generation in different variants is visualized in sections 6.11 and 6.12.

The simulation results in sections 6.1 to 6.10 are grouped thematically. The first 21 variants are grouped by HP technology and building envelope. Variants 22 – 33 are grouped by climate, with 3 variants per climate. The Base Variant in every climate is compared to the Base Variant with DR to ascertain, how much the Residual Load can be decreased without altering the system configuration. Additionally, the Base Variant is compared to a variant with a variable speed GSHP, active PCM and a great temperature control range to determine the maximum possible reduction in Residual Load.

The first graph displayed for every group consists of 3 stacked columns per variant. The heating, cooling and DHW demand are key parameters for understanding the impact of different system configurations on the total annual energy demand. These loads are different for every variant and are summarized as 'Demand' in this graph. The demand from ventilation, plug loads, appliances and lighting is not included, because it is based on the same input files in every variant and therefore identical.

The main objective of this paper is to reduce Residual Loads. Both positive and negative Residual Loads are computed as the average load over one hour. The absolute value of the negative Residual Load is added to the positive Residual Load and the sum is displayed in kWh as 'ResLoad'.

Another priority is to maintain thermal comfort i.e. a PPD smaller than 10 %. The percentage of annual hours when the PPD exceeds 10 % is split into 2 categories of PPD (10 % to 15 % and > 15 %), to be able to judge the extent of thermal discomfort. The results are displayed as 'PPD' on the secondary y-axis.

The second graph shows annual hours at a certain Residual Load in descending order. The leftmost values are the greatest positive Residual Loads, whereas the rightmost values are the greatest negative Residual Loads. The area between the graph and the x-axis is the total absolute Residual Load during the year.

## **6.1 Variants 1 – 2**

### **Variant 1**

The use of DR while leaving other system parameters unchanged results in a decrease of Residual Load of 19.5 % compared to the Base Case as shown in Figure 40 and Figure 41. The x-axis of Figure 41 shows the distribution of Residual Load across all hours of the year plotted in descending order by Residual Load.

The increase in DHW demand by the DR control is used to decrease negative Residual Load. Lower heating setpoint temperatures lead to a decreased heating demand which reduces positive Residual Load during Winter. The increase in DHW demand is offset by the reduced heating demand so the overall energy demand is approximately equal to that of the Base Variant.

The overall PPD > 10 % is reduced from 17.2 % to 15.3 %. This reduction is caused by a lower cooling setpoint compared to the Base Variant. Cooler temperatures increase comfort during periods of high relative humidity during summer.

## **Variant 2**

The use of DR while increasing the ASHP's power threefold results in a decrease of Residual Load of 18.8 %. While there is an increased potential to reduce high negative Residual Loads caused by appliances (washing machine, dryer), the HP demand cannot be matched to the Residual Load accurately enough with only 2 stages. The 5-minute minimum runtime per stage leads to a delayed response to the Residual Load signal. The control of the high-powered HP must ignore small Residual Loads because turning on the HP would lead to overcompensation (turning a small negative Residual Load into a large positive Residual Load and vice versa). Therefore, the times when the control algorithm can take advantage of the high-powered HP are limited.

This system configuration fails to decrease either positive or negative Residual Load compared to Variant 1. The increased HP power leads to less runtime throughout the year compared to the Base Variant and Variant 1. During winter, this reduced runtime means that there are fewer defrost cycles which require up to 10 kW for several minutes. Because of this reduction in defrost cycles, the heating demand can be decreased by 10.3 % compared to Variant 1.

The overall PPD > 10 % is reduced from 17.2 % to 13.7 %. The slightly higher comfort compared to Variant 1 is caused by overcooling during summer resulting from the threefold increase in HP power. Overcooling occurs when the ASHP is turned on because of the DR signal. Each stage has a minimum runtime and, even if the inside air temperatures fall below the setpoint temperature, the ASHP continues to operate until the end of its minimum runtime. Therefore, temperatures can temporarily fall below the setpoint temperature during summer. This aspect of its operation also leads to a higher cooling demand compared to Variant 1.

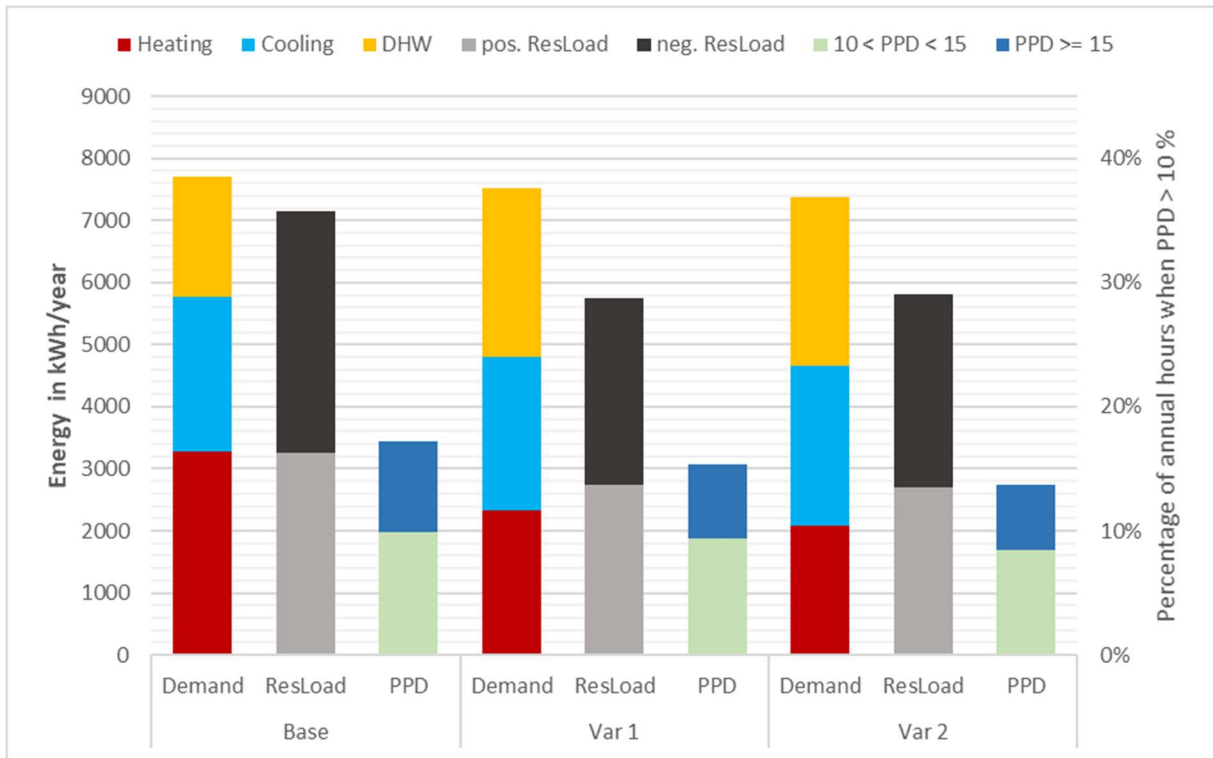


Figure 40: Results Variants 1 and 2

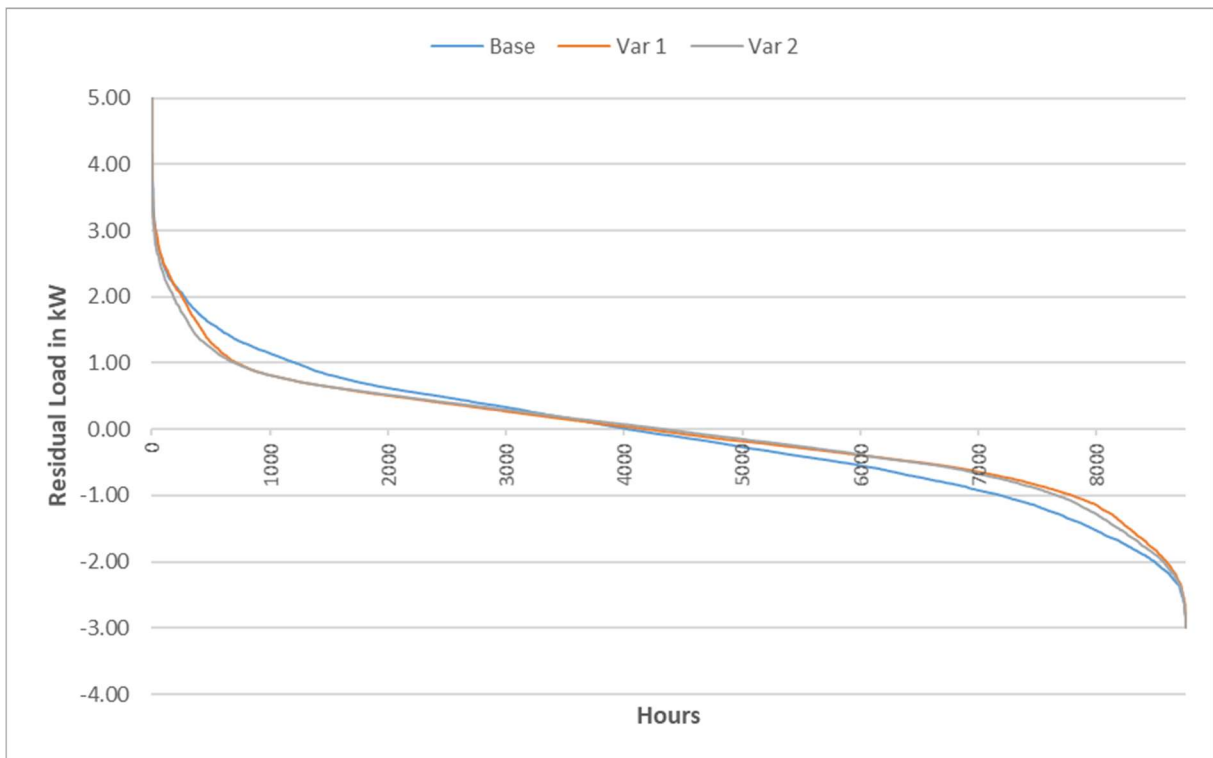


Figure 41: Annual Residual Loads Variants 0 and 2

## 6.2 Variants 3 – 5

### Variant 3

The use of DR in combination with massive construction results in a decrease of Residual Load of 21.8 % compared to the Base Case as shown in Figure 42 and Figure 43. The heat transfer between the storage mass and the interior air is not great enough to make significant use of the extra heat storage capacity. Therefore, the reduction in Residual Load is similar to that observed for Variant 1 which uses lightweight construction. The increased DHW demand reduces negative Residual Load, whereas the reduced heating demand reduces positive Residual Load.

The heating demand is reduced by 32.8 % because of lower heating temperatures during winter.

The overall PPD > 10 % is reduced from 17.2 % to 12.8 %. While the heat transfer between air and the storage mass is insufficient to impact DR, there is still a slight comfort benefit in the massive construction compared to lightweight construction.

### Variant 4

Increasing the ASHP power threefold in combination with massive construction results in a decrease of total Residual Load of 18.9 %. As in Variant 3, the heat transfer is too low to make use of the building's heat storage capacity. An ASHP with greater capacity does not improve a building's potential for DR. As in Variant 2, the HP demand cannot be matched to the Residual Load accurately enough with only 2 stages and a minimum runtime of 5 minutes.

The heating demand is reduced by 38.6 % because of fewer reheat cycles and lower heating temperatures during winter. The PPD > 10 % is reduced from 17.2 % to 11.5 %. The PPD is lower than in Variant 3 because of unintentional overcooling during summer.

### Variant 5

A building envelope that conforms to the IECC minimum standards results in a decrease of total Residual Load by 1.9 %. The increased energy demand during winter when renewable resources are not readily available causes an increase in positive Residual Load of 39.2 %.

The negative Residual Load is decreased by 36.2 %. The lower insulation standard results in a 42.0 % increase in heating energy demand compared to the Base Variant. The increased heating energy demand during spring and autumn leads to a lower negative Residual Load because the increasing renewable generation can be compensated by the heat pump's demand. The cooling load during summer is mainly due to dehumidification, and relative humidity is not affected by the building's insulation standard. Therefore, the energy demand during summer is nearly identical to Variants 3 and 4.

The PPD > 10 % is increased from 17.2 % to 26.7 %. Lower u-values result in a higher difference in mean radiant temperature compared to the inside air temperature. This temperature difference leads to thermal discomfort especially during cold winter days.

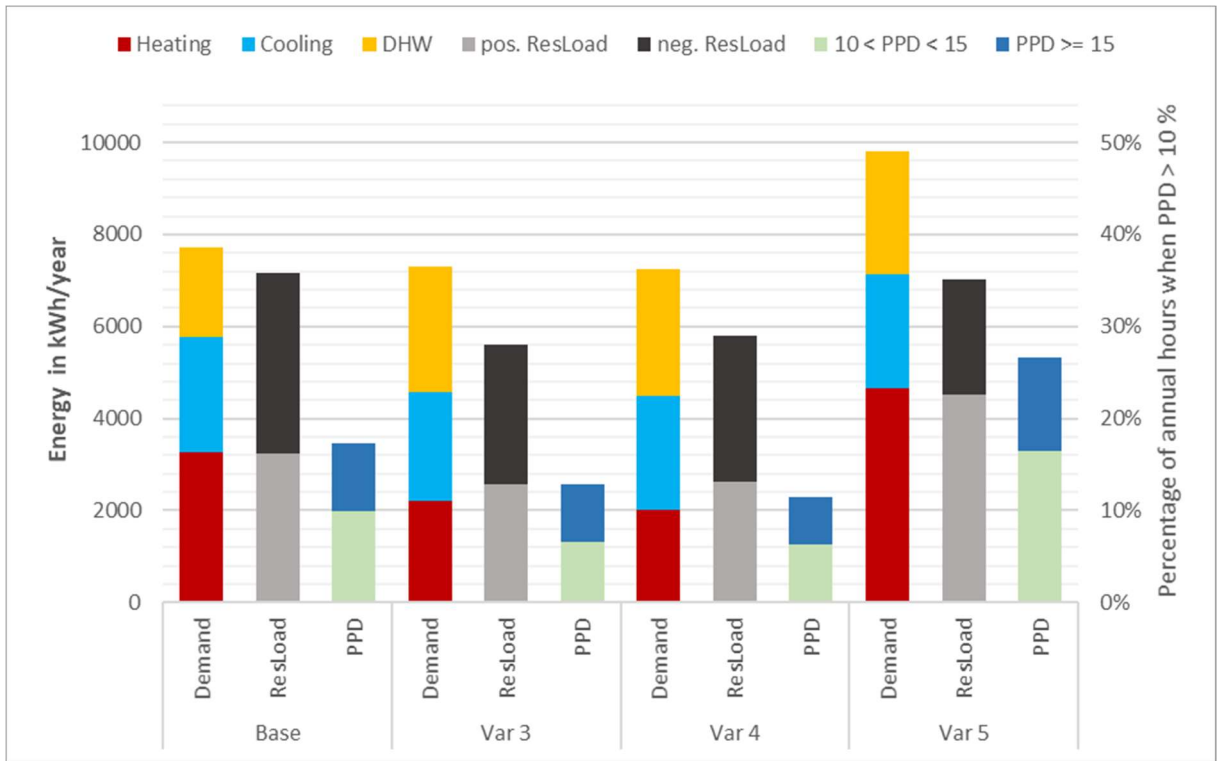


Figure 42: Results Variants 3 – 5

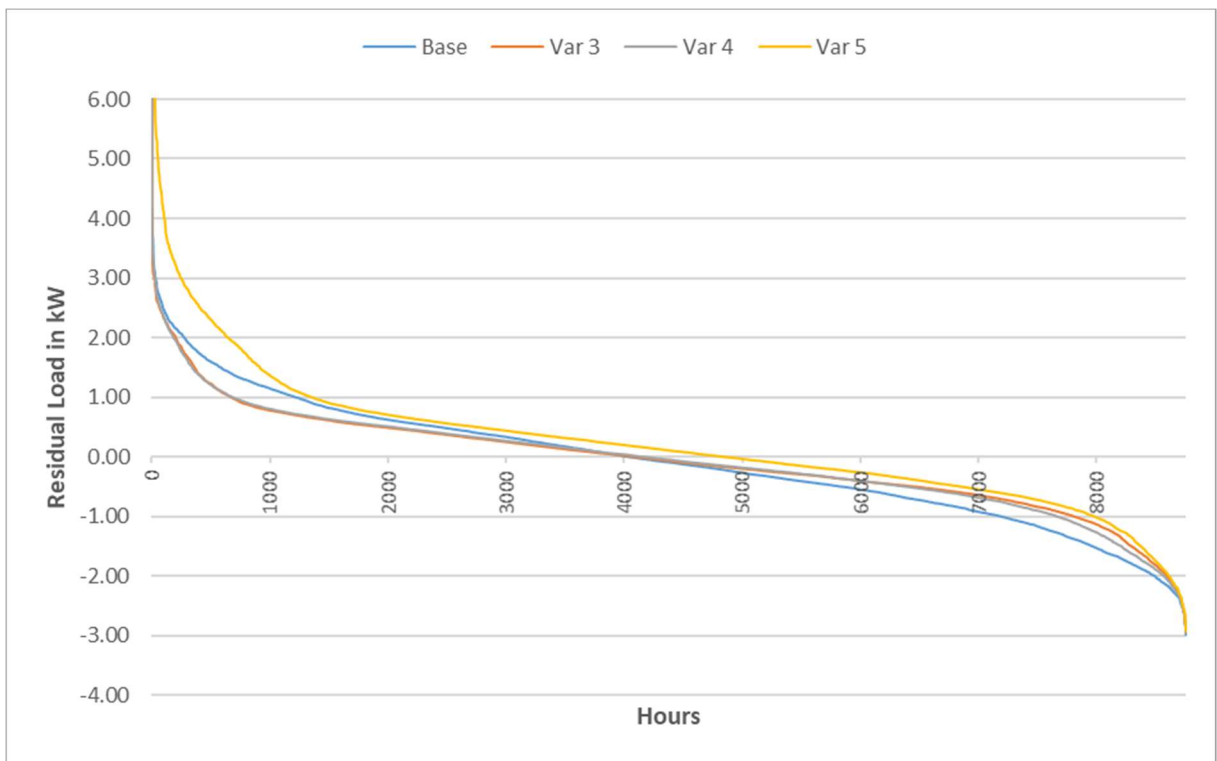


Figure 43: Annual Residual Loads Variants 3 – 5

## 6.3 Variants 6 – 9 (PCM with ASHP)

### Variant 6

Applying PCM gypsum boards to the inside of the exterior walls of the Base Variant results in a decrease of total Residual Load of 19.8 % as shown in Figure 44 and Figure 45. This variant's building model has greater thermal storage capacity than the lightweight Variants 1 and 2 but the decrease in Residual Load is identical.

Inside surface temperatures and air temperatures in buildings that approach passive house standard are nearly identical which leads to high thermal comfort with or without the PCM. The PCM's low heat transfer coefficient in combination with the aforementioned small temperature difference ( $< 2$  K) between gypsum board and indoor air lead to an insufficient heat flux for load shifting.

The PPD  $> 10$  % is decreased from 17.2 % to 14.9 % which is also nearly identical to the Variant 1. The comfort benefits of high thermal storage capacity cannot be utilized properly with this passive system configuration.

### Variant 7

Increasing the range of heating setpoints from (20 °C to 22 °C) to (19 °C to 23 °C) and cooling setpoints from (24 °C to 26 °C) to (23 °C to 26 °C) results in a decrease of total Residual Load of 21.8 %. Even with a passive PCM system the increased temperature range leads to a greater decrease of Residual Load compared to Variant 6.

The heating demand and cooling demand are increased compared to Variant 6 by 5.6 % and 3.7 % respectively. This increase in demand results because of the higher heating and lower cooling temperatures in the DR control strategy.

The PPD  $> 10$  % is decreased from 17.2 % to 12.6 %. The majority of this decrease is due to the lower cooling setpoint during summer. The modelling results show that because of temperature stratification, temperatures on the second floor can be up to 2 K greater compared to temperatures on the first floor. The hours of operative temperatures between 25 °C and 26 °C are reduced from 1046 in Variant 6 to 106 in Variant 7. Consequently, the annual share of hours with a PPD of over 15 % is reduced from 5.2 % in Variant 6 to 1.8 % in Variant 7.

### Variant 8

By decreasing the ASHP's capacity by 30 % the total Residual Load is decreased by 19.3 %. A smaller sized HP is better at compensating for small Residual Loads and less prone to overcompensation. A longer running time is necessary for a HP with lower capacity to deliver the same energy as a normal sized HP. Because of the longer running times during winter the ASHP goes through more defrost cycles which increases energy consumption as well as positive Residual Load. Thus, the total heating demand is increased by 7.9 % compared to the Base Variant.

The PPD  $> 10$  % is decreased from 17.2 % to 13.6 %. The ASHP still has enough capacity to sustain similar comfort levels as in Variant 7.

## Variant 9

By increasing the ASHP's capacity by 200 % the total Residual Load is decreased by 19.0 %. Because of the effects of overcompensation, as first mentioned in Variant 2, Variant 9 reduces the Residual Load by a smaller magnitude compared to Variants 6 through 8. Even with increased HP capacity the passive PCM cannot be utilized for DR. The only way to increase the heat flux between PCM and indoor air is to increase the temperature difference which would lead to thermal discomfort and is therefore not examined.

The heating demand is reduced by 36.4 % compared to the Base Variant. Because of the increased ASHP capacity the total annual runtime is lower. During winter less defrost cycles are necessary which decreases energy consumption.

The PPD > 10 % is decreased from 17.2 % to 13.4 %.

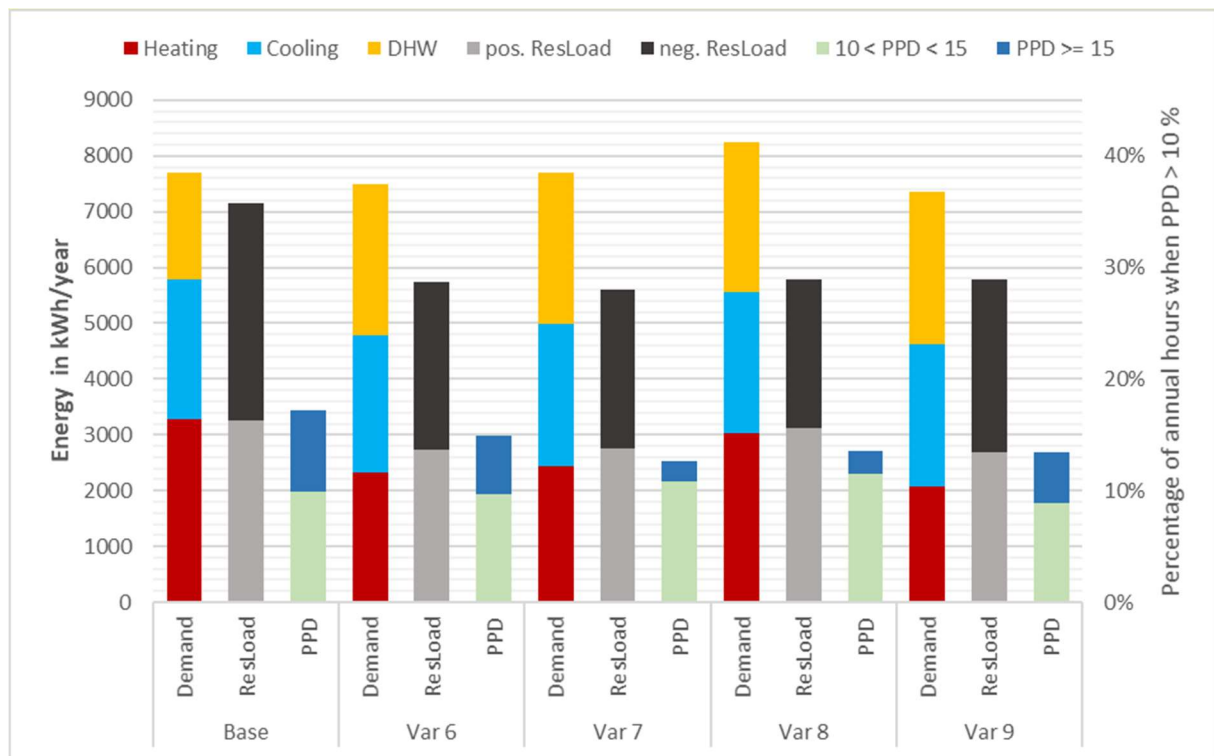


Figure 44: Results Variants 6 – 9

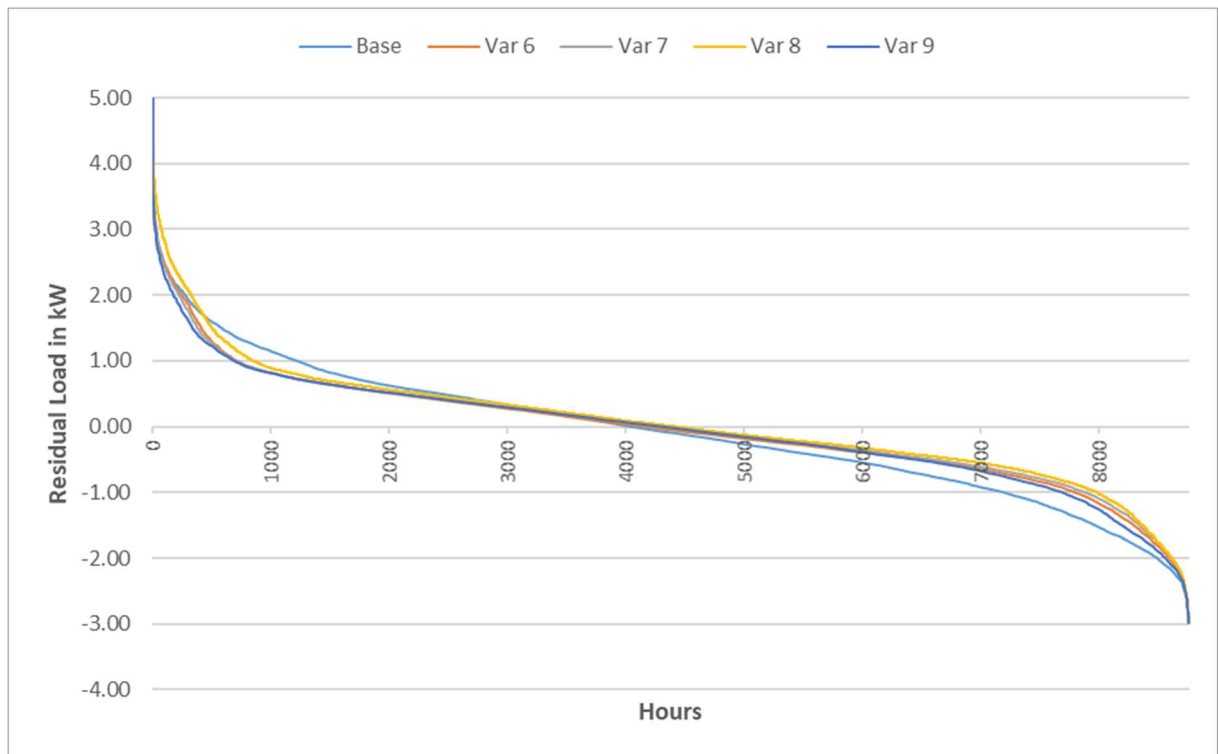


Figure 45: Annual Residual Loads Variants 6 – 9

## 6.4 Variants 10 – 13 (PCM with GSHP)

### Variant 10

Exchanging the 2-stage ASHP for a single-stage GSHP leads to a 29.1 % reduction in Residual Load as shown in Figure 46 and Figure 47. In this variant the PCM can actively be used to store energy during times of negative Residual Load. Therefore, the negative Residual Load is reduced by 31.9 % compared to the Base Variant. For reference, in Variant 6 with a passive PCM layer the negative Residual Load is reduced by 20.8 %.

The total annual energy demand is decreased by 2.2 %. The energy savings from the more efficient heat pump are greater than the increased DHW demand, caused by higher storage temperatures of up to 80 °C.

The PPD > 10 % is decreased from 17.2 % to 5.6 %. The activated PCM layer manages to keep operative temperatures below 25 °C as shown in Table 15.

Table 15: Operative Temperature Distribution Variant 10

T [°C]	Base Variant		Variant 10	
	Zone 2 time [h]	Zone 3 time [h]	Zone 2 time [h]	Zone 3 time [h]
17	0	0	0	0
18	199	62	196	57
19	413	272	307	249
20	1353	730	1419	675
21	2736	2615	2786	1931
22	2753	2658	2737	3397
23	1235	1905	1256	1986
24	71	518	59	465
25	221	833	0	0
26	0	351	0	0
27	0	1	0	0

#### Variant 11

Increasing the range of the previous variant's heating setpoints from (20 °C to 22 °C) to (19 °C to 23 °C) and cooling setpoints from (24 °C to 26 °C) to (23 °C to 26 °C) results in a decrease of total Residual Load of 31.2 %. The greater temperature range further decreases Residual Load compared to Variant 10. This decrease is mainly due to lower cooling temperatures during summer which help to reduce negative Residual Loads by 37.5 % compared to the Base Variant.

The total annual energy demand is increased by 1.4 %. Lower cooling temperatures result in an increased cooling demand of 4.5 % compared to Variant 10.

The PPD > 10 % is decreased from 17.2 % to 13.7 %. The greater temperature range leads to more discomfort compared to Variant 10.

#### Variant 12

Exchanging the single-stage GSHP for a 2-stage GSHP results in a decrease of Residual Load of 34.8 %. A 2-stage compressor improves the GSHP's potential for DR, because it can track the Residual Load more accurately compared to a single-stage HP.

The total annual energy demand for heating and cooling is increased by 2.4 % compared to the Base Variant. The PPD > 10 % is decreased from 17.2 % to 9.6 %.

### Variants 10 – 13

Using a variable-speed GSHP leads to a 35.5 % reduction in Residual Load. Instantaneous changes to the compressor power allow for a more accurate tracking of the Residual Load signal by the controller. The intermittent speeds between 50 % power and 100 % power are rarely used. Negative Residual Loads mostly exceed the maximum heat pump power and positive Residual Loads force the heat pump to turn off. Therefore, the variable speed heat pump usually operates either at full power or is turned off. For that reason, the improvement over the 2-stage heat pump is minor. Negative Residual Load is reduced by 42.0 % compared to the Base Variant. One of the instances where the compressor cannot compensate for Residual Loads is the use of the dryer (4 kW positive Residual Load) as shown in Figure 47. Peak photovoltaic generation (3 kW negative Residual Load) can also not be compensated, since the load is greater than the maximum heat pump power. The total annual energy demand is increased by 2.0 % compared to the Base Variant, as a result of a greater temperature range for space conditioning and an increased DHW demand. The PPD > 10 % is decreased from 17.2 % to 12.7 %.

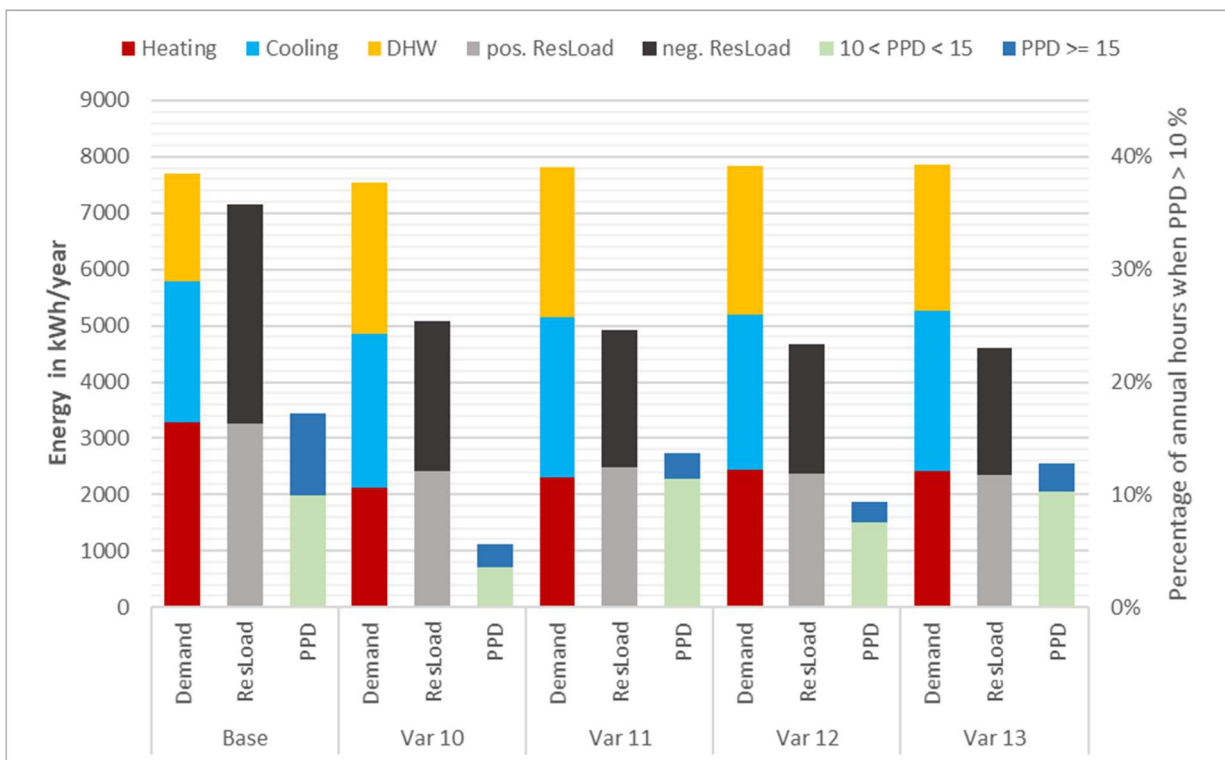


Figure 46: Results Variants 10 – 13

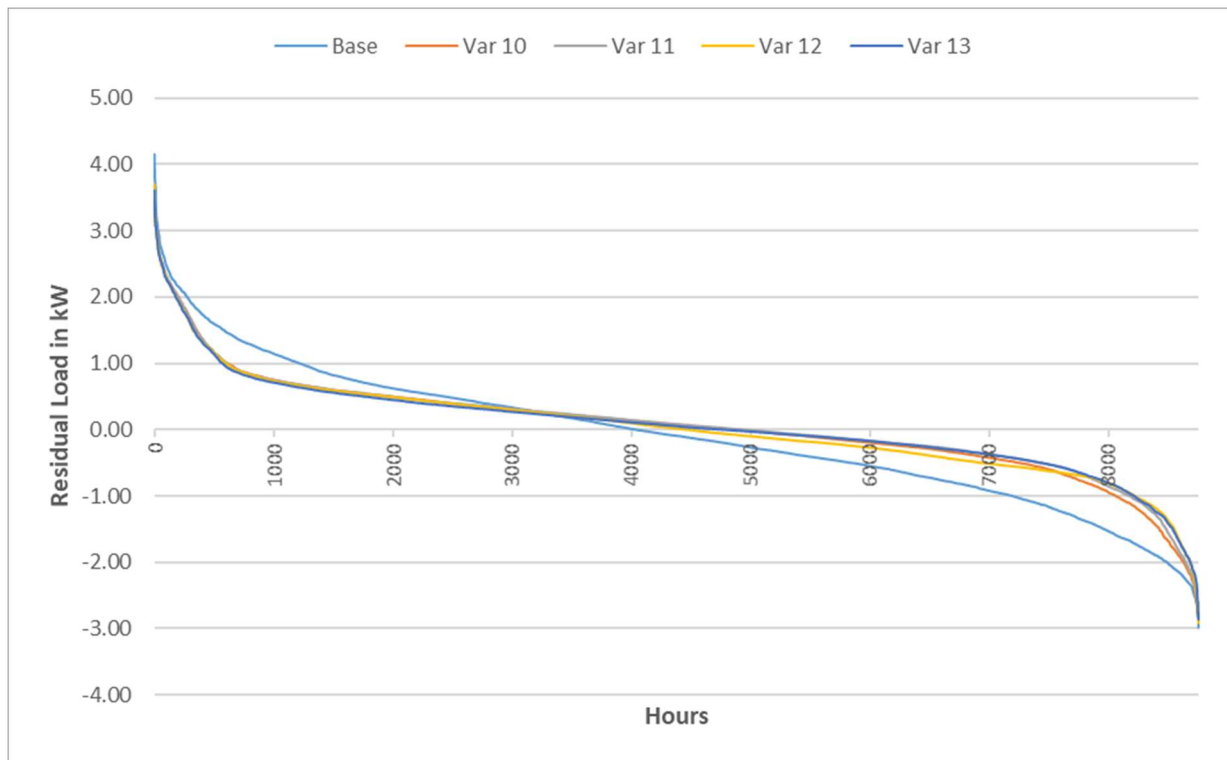


Figure 47: Annual Residual Loads Variants 10 – 13

## 6.5 Variant 14 – 17 (Concrete Core Activation with AWHP)

### Variant 14

A massive building envelope in combination with Concrete Core Activation and an AWHP leads to a 22.8 % decrease in Residual Load as shown in Figure 48 and Figure 49. An AWHP has the same drawbacks as an ASHP during winter. Defrost cycles result in an increased energy consumption and higher positive Residual Loads.

The total annual energy demand is increased by 6.7 %. The lower heating demand, due to lower heating setpoints during winter, is offset by the increased DHW demand.

The PPD > 10 % is decreased from 17.2 % to 1.2 %. The great thermal storage capacity of the concrete ceiling is used to keep operative temperatures within a comfortable range between 21 °C and 24 °C for most of the year. The thermal storage mass compensates all potential temperature spikes. Therefore, the PPD never exceeds 15 %.

### Variant 15

Increasing the range of the previous variant's heating setpoints from (20 °C to 22 °C) to (19 °C to 23 °C) and cooling setpoints from (24 °C to 26 °C) to (23 °C to 26 °C) results in a 23.5 % decrease in total Residual Load. As in previous variants, a larger temperature range provides a greater potential to reduce negative Residual Load during the cooling period. The negative Residual Load is decreased by 43.2 % compared to 34.9 % in Variant 14.

The total annual energy demand is increased by 14.4 % due to the increased cooling and heating demand.

The PPD > 10 % is decreased from 17.2 % to 9.8 %. The greater temperature band leads to a small increase in thermal discomfort compared to Variant 14.

#### **Variant 16**

Reducing the AWHP's power by 30 % leads to a reduction in total Residual Load of 22.2 %. The smaller sized AWHP reduces Residual Load 1 % more than the normal sized AWHP in Variant 14. This result is because during the majority of the year absolute Residual Loads are lower than 1 kW as shown in Figure 49. A smaller sized HP performs better at reducing Residual Loads in this range because it is less prone to overcompensation.

The total annual energy demand is increased by 10.0 % because of the AWHP's longer running time during winter, which results in more defrost cycles.

The PPD > 10 % is decreased from 17.2 % to 1.8 %. The smaller sized AWHP, in combination with high thermal storage mass, has enough capacity to keep operative temperatures in a comfortable temperature range throughout the year. Therefore, it performs nearly identical to the normal sized AWHP from Variant 14 regarding thermal comfort.

#### **Variant 17**

By increasing the AWHP's capacity by 200 % the total Residual Load is decreased by 17.6 %. The times when the increased power draw can be used to compensate peak negative Residual Loads are too infrequent to offset the lost potential of reducing small (–1 kW to 0 kW) negative Residual Loads. Because of the effects of overcompensation this variant performs worse than Variants 15 and 16 at decreasing the Residual Load.

The total annual energy demand is increased by 4.7 % and the PPD > 10 % is decreased from 17.2 % to 1.0 %. The AWHP's high capacity leads to overcooling during summer, where the operative temperature falls lower than the setpoint. Thus, the concrete ceiling manages to keep operative temperatures between 21 °C and 24 °C for most of the year as shown in Table 16. During summer, only 288 hours exceed 24 °C with a maximum temperature of 24.2 °C in zone 3.

Table 16: Operative Temperature Distribution Variant 17

T [°C]	Base Variant		Variant 17	
	Zone 2 time [h]	Zone 3 time [h]	Zone 2 time [h]	Zone 3 time [h]
17	0	0	0	0
18	101	18	0	0
19	276	1503	0	0
20	4570	2606	83	66
21	1071	1443	2586	391
22	629	517	3716	5522
23	1027	602	2345	2493
24	865	886	30	288
25	221	833	0	0
26	0	351	0	0
27	0	1	0	0

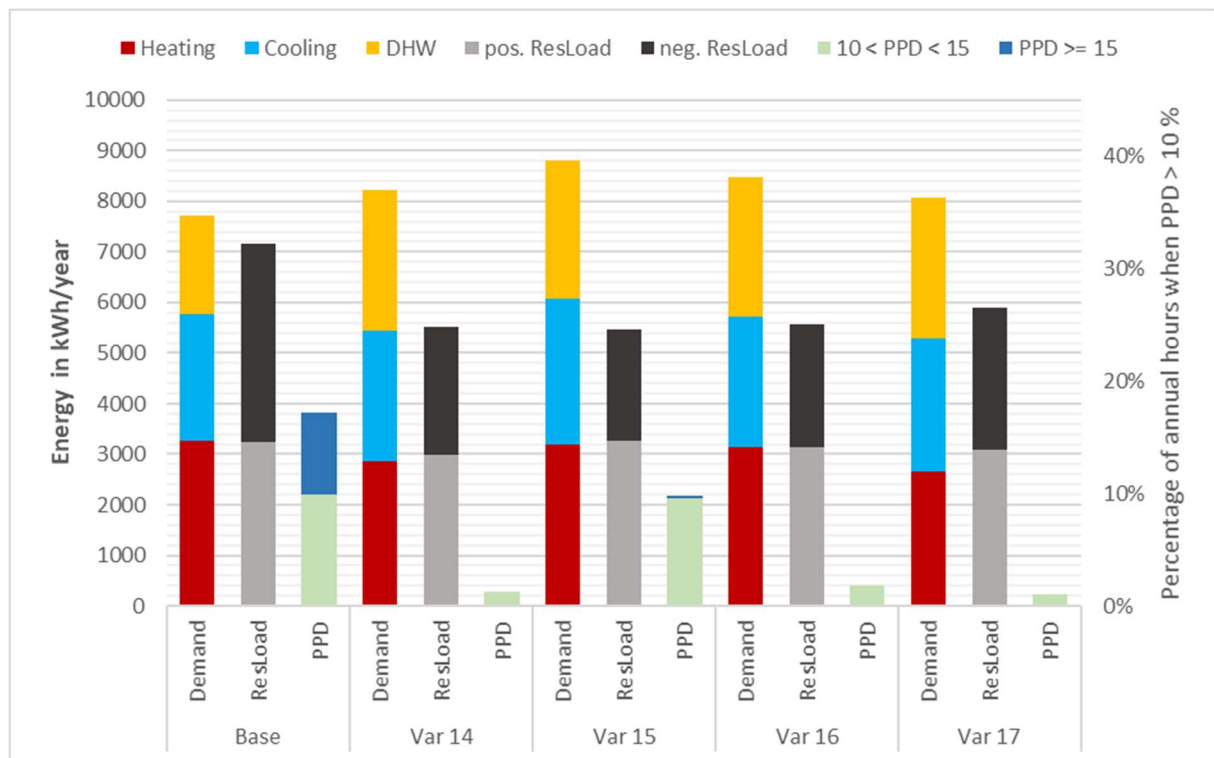


Figure 48: Results Variants 14 – 17

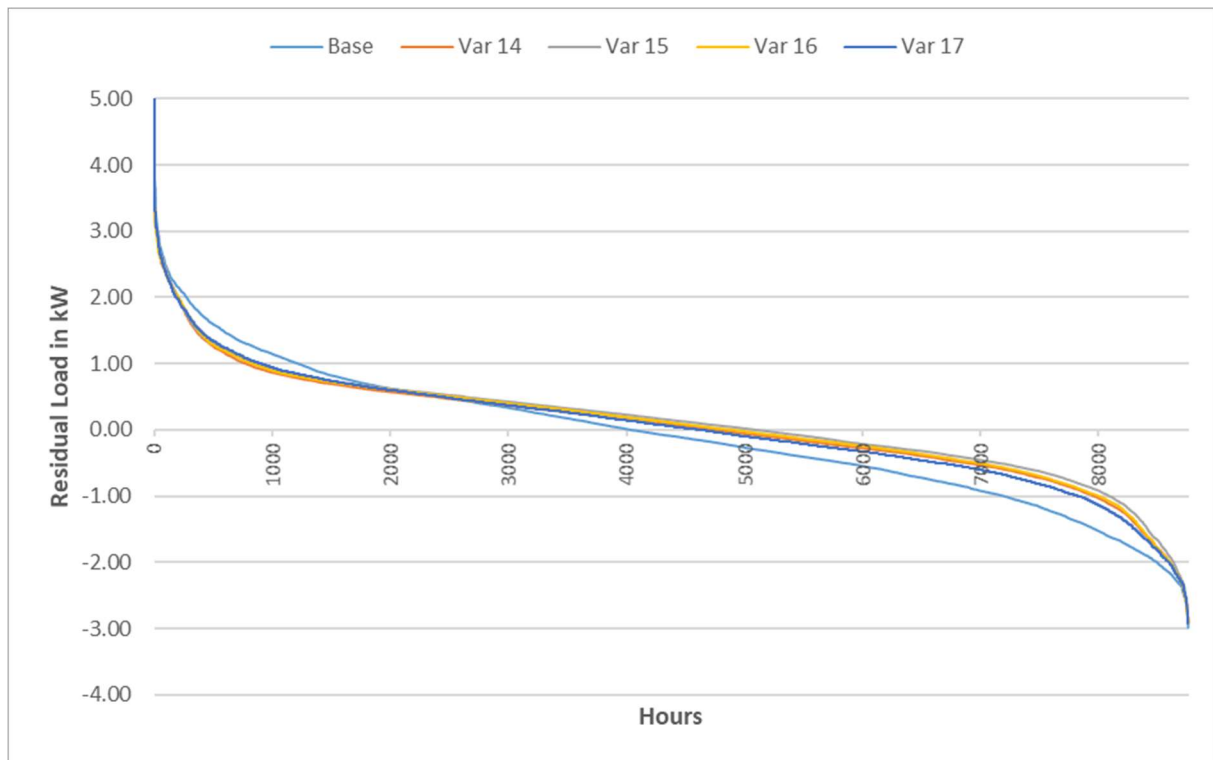


Figure 49: Annual Residual Loads Variants 14 – 17

## 6.6 Variant 18 – 21 (Concrete Core Activation with GSHP)

### Variant 18

Combining a single-stage GSHP with concrete core activation results in a 27.5 % decrease in total Residual Load as shown in Figure 50 and Figure 51.

The total annual energy demand is decreased by 7.8 %. The heating energy demand is reduced by 44.8 %, mainly because of the lack of defrost cycles. The increased DHW demand, due to DR, is smaller than the total annual energy savings. Therefore, this variant does not only have a lower Residual Load than the Base Variant but also a lower annual energy demand.

The PPD > 10 % is decreased from 17.2 % to 1.0 %. Similar to previous variants with an active concrete ceiling, the operative temperature is kept in a range between 21 °C and 24 °C for the majority of the year.

### Variant 19

Increasing the range of the previous variant's heating setpoints from (20 °C to 22 °C) to (19 °C to 23 °C) and cooling setpoints from (24 °C to 26 °C) to (23 °C to 26 °C) results in a 30.4 % decrease in total Residual Load. The greater temperature range increases the building's potential for DR. More energy can be stored in the ceiling when heating it from (19 °C to 23 °C) compared to heating it from (20 °C to 22 °C). Additionally, the GSHP can be turned off

longer during times of positive Residual Load. As a result, the negative Residual Load is reduced by 33.7 % compared to a 25.1 % reduction in Variant 18.

The total annual energy demand is decreased by 1.6 %. This variant's annual energy demand is 6.6 % greater compared to Variant 18 because of higher heating and lower cooling setpoints. The PPD > 10 % is decreased from 17.2 % to 10.3 %. The greater temperature band leads to a small increase in thermal discomfort compared to Variant 18.

### **Variant 20**

Reducing the GSHP's power by 30 % leads to a reduction in total Residual Load of 30.7 %. This decrease is nearly identical to Variant 19. A smaller sized GSHP heat pump in combination with Concrete Core Activation does improve the building's capabilities for DR.

The total annual energy demand is decreased by 3.6 %. The annual heating demand is reduced by 6.2 % compared to Variant 19. A single-stage heat pump with decreased power is better at tracking low Residual Loads. The heat pump's lower capacity results in longer running times. There are no drawbacks to longer running times during winter when using a GSHP. Defrost cycles are not necessary.

The PPD > 10 % is decreased from 17.2 % to 8.65 %. Similar to the previous variant the greater temperature band leads to a small increase in thermal discomfort compared to Variant 18.

### **Variant 21**

Using a variable-speed GSHP leads to a 32.0 % reduction in Residual Load. Negative Residual Load is reduced by 34.3 %. Similar to Variant 13 the instantaneous changes to compressor power allow a more accurate tracking of the Residual Load, especially when reducing negative Residual Load. The total annual energy demand is decreased by 2.5 % compared to the Base Variant. The savings from the efficient heat pump outweigh the increased DHW demand.

The PPD > 10 % is decreased from 17.2 % to 9.7 %.

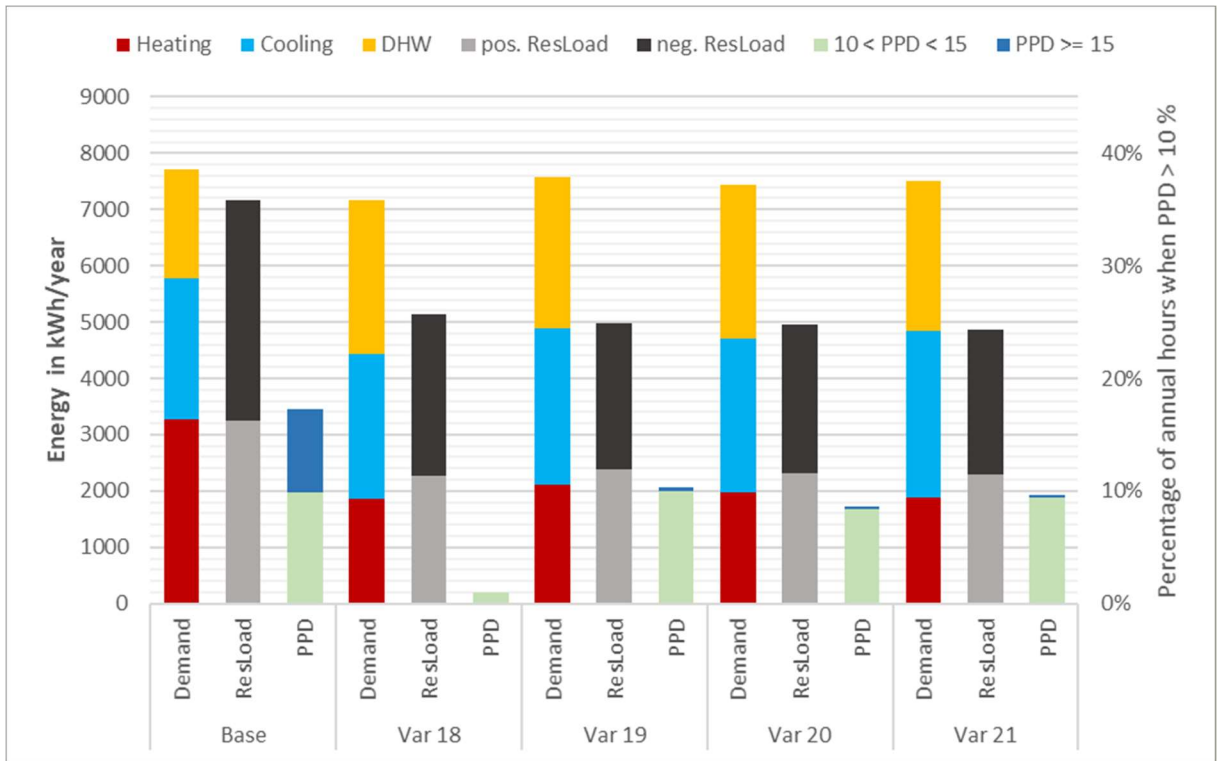


Figure 50: Results Variants 18 – 21

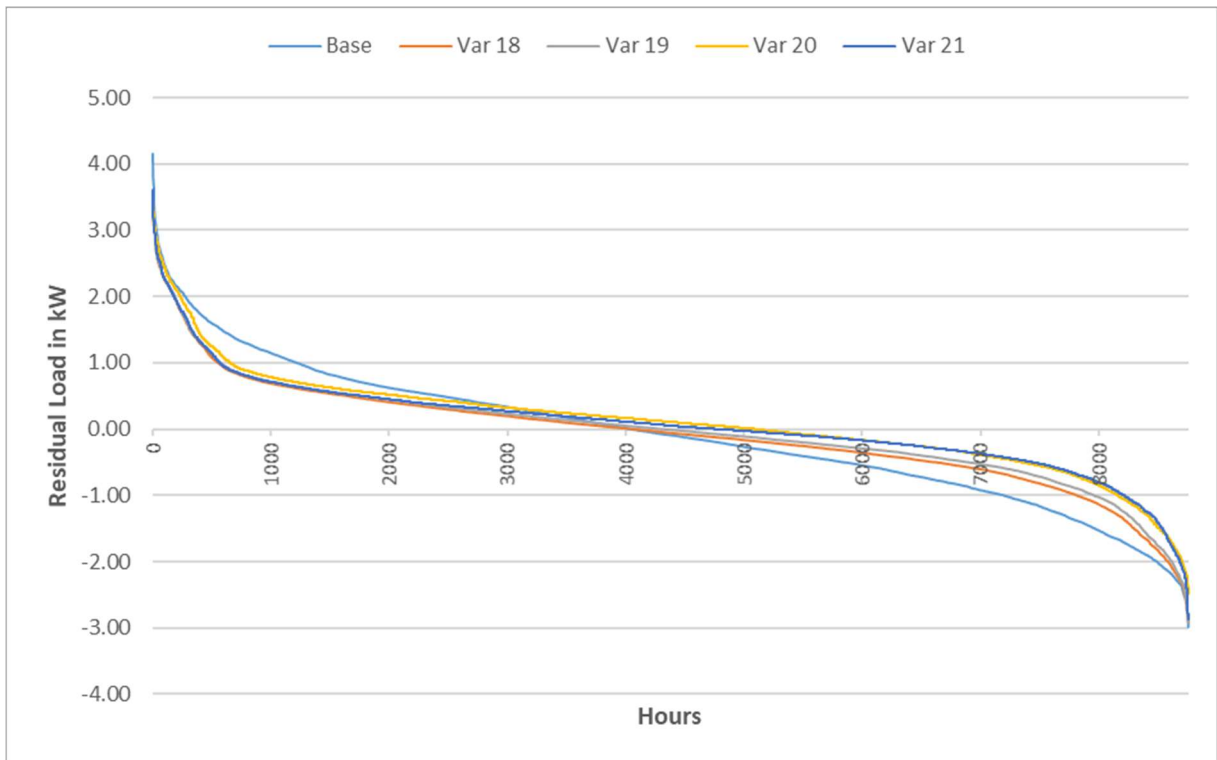


Figure 51: Annual Residual Loads Variants 18 – 21

## 6.7 Variants 22 – 24 (Vienna)

### Variant 22

Changing the location of the Base Variant to Vienna in Austria results in an absolute annual Residual Load of 7780 kWh as shown in Figure 52 and Figure 53. The building's cooling demand is greatly reduced by 78.7 % compared to the Base Variant in Gaithersburg. This explains the 14.1 % higher annual negative Residual Load. With little cooling or dehumidification, the only potential for eliminating negative Residual Loads during summer is DHW.

The total annual energy demand is decreased by 14.2 % because of the lower cooling demand. The annual heating demand is increased by 26.4 %.

The cooler climate also results in a lower PPD > 10 % of 7.4 %. There are fewer hours during which the operative temperature exceeds 25 °C during summer. Additionally, the climate in Vienna is less humid compared to Gaithersburg. A person's tolerance for warm temperatures is greater if humidity is lower (ASHRAE 2013). Therefore, temperatures that would lead to discomfort in Gaithersburg are still comfortable in Vienna at lower humidity levels.

### Variant 23

Implementing a DR control strategy for Variant 22 results in a 24.8 % decrease in total Residual Load. The positive Residual Load is reduced by 29.4 % mainly because of lower heating setpoint temperatures during winter. The negative Residual Load is reduced by 14.5 % mainly because of increased DHW setpoint temperatures. Cooling is not a major contributor to reducing Residual Load due to the building's low cooling demand in Vienna's climate.

The total annual energy demand is decreased by 9.6 %. Lower heating setpoints during the winter lead to a 36.4 % reduction in heating demand. DHW demand is increased by 47.1 % because of the DR control strategy.

The PPD > 10 % is decreased from 7.4 % to 5.2 % and the PPD > 15 % is decreased from 2.2 % to 0.6 %. Hours with a PPD of over 15 % are reduced because of the lower cooling setpoint during hot summer days. Hot summer days are also days of peak renewable generation. Therefore, cooling setpoints are lowered by the DR control which reduces not only negative Residual Load but also peak operative temperatures.

### Variant 24

Changing the 2-stage ASHP from Variant 23 to a variable speed GSHP in combination with an active PCM layer results in a 37.9 % decrease in total Residual Load.

The total annual energy demand is increased by 1.5 %. Lower cooling temperatures during summer, higher heating temperatures during winters and higher warm water storage temperatures outweigh the savings of the efficient GSHP.

The PPD > 10 % is decreased from 7.4 % to 0.1 %. The high thermal storage capacity of the active PCM in combination with lower cooling temperatures during summer can prevent thermal discomfort throughout the year under the climate conditions in Vienna.

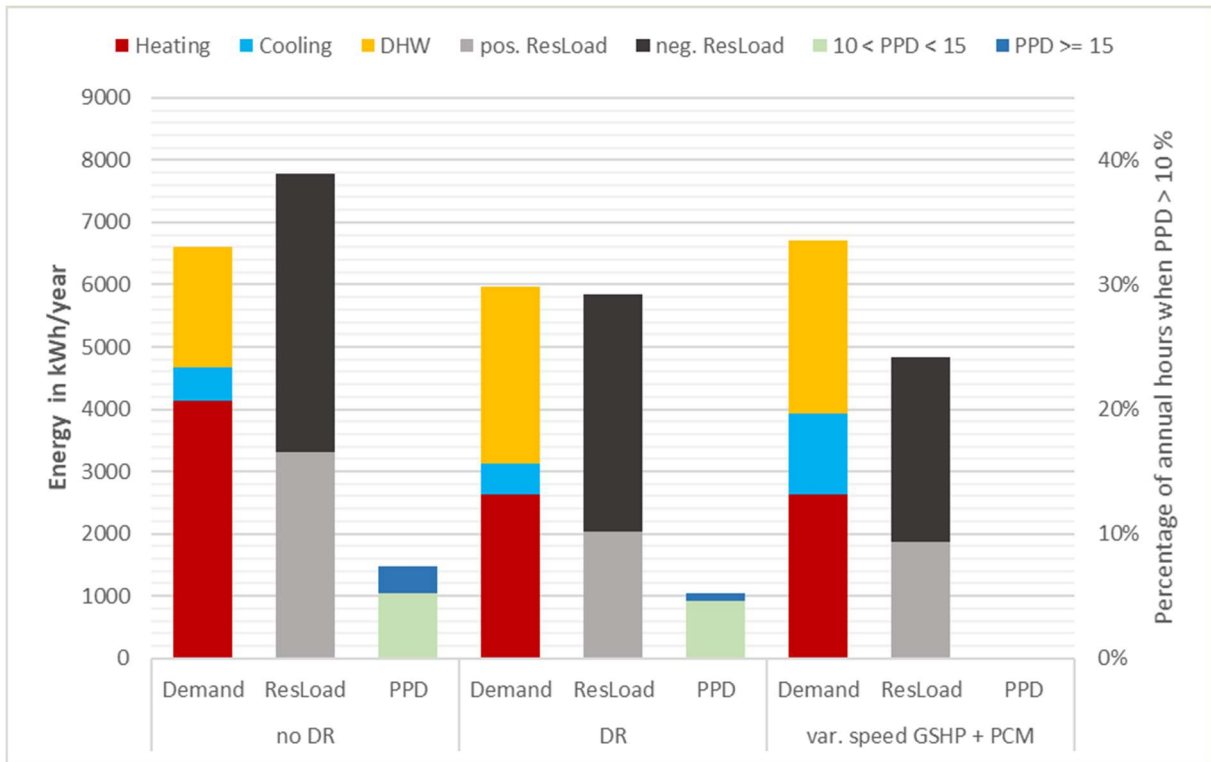


Figure 52: Results Variants 22 – 24

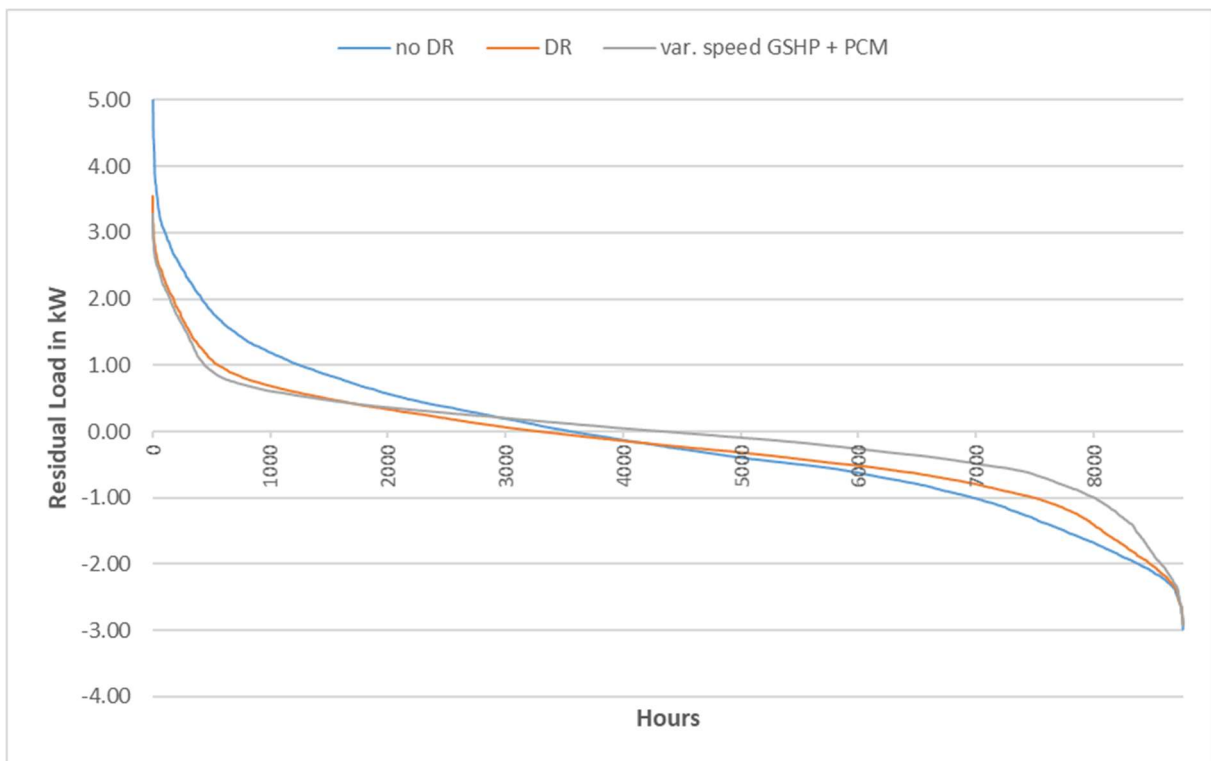


Figure 53: Annual Residual Loads Variants 22 – 24

## 6.8 Variants 25 – 27 (Phoenix)

### Variant 25

Changing the location of the Base Variant to Phoenix, Arizona results in an absolute annual Residual Load of 8253 kWh as shown in Figure 54 and Figure 55. The building's cooling demand is increased by 46.6 % compared to the Base Variant in Gaithersburg. The heating demand is reduced by 83.4 %.

The total annual energy demand is decreased by 19.9 % because of the lower heating demand.

Even though Phoenix is located in a desert climate zone, temperature peaks during summer have less of an impact on thermal comfort compared to the Base Variant in Gaithersburg. This lesser impact is because of low humidity and its effects on thermal comfort as mentioned in (ASHRAE 2013). The lack of dehumidification also keeps the cooling demand relatively low in relation to outdoor temperatures.

The hot and dry climate results in a PPD > 10 % of 5.5 %. The ASHP keeps operative temperatures lower than 25 °C while relative humidity never exceeds 60 %

### Variant 26

Implementing a DR control strategy for Variant 25 results in a 23.8 % decrease in total Residual Load. Changing cooling and DHW setpoint temperatures provides the main potential for DR in this climate zone. Heating is not a major contributor to reducing Residual Load due to the building's low heating demand.

The total annual energy demand is increased by 4.7 % compared to Variant 25. The increase in DHW demand is greater than the decrease in cooling demand. The cooling demand is decreased by 17.1 % as a response to positive Residual Load. Setpoint temperatures are increased to 26 °C which reduces the cooling energy demand.

The PPD > 10 % is similar to the previous variant at 6.3 %. Lower cooling temperatures during times of negative Residual Load do not improve thermal comfort. There is no discomfort due to high relative humidity which could be compensated by lowering operative temperatures. The ASHP keeps operative temperatures lower than 25 °C throughout the year similarly to Variant 25.

### Variant 27

Changing the 2-stage ASHP from Variant 25 to a variable speed GSHP in combination with an active PCM layer results in a 35.1 % decrease in total Residual Load.

The total annual energy demand is decreased by 2.9 %, because the energy savings of the GSHP outweigh the higher DHW demand in this climate.

The PPD > 10 % is decreased to 1.3 % due to lower cooling temperatures.

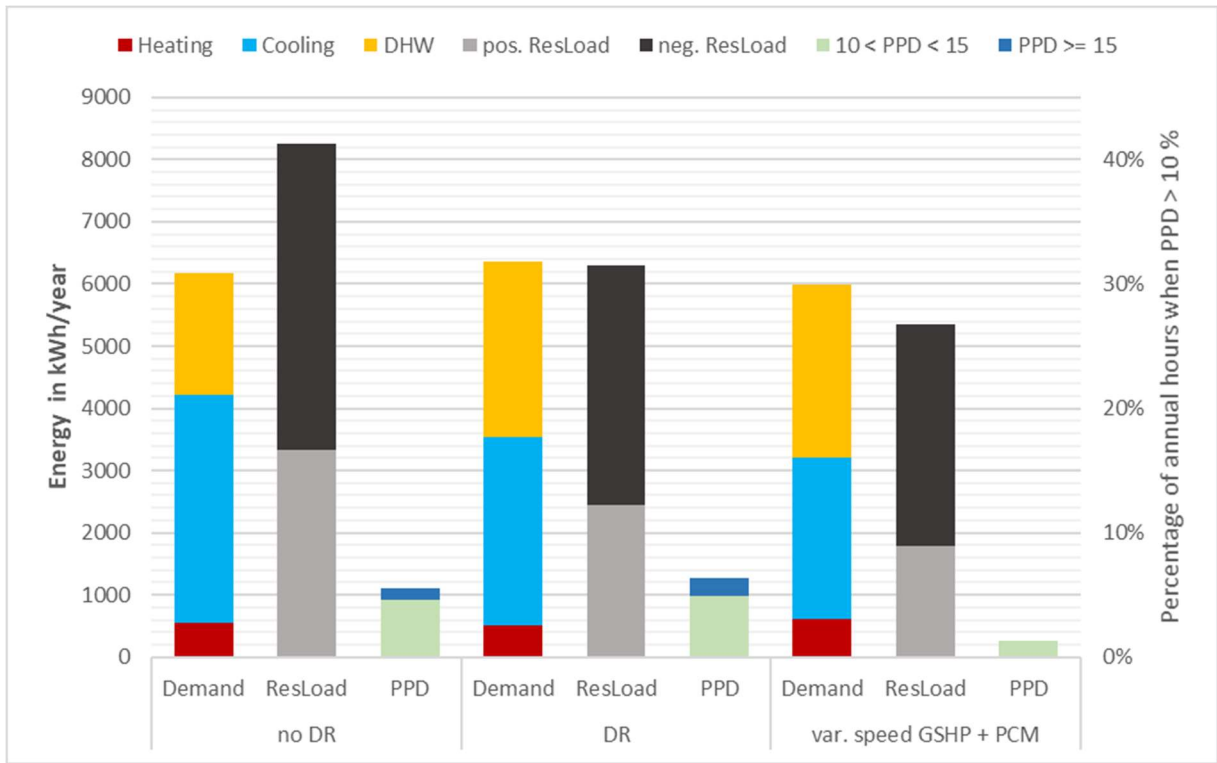


Figure 54: Results Variants 25 – 27

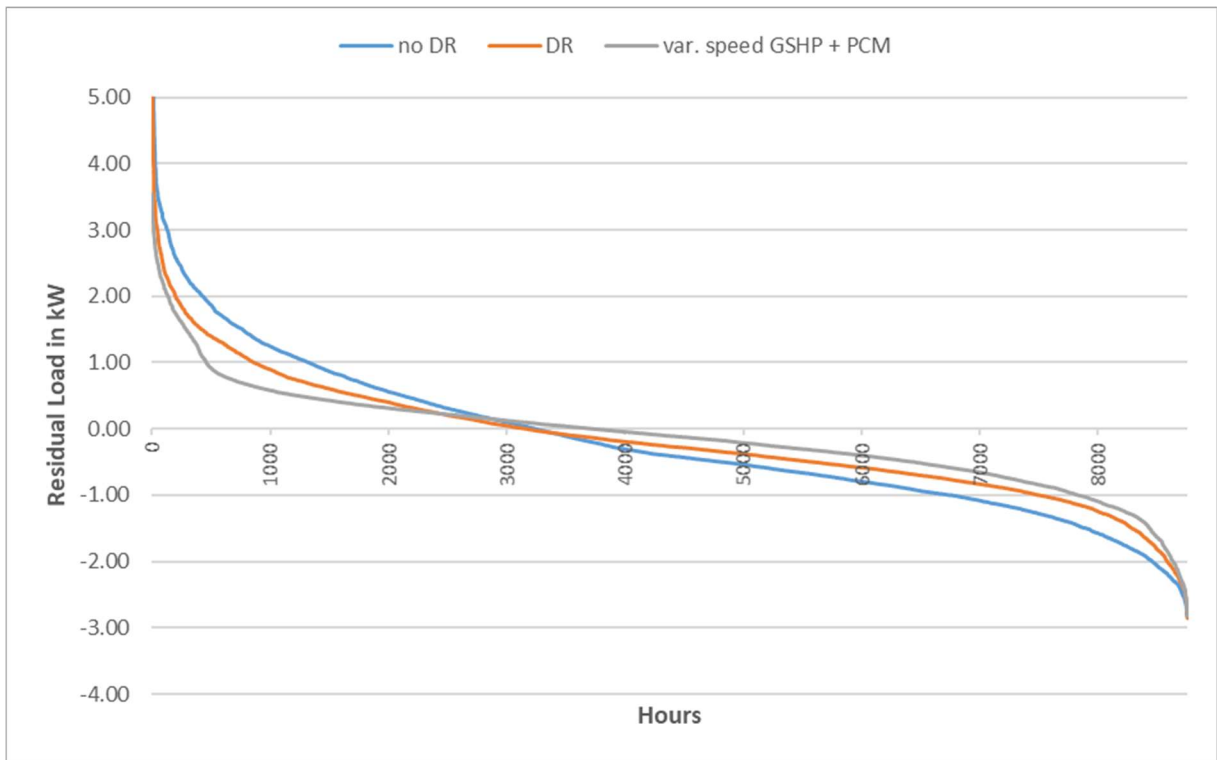


Figure 55: Annual Residual Loads Variants 25 – 27

## 6.9 Variants 28 – 30 (Miami)

Changing the location of the Base Variant to Miami, Florida results in an absolute annual Residual Load of 7590 kWh as shown in Figure 56 and Figure 57.

The building's cooling demand is increased by 268.5 % compared to the Base Variant in Gaithersburg. Dehumidification is necessary throughout the year to maintain thermal comfort in Miami's humid tropical climate. The heating demand is reduced by 87.5 %. Outside air temperatures fall below 15 °C for fewer than 500 hours per year.

The total annual energy demand is increased by 49.5 % because of the greatly increased cooling demand.

Constant cooling and dehumidification greatly reduce negative Residual Load. The heating demand is negligible compared to the cooling demand and the ASHP never goes into defrost mode. For these reasons the total Residual Load is similar to the Base Variant in Gaithersburg even though the total annual energy demand is nearly 50 % higher.

The PPD > 10 % is 6.9 %. Constant dehumidification provides high thermal comfort despite the hot and humid climate.

### Variant 29

Implementing a DR control strategy for Variant 28 results in a 24.4 % decrease in total Residual Load. Changing cooling and DHW setpoint temperatures provides the main potential for DR in this climate zone. Heating is not a major contributor to reducing Residual Load due to the building's low heating demand. The DR potential of cooling temperatures is limited by the dehumidification demand. Even if there is positive Residual Load and the building's operative temperature is still within a comfortable range, the HP is turned on if relative humidity exceeds 50 %.

The total annual energy demand is decreased by 2.2 % compared to Variant 28. The cooling demand is decreased by 5.1 %. As a response to positive Residual Load setpoint temperatures are increased to 26 °C which reduces the cooling energy demand. The PPD > 10 % is similar to the previous variant at 6.7 %.

### Variant 30

Changing the 2-stage ASHP from Variant 28 to a variable speed GSHP in combination with an active PCM layer results in a 26.2 % decrease in total Residual Load. Either the separate dehumidifier or the GSHP are on during times of negative Residual Load. Therefore, further increasing energy consumption to reduce negative Residual Load is not possible.

Reducing energy consumption by increasing cooling setpoints is not an effective way to reduce positive Residual Loads in hot and humid climates. The dehumidifier is the main contributor to cooling load with a fixed relative humidity setpoint. Even if the GSHP is turned off the dehumidifier is running to keep the relative humidity in a comfortable range while also cooling the indoor air.

The total annual energy demand is decreased by 4.6 %. The PPD > 10 % is increased from 6.9 % to 10.7 %. By constantly using the GSHP to cool the building, even for small Residual Loads, the operative temperature is at the minimum of 23 °C for the majority of the year. Even if there is demand for dehumidification, the dehumidifier is not turned on if the temperature falls below the lower threshold of 23 °C. Therefore, discomfort due to high relative humidity levels is increased resulting in the higher PPD value.

Constant reheating would be required to keep the temperature above 23 °C. This reheating would greatly increase cooling demand while not providing a great decrease in total Residual Load. This is because negative Residual Load contributes only 23.7 % to the total Residual Load.

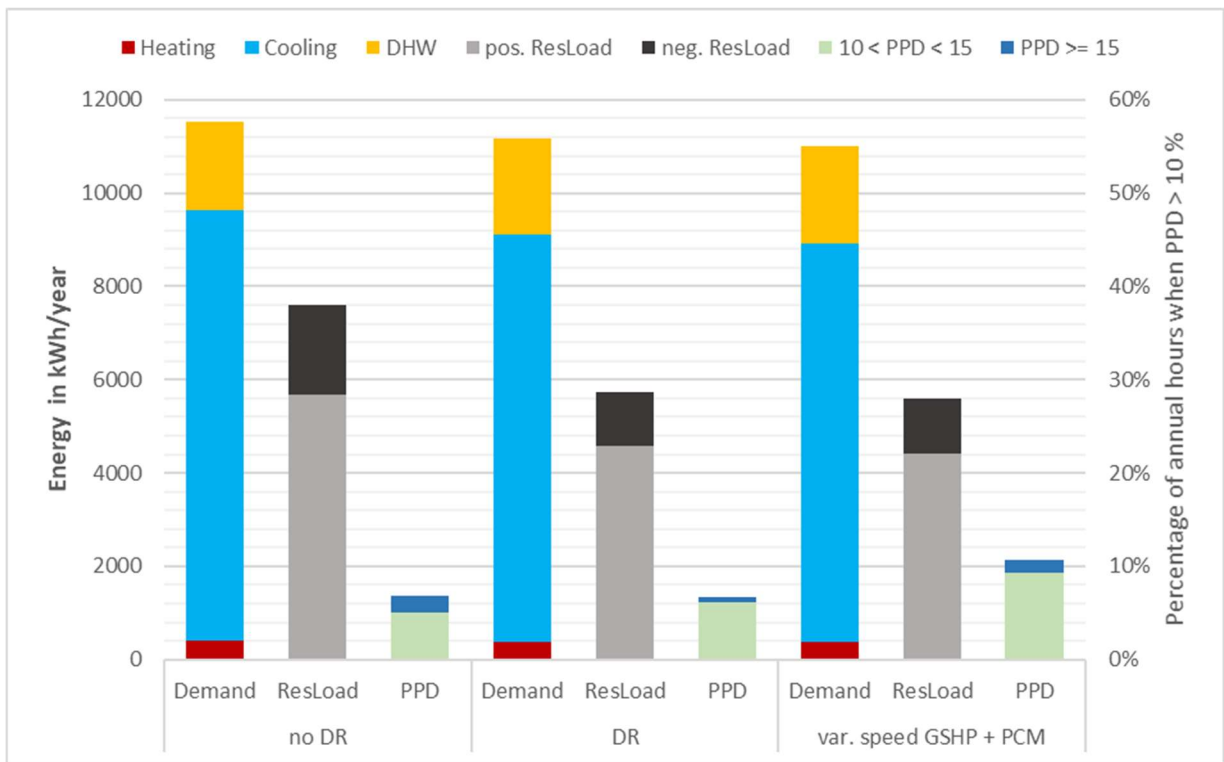


Figure 56: Results Variants 28 – 30

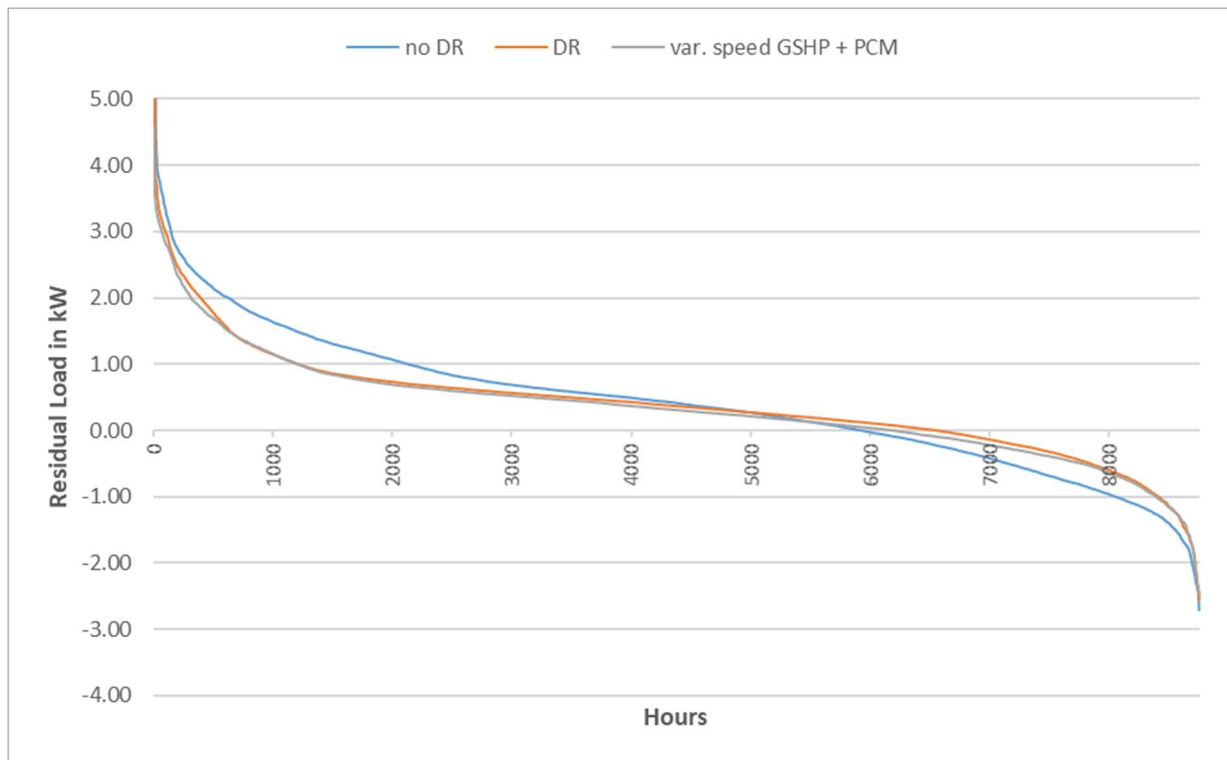


Figure 57: Annual Residual Loads Variants 28 – 30

## 6.10 Variants 31 – 33 (Fairbanks)

### Variant 31

Changing the location of the Base Variant to Fairbanks, Alaska results in an absolute annual Residual Load of 17 100 kWh as shown in Figure 58 and Figure 59.

The building's cooling demand is decreased by 90.1 % compared to the Base Variant in Gaithersburg. The heating demand is increased by 512.4 %. Fairbanks' average annual outside air temperature is  $-0.1$  °C compared to  $11.7$  °C in Gaithersburg. The outside air temperature exceeds  $20$  °C during 430 hours per year.

The total annual energy demand is increased by 146.0 %. The efficiency of ASHPs is greatly decreased when outdoor air temperatures fall below the freezing point. Frequent defrost cycles and COPs close to 1 during winter result in a system performance similar to that of resistance heat. The high heating energy demand and frequent defrost cycles lead to a 138.9 % increase in absolute annual Residual Load compared to Gaithersburg. This increase is of a similar magnitude than the increase in total annual energy demand. The effect of the great power draw of the auxiliary heating stage on positive Residual Load is shown in Figure 59. There are over 2000 hours during which positive Residual Loads exceed 2 kW. In the climate of Gaithersburg there are approximately 100 such hours, mainly caused by the dryer.

The PPD > 10 % is 4.9 %. The indoor air is dry with a relative humidity of less than 30 % for 65 % of the year. Indoor operative temperatures are kept in a comfortable range between 20 °C and 24 °C throughout the year.

### **Variant 32**

Implementing a DR control strategy for Variant 31 results in a 12.5 % decrease in total Residual Load. The positive Residual Load is reduced by 9.3 % and the negative Residual Load is reduced by 27.6 %. Cooling is not a major contributor to reducing Residual Load due to the building's negligible cooling demand in Fairbanks' climate.

The total annual energy demand is decreased by 2.6 % compared to Variant 31. The heating demand is decreased because of lower heating setpoint temperatures. The PPD > 10 % is 3.1 %.

### **Variant 33**

Changing the 2-stage ASHP from Variant 31 to a variable speed GSHP in combination with an active PCM layer results in a 74.4 % decrease in total Residual Load. Negative Residual Loads are decreased by 30.9 %. Positive Residual Loads are decreased by 83.8 %. The majority of the decrease in positive Residual Load is due to the GSHP's greater efficiency, especially in cold climates. The total annual energy demand is decreased by 57.6 %. The performance of a GSHP is not dependent on outdoor air temperatures. Soil temperatures stay above the freezing point throughout the year which results in greater system efficiency compared to the ASHP. Additionally, there is no need for defrost cycles which decreases energy demand as well as positive Residual Load. The PPD > 10 % is 4.9 %.

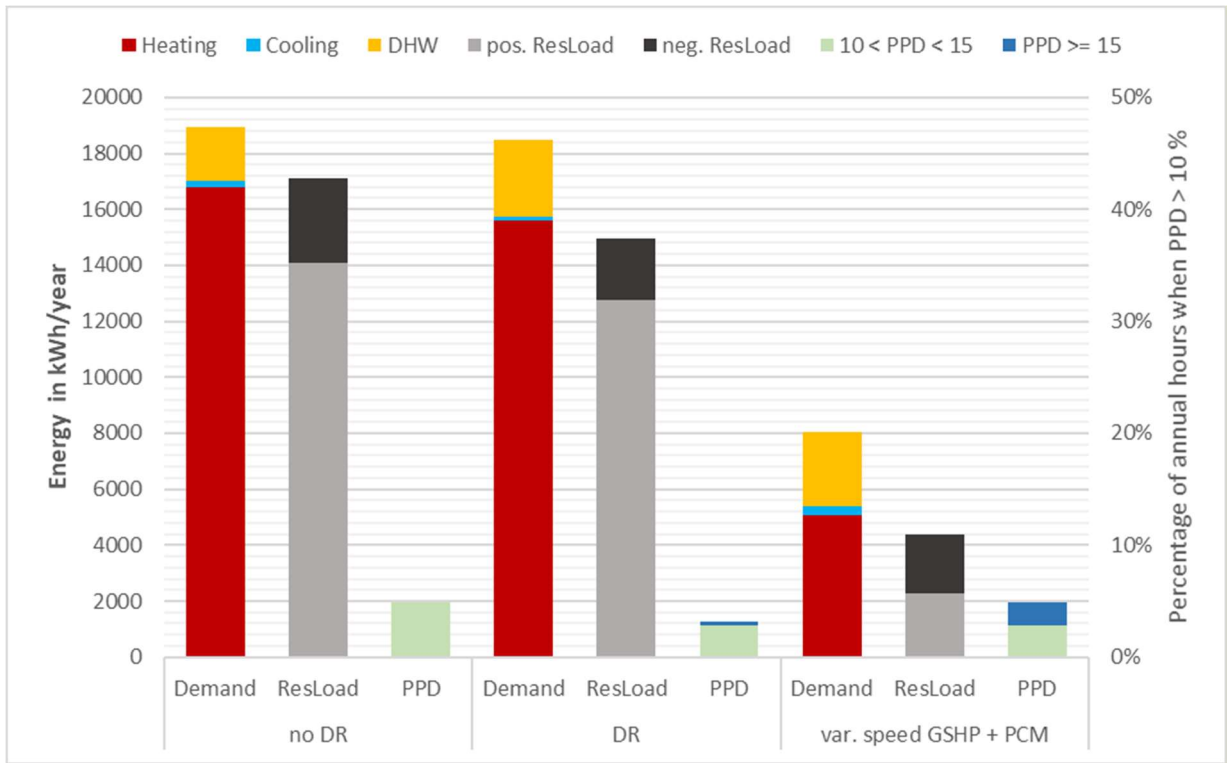


Figure 58: Results Variants 31 – 33

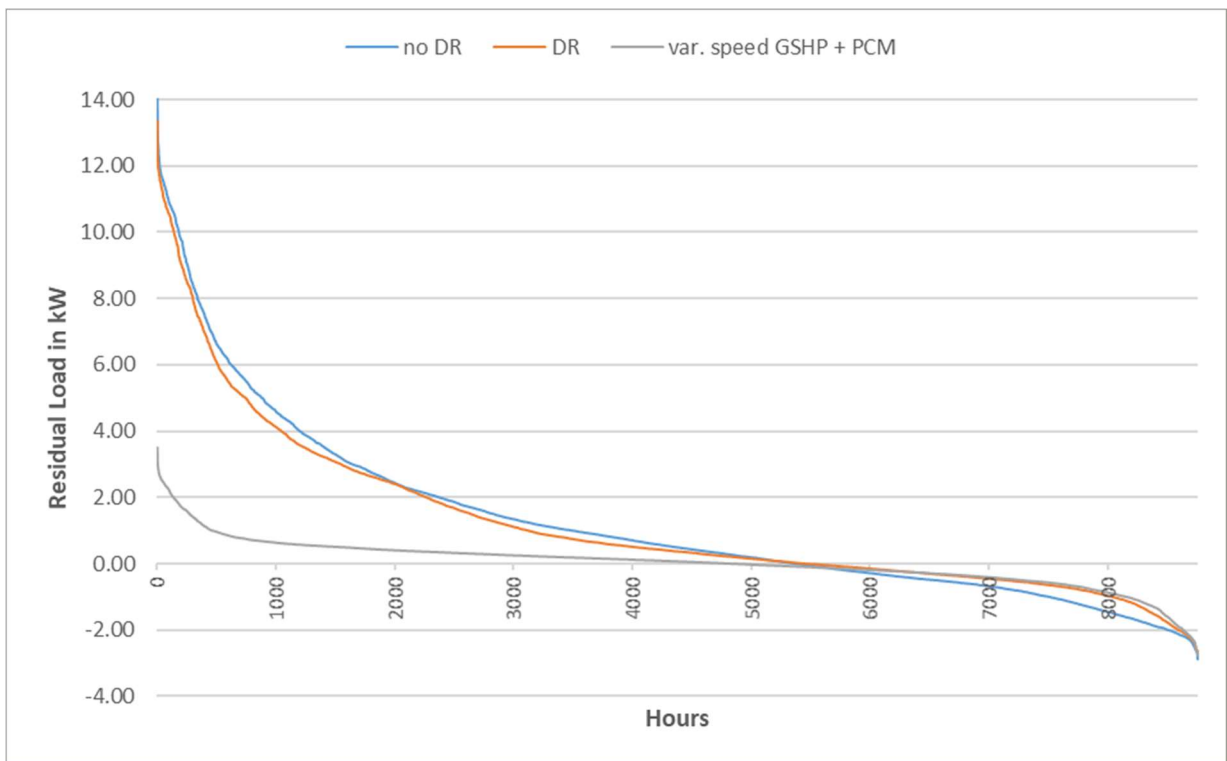


Figure 59: Annual Residual Loads Variants 31 – 33

## 6.11 Typical Winter Week Gaithersburg

A typical winter week without DR is shown in Figure 60. The total absolute Residual Load during this week is 169 kWh. The building's load fluctuates heavily and rarely matches the grid generation. The peaks are mainly caused by the ASHP's defrost cycle. Additionally, peaks are typically caused by the electrical stove/oven, dishwasher, hairdryer and clothes dryer.

A typical winter week with DR is shown in Figure 61. The total absolute Residual Load during this week is 105 kWh. Defrost cycles still cause peak loads but the overall heating demand is better matched to the grid generation compared to the Base Variant.

A typical winter week with DR, a variable speed GSHP and active PCM is shown in Figure 62. The total absolute Residual Load during this week is 57 kWh. No defrost cycles are necessary when using a borehole heat exchanger. Therefore, the major peak loads is the dryer which is now clearly visible in the graph. High thermal capacitance provides a greater potential for peak shifting compared to the lightweight construction. Especially on the third, sixth and seventh day the increased load, caused by the DR strategy, accurately tracks the grid's peak generation until the thermal storage capacity is fully charged.

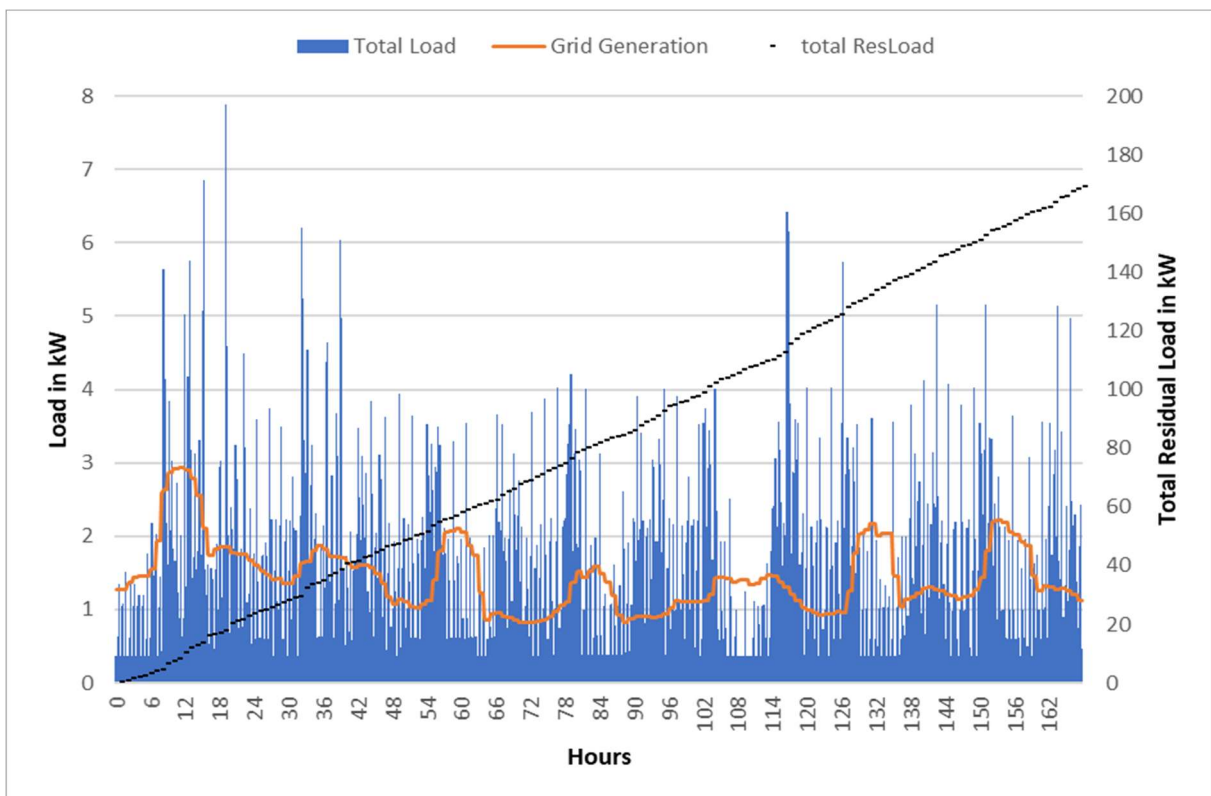


Figure 60: Typical winter week Base Variant

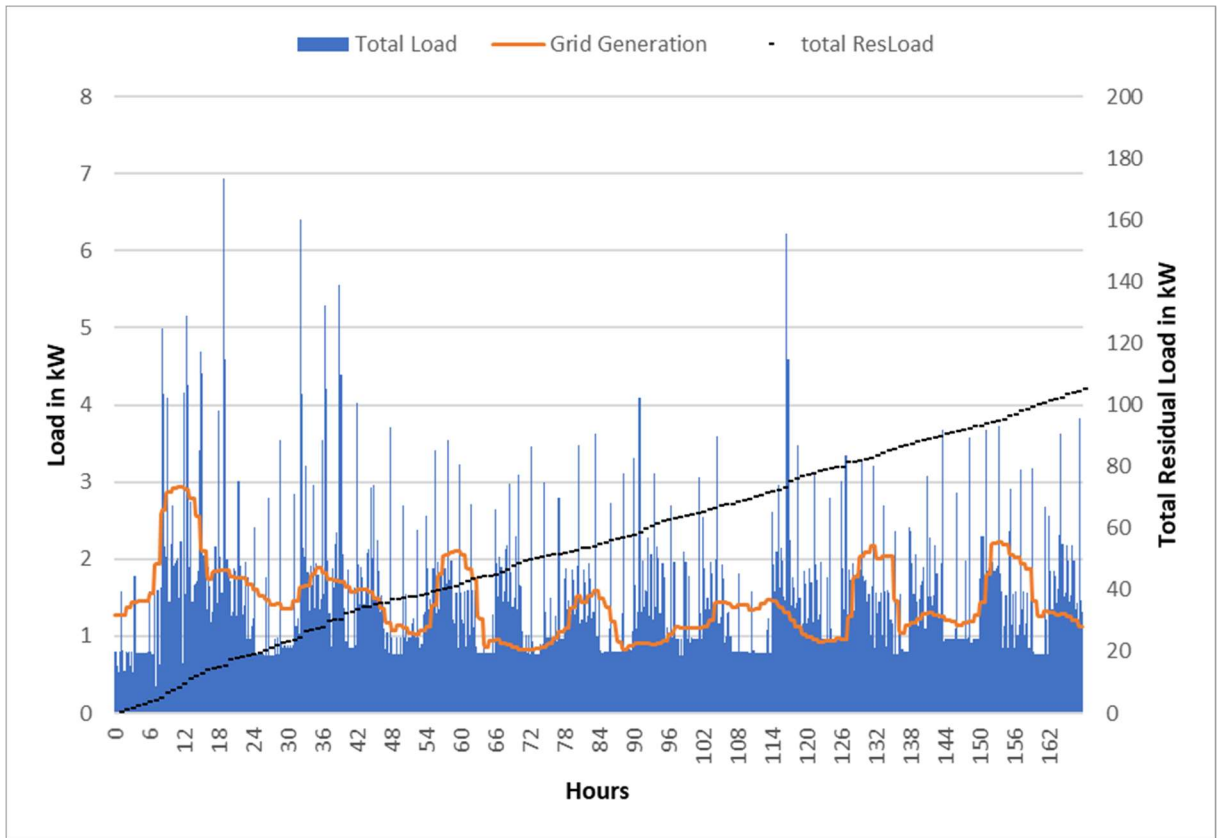


Figure 61: Typical winter week Base Variant with DR

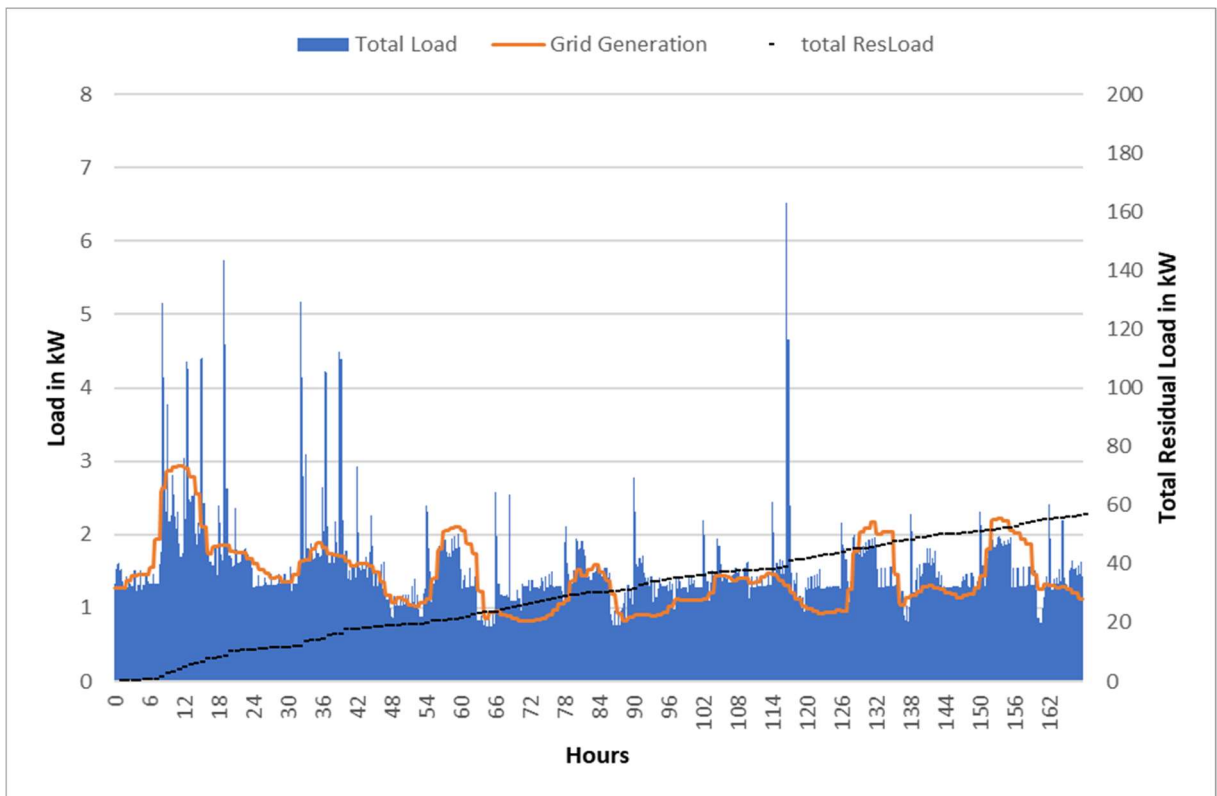


Figure 62: Typical winter week variable speed GSHP with PCM and DR

## 6.12 Typical Summer Week Gaithersburg

A typical summer week without DR is shown in Figure 63. The total absolute Residual Load during this week is 162 kWh. The building's load fluctuates heavily and rarely matches the grid generation. Especially during the sixth and seventh day there is only a base load during times of peak renewable generation. The peaks, with a power greater than 5 kW, are typically caused by the dryer. This appliance is turned on during the first, second, and fifth day. The other peaks are mainly caused by household appliances, such as toasters, microwaves, and hair dryers.

A typical summer week with DR is shown in Figure 64. The total absolute Residual Load during this week is 120 kWh. The reduction in absolute Residual Load between this variant and the Base Variant is not as great as the reduction during winter. This difference is because there is a dehumidification demand that is independent of the outside temperature. Dehumidification is not altered by the DR controller since it would negatively impact thermal comfort.

A typical summer week with DR, a variable speed GSHP and active PCM is shown in Figure 65. The total absolute Residual Load during this week is 99 kWh. The major peak load is the dryer. On the sixth and seventh day the increased load, caused by the DR strategy, accurately tracks the grid's peak generation until the thermal storage capacity is fully charged. The grid generation during these days greatly exceeds the building's potential for demand response. Therefore, only about a third of the peak is compensated.

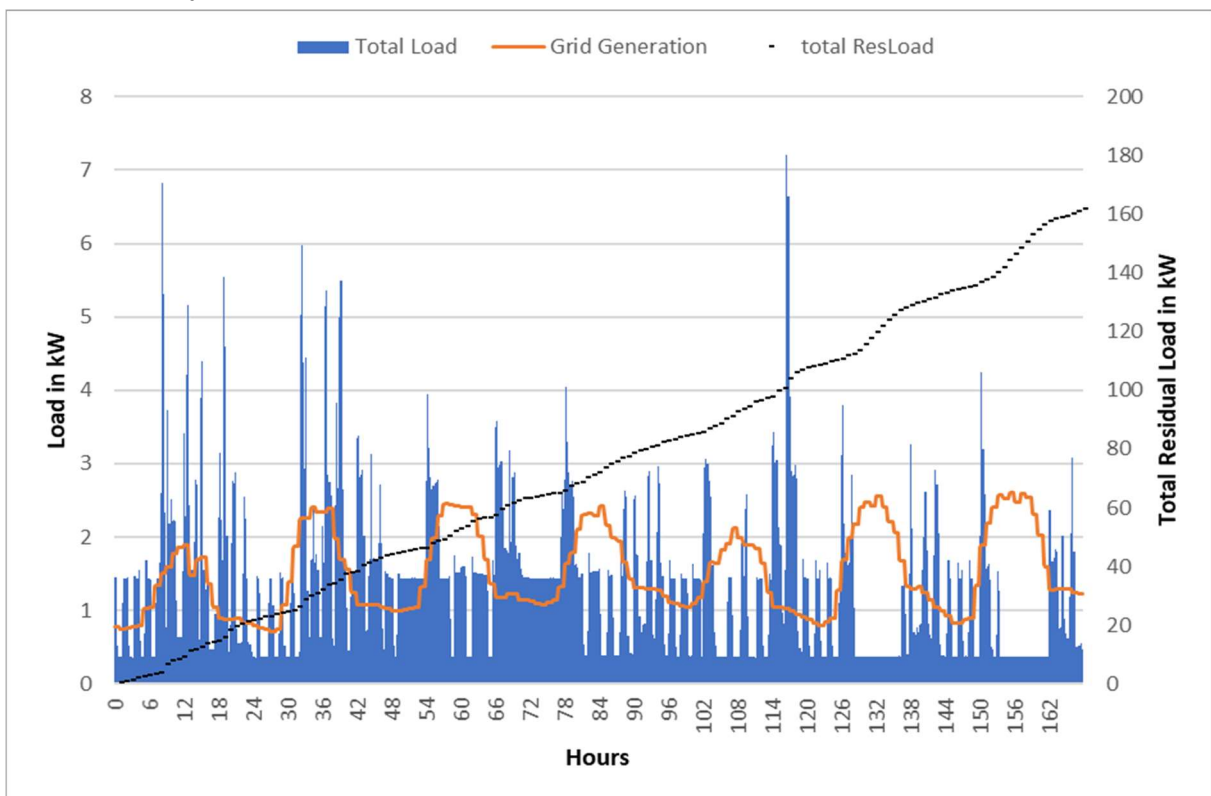


Figure 63: Typical summer week Base Variant

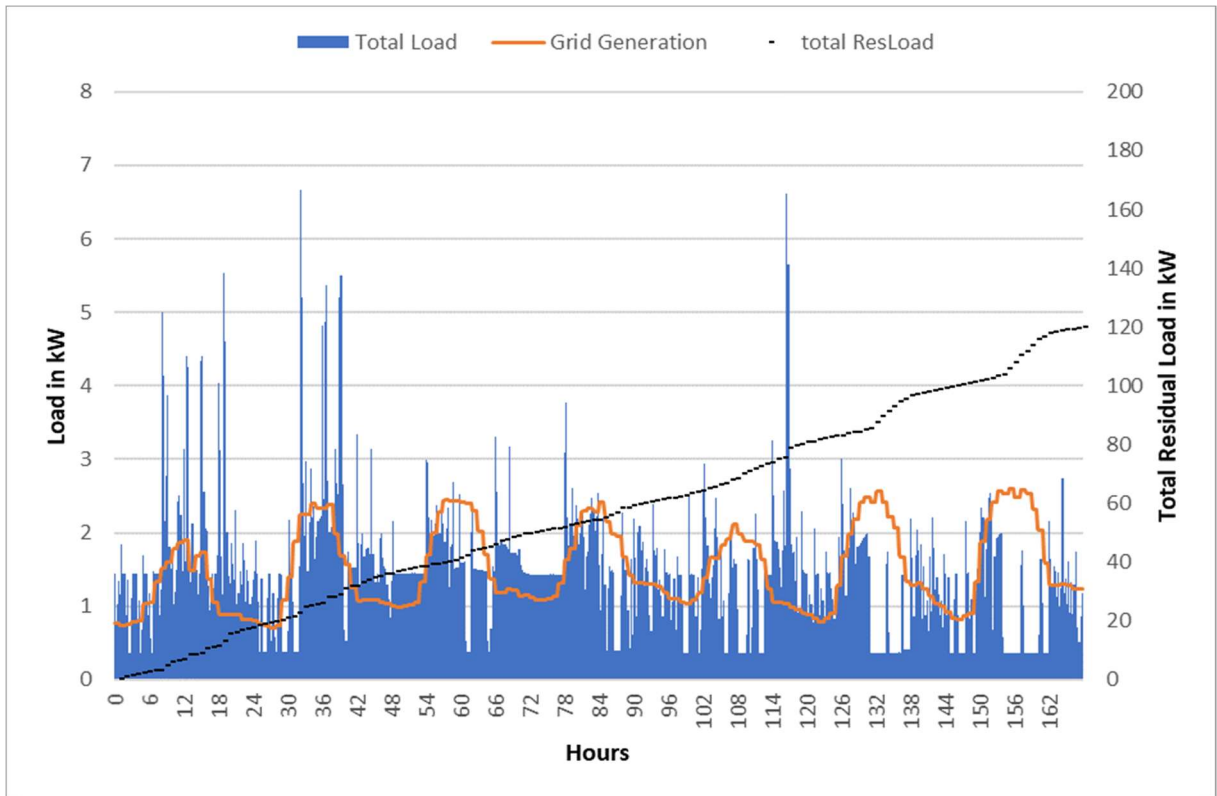


Figure 64: Typical summer week Base Variant with DR

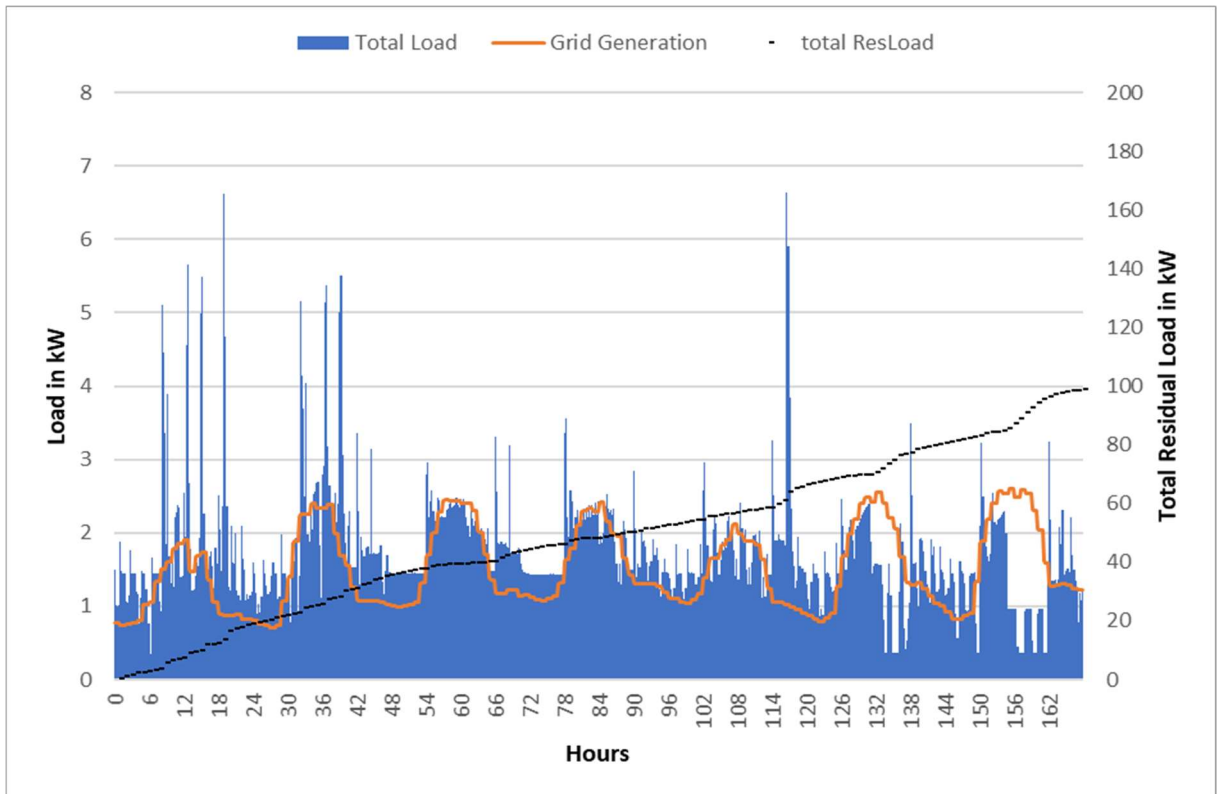


Figure 65: Typical summer week variable speed GSHP with PCM and DR

## 7 Conclusion

The objective of this paper is to show the effectiveness of Demand Response (DR) with Thermostatically Controlled Loads (TCL) to reduce Residual Loads (RL) in US detached single-family house that is expected to be typical of construction in 2050. The impact of different thermal storage capacities, heat pump technologies, and climates on a building's potential for DR is investigated. A 50 % share of renewable generation in 2050 is assumed for the simulation.

Using a DR strategy, which varies the setpoint temperatures of building equipment based on RL, results in a 19.5 % reduction in RL in the climate of Gaithersburg, Maryland. The control for DHW can be implemented with either a resistance heat element or a heat pump water heater.

The lightweight variant of the building has minimal thermal storage capacity compared to a building constructed from massive materials. Nevertheless, the DR control strategy succeeds in reducing positive as well as negative RL. The DR strategy does not cause an increase in energy demand. Energy savings during winter cancel out higher consumption caused by DHW and cooling. It can be concluded that there is no technical reason not to use DR to reduce RL in detached single-family homes in Maryland. This finding applied even when DR was applied to a home built to current building energy efficiency standards in the US.

Increasing the heat pump's power does not necessarily improve a building's capabilities for DR. The majority of RLs are less than 1000 W, which is close to the heat pump's load of 800 W. Peaks in positive RL, caused often by the dryer, cannot be compensated by turning off the HP. Peaks in negative RL, caused by high renewable generation during summer, can also not be decreased by increasing HP power. The building is already cooled down to the lower end of the control's temperature range during summer. So even if there is high negative RL in the grid, the controller prioritizes thermal comfort and the HP is not turned on. Conversely, a high-power single-stage or two-stage HP might overcompensate as a response to the control signal by turning a negative RL into a positive RL and vice versa. Additionally, every compressor stage has a minimum runtime which delays tracking of the RL signal and can counteract the reduction in RL.

Therefore, intentionally oversizing a HP just for the sake of increasing a building's potential for DR is not an effective measure for reducing RL.

Decreasing the heat pump's power does not lead to lower RL in the climate of Gaithersburg. Especially for ASHPs there are drawbacks associated with a lower capacity. More defrost cycles are necessary because of increased compressor runtimes. The increased electricity demand in winter leads to an increase in positive RL and a decrease in negative RL. The colder the climate, the more the disadvantages (increased positive RL) outweigh the advantages (decreased negative RL). Additionally, the annual heating demand is increased. Low powered heat pumps might perform differently in various climates but are not within the scope of this paper.

In the climate of Maryland, a lower insulation standard leads to a higher annual energy demand and a nearly unchanged total RL, compared to the variant with a near passive house standard of insulation and DR. Even though negative RLs are reduced because of the increased heating demand, positive RLs are increased by a similar magnitude. Additionally, the lower insulation standard can lead to thermal discomfort because of the differences between surface temperatures and air temperatures.

Therefore, it can be concluded that a higher insulation standard not only reduces annual energy demand and PPD but also has no adverse effects on absolute annual RL.

This study highlights the effectiveness of a variable speed heat pump at reducing RL. All variable speed heat pumps examined in this paper (ASHP, AWHP, GSHP) perform as good as or better than their single-stage or 2-stage counterpart at reducing RL. Single and multi-stage heat pumps have minimum stage runtimes, which delays their response to a real-time generation signal. A real-time generation profile fluctuates and changes every second. A variable speed heat pump can respond to these changes instantaneously by adjusting compressor speed and therefore power consumption.

The choice of heat pump technologies can play an important role in reducing the RL generated by a building. Especially in cold climates, a highly efficient GSHP greatly reduces positive RL compared to an ASHP. Energy efficiency measures are of paramount importance for reducing positive RL and should be implemented before developing a DR strategy. DR cannot make up for a building's overall poor energy efficiency.

The heat flux between PCM and the indoor air in a passive PCM system is not sufficient for effectively improving DR capabilities. Nevertheless, the thermal comfort of a building with lightweight construction can be improved when using PCMs for peak shifting. In Gaithersburg the thermal comfort in a lightweight building with PCMs is comparable to the thermal comfort in a building made of massive construction materials. Therefore, PCMs are a viable option to improve thermal comfort in buildings made of lightweight materials.

The heat flux between the heat transfer fluid and PCM of an active PCM system is large enough to make it a viable option for improving DR. In the climate of Gaithersburg, an active PCM system can decrease negative RL by 36 % compared to a 20 % decrease of the passive system. This improvement is accomplished by charging the PCM with a heat transfer fluid during times of high renewable generation. Thermal comfort is also improved compared to the passive PCM system because of nearly constant surface temperatures throughout the year.

Increasing the range for temperature setpoints results in an average decrease of total annual RL of 3 % across all variants. Thermal comfort is equal to or greater than in the Base Variant, even with a greater temperature range. Variants with high thermal capacitance provide greater thermal comfort than variants with low thermal capacitance. While it is true that a greater temperature range slightly increases thermal discomfort, it is up to the user to decide which temperature thresholds are still acceptable. In general, a greater range for temperature

setpoints enables the DR control to store more thermal energy in the building and thus decrease RL. These results may vary widely in different climate conditions.

The best performing variants make use of variable speed GSHP and operate in a temperature range between 20 °C and 26 °C. The variant with activated PCM achieves a total reduction of annual RL of approximately 36 %.

There are multiple ways to reduce positive Residual Load apart from lowering the heating setpoint and DHW temperature during winter. The best ways to reduce positive Residual Load are energy efficiency measures. More efficient household appliances (e.g., washers, dryers, microwaves, etc.), heat pumps, HRV, and higher insulation standards are the major ways to reduce positive Residual Load. DR is also only one part of the equation for reducing negative Residual Load. In an electrical grid without vast storage capacity, limiting the active power of renewable power plants will be necessary. Feeding reactive power into the grid will not be sufficient to keep voltage levels in the required range.

A variety of different storage technologies (electrochemical, mechanical, chemical, etc.) will be necessary along with DR to transition to 100 % renewable energy generation.

To improve energy flexibility in buildings, space and hot water heating based on fossil fuels needs to be phased out. A furnace cannot provide any grid services. The electrification of the energy system will be one of the most important aspects for transitioning to 100 % renewable energy. Grid operators will be able to develop algorithms to control a great number of residential heat pumps to keep the grid operational even during times of peak demand or generation. In combination with storage infrastructure, DR will play a vital role in the energy system.

The controlling strategy used in this paper is a simple proof of concept. The interconnections between the electricity grid and consumers are complex and more sophisticated models will be necessary. Furthermore, complexity is only going to increase when smart meters are rolled out on a large scale and more and more stakeholders join the smart grid.

Future research should consider how to use monetary incentives for consumers to allow DR. Without receiving a discount on electricity prices or direct payments from the electricity supplier, consumers will most likely not be ready to give up control over their TCLs. Additionally, an integration study of large-scale DR strategies for residential housing will be essential. The possibility of combining communities into microgrids should be considered to determine potential benefits and drawbacks regarding grid services.

## Bibliography

ASHRAE, 2013, ASHRAE Standard 55 - Thermal Environmental Conditions for Human Occupancy.

AWS Truepower, 2012, PJM Renewable Integration Study. <https://www.pjm.com/~media/committees-groups/subcommittees/irs/postings/pris-task-1-wind-and-solar-power-profiles-final-report.ashx>

Balke, E., 2016, Modeling, Validation and Evaluation of the NIST Net Zero Energy Residential Test Facility.

Callaway, D., 2009, Tapping the energy storage potential in electric loads to deliver load following and regulation, with application to wind energy.

DOE, 2015, United States Electricity Industry Primer.

EIA, 2019a, Annual Energy Outlook 2019 with projections to 2050.

EIA, 2019b, Electric Power Monthly with Data for December 2018. [https://www.eia.gov/electricity/monthly/current\\_month/epm.pdf](https://www.eia.gov/electricity/monthly/current_month/epm.pdf)

General Electric, 2014, PJM Renewable Integration Study.

ICC, 2016, IECC - International Energy Conservation Code 2015.

IEA, 2017, IEA EBC Annex 67 Common exercise 4: Evaluation of characterization methodology for energy flexibility based on Flexibility Function and Flexibility Characteristics.

IEA, 2003, The Power to Choose - Demand Response in Liberalised Electricity Markets.

IEEE, 2013, A Framework for and Assessment of Demand Response and Energy Storage in Power Systems. ETH Zurich, Switzerland

Li, G., 2015, Sensible heat thermal storage energy and exergy performance evaluations. Elsevier Ltd.

MA23, 2019, Wetter seit 1955 Hohe Warte Wien - Weather since 1955 Hohe Warte Vienna. <https://www.data.gv.at/katalog/dataset/wetter-seit-1955-hohe-warte-wien>

NIST, 2015, NIST Technical Note 1869 – Research and Development Opportunities for the NIST Net Zero Energy Residential Test Facility.

NOAA, 2017, Monthly Weather Data US Weather Stations. <https://www.ncdc.noaa.gov/cdo-web/datatools/findstation>; 03/25/2019

NREL, 1990, 30-Year Average of Monthly Solar Radiation, 1961-1990, Baltimore MD. [https://rredc.nrel.gov/solar/old\\_data/nsrdb/1961-1990/redbook/sum2/state.html](https://rredc.nrel.gov/solar/old_data/nsrdb/1961-1990/redbook/sum2/state.html)

Omar, F., Bushby, S., 2013, Simulating Occupancy in the NIST Net-Zero Energy Residential Test Facility.

PJM, 2019a, PJM's Role as an RTO. <https://www.pjm.com/~media/about-pjm/newsroom/fact-sheets/pjms-role-as-an-rto-fact-sheet.ashx>

PJM, 2019b, Fuel mix of generation resources operating under PJM direction for each hour. [http://dataminer2.pjm.com/feed/gen\\_by\\_fuel/definition](http://dataminer2.pjm.com/feed/gen_by_fuel/definition); 03/13/2019

Pomianowski, M., Heiselberg, P., Zhang, Y., 2013, Review of thermal energy storage technologies based on PCM application in buildings. Elsevier Ltd.

Rathod, M.K., 2018, Thermal Stability of Phase Change Material. IntechOpen

Reddy, K.S., Mudgal, V., Mallick, T.K., 2017, Review of latent heat thermal energy storage for improved material stability and effective load management. Elsevier Ltd.

Richarz, C., Schulz, C., 2013, Energy efficiency refurbishments. , 978-3-920034-90-4;

Schill, W., 2013, Residual Load, Renewable Surplus Generation and Storage Requirements in Germany. German Institute for Economic Research, Berlin

US Census, 2018, Historical Households Tables. <https://www.census.gov/data/tables/time-series/demo/families/households.html>; 03/07/2019

US Census, 2017, Square Feet of Floor Area in New Single-Family Houses Completed. <https://www.census.gov/construction/chars/pdf/squarefeet.pdf>; 02/21/2019

US Census, 2015, Projections of the Size and Composition of the U.S. Population: 2014 to 2060.

## List of Figures

Figure 1: Map of Four North American Power Grid Interconnections (DOE 2015).....	10
Figure 2: Map of North American Transmission Operators (DOE 2015).....	11
Figure 3: Electricity Mix PJM 2018 (PJM 2019b).....	12
Figure 4: Electricity Generation Profile PJM 2018 (PJM 2019b).....	13
Figure 5: Selected centralized solar power plants PJM (AWS Truepower 2012).....	14
Figure 6: Selected onshore and offshore wind sites PJM (AWS Truepower 2012).....	14
Figure 7: Electricity Mix PJM 2030 (own illustration).....	15
Figure 8: Electricity Generation Profile PJM 2030 (own illustration).....	15
Figure 9: Electricity Mix PJM 2050 (own illustration).....	16
Figure 10: Electricity Generation Profile PJM 2050 (own illustration).....	17
Figure 11: Flexibility function for reduced consumption utilizing a price control signal (IEA 2017).....	21
Figure 12: Flexibility function for increased consumption utilizing a Residual Load control signal (IEA 2017, altered).....	21
Figure 13: Phase transition profile of phase change material (Reddy et al. 2017).....	23
Figure 14: Working principle and structure of encapsulated PCM (Reddy et al. 2017).....	24
Figure 15: Clothing insulation as a function of outdoor temperature (ASHRAE 2013).....	26
Figure 16: Acceptable range of operative temperature and humidity (ASHRAE 2013).....	27
Figure 17: PPD as a function of PMV (ASHRAE 2013).....	28
Figure 18: Local thermal discomfort caused by radiant asymmetry (ASHRAE 2013).....	29
Figure 19: NZERTF Zones (Balke 2016).....	29
Figure 20: NZERTF south view.....	30
Figure 21: NZERTF north view.....	31
Figure 22: NZERTF 1st Floor (NIST).....	31
Figure 23: NZERTF 2nd Floor (NIST).....	32
Figure 24: Climate Zones US (ICC 2016).....	33
Figure 25: Climate diagram Washington Dulles (2010-2017) (NOAA 2017).....	34
Figure 26: Roof geometry of the NZERTF (own illustration).....	42
Figure 27: Resistance heaters, sensors for dry air temp, relative humidity and radiant temperature (NIST).....	44
Figure 28: Latent Heat Generators (Ultrasonic humidifiers) (Omar and Bushby 2013).....	44
Figure 29: Variants Simulated in Gaithersburg Climate.....	45
Figure 30: Variants Simulated in Climates of Vienna, Phoenix, Miami, and Fairbanks.....	45
Figure 31: Single-Stage Heat Pump Control.....	47
Figure 32: 2-Stage Heat Pump Control - Stage Selection.....	50
Figure 33: Variable Speed Heat Pump Control - Power Selection.....	51
Figure 34: Climate Diagram Vienna, Austria (MA23 2019).....	53
Figure 35: Climate Diagram Phoenix, AZ (NOAA 2017).....	54
Figure 36: Climate Diagram Miami, FL (NOAA 2017).....	55

Figure 37: Climate Diagram Fairbanks, AL (NOAA 2017).....	56
Figure 38: Typical summer week July 23 to August 2.....	57
Figure 39: Typical winter week February 3 – February 9.....	57
Figure 40: Results Variants 1 and 2 .....	60
Figure 41: Annual Residual Loads Variants 0 and 2.....	60
Figure 42: Results Variants 3 – 5 .....	62
Figure 43: Annual Residual Loads Variants 3 – 5.....	62
Figure 44: Results Variants 6 – 9 .....	64
Figure 45: Annual Residual Loads Variants 6 – 9.....	65
Figure 46: Results Variants 10 – 13 .....	67
Figure 47: Annual Residual Loads Variants 10 – 13.....	68
Figure 48: Results Variants 14 – 17 .....	70
Figure 49: Annual Residual Loads Variants 14 – 17.....	71
Figure 50: Results Variants 18 – 21 .....	73
Figure 51: Annual Residual Loads Variants 18 – 21.....	73
Figure 52: Results Variants 22 – 24 .....	75
Figure 53: Annual Residual Loads Variants 22 – 24.....	75
Figure 54: Results Variants 25 – 27 .....	77
Figure 55: Annual Residual Loads Variants 25 – 27.....	77
Figure 56: Results Variants 28 – 30 .....	79
Figure 57: Annual Residual Loads Variants 28 – 30.....	80
Figure 58: Results Variants 31 – 33 .....	82
Figure 59: Annual Residual Loads Variants 31 – 33.....	82
Figure 60: Typical winter week Base Variant.....	83
Figure 61: Typical winter week Base Variant with DR .....	84
Figure 62: Typical winter week variable speed GSHP with PCM and DR.....	84
Figure 63: Typical summer week Base Variant .....	85
Figure 64: Typical summer week Base Variant with DR .....	86
Figure 65: Typical summer week variable speed GSHP with PCM and DR.....	86

## List of Tables

Table 1: Development of residential sector in PJM (own illustration) .....	18
Table 2: Metabolic Rates for Typical Tasks (ASHRAE 2013) .....	25
Table 3: Clothing Insulation Values for Typical Ensembles (ASHRAE 2013).....	26
Table 4: Minimum requirement for U-Values by the IECC in W/m <sup>2</sup> K (ICC 2016).....	33
Table 5: NZERTF Lightweight Roof (IBO 2019) .....	35
Table 6: NZERTF Lightweight Wall (IBO 2019) .....	35
Table 7: NZERTF Lightweight Ceiling (IBO 2019) .....	36
Table 8: NZERTF Lightweight Interior Wall (IBO 2019) .....	36
Table 9: NZERTF Basement Wall (IBO 2019) .....	36
Table 10: NZERTF Basement Floor (IBO 2019).....	37
Table 11: NZERTF Concrete Roof (IBO 2019).....	37
Table 12: NZERTF Brick Wall (IBO 2019) .....	38
Table 13: NZERTF Concrete Ceiling (IBO 2019).....	38
Table 14: NZERTF Brick interior wall (IBO 2019) .....	39
Table 15: Operative Temperature Distribution Variant 10.....	66
Table 16: Operative Temperature Distribution Variant 17.....	70

## List of Abbreviations

ASHRAE	American Society of Heating, Refrigerating and Air-Conditioning Engineers
ASHP	Air Source Heat Pump
AWHP	Air-Water Heat Pump
DOC	U.S. Department of Commerce
DOE	U.S. Department of Energy
DHW	Domestic Hot Water
EIA	U.S. Energy Information Administration
FERC	Federal Energy Regulatory Commission
GSHP	Ground Source Heat Pump
HUD	U.S. Department of Housing and Urban Development
IBC	International Building Code
IBO	Austrian Institute for Healthy and Ecological Building
ICC	International Code Council
IEA	International Energy Agency
IECC	International Energy Conservation Code
IEEE	Institute of Electrical and Electronics Engineers
MA23	Magistrate Vienna - Department 23 - Economy, Labor and Statistics
NOAA	National Oceanic and Atmospheric Administration
NIST	National Institute for Science and Technology
NREL	National Renewable Energy Laboratory
NZERTF	Net-Zero Energy Residential Test Facility
PCM	Phase Change Material

PJM	PJM Interconnection LLC
RES	Renewable Energy Sources
TCL	Thermostatically Controlled Loads
US Census	United States Census Bureau